PHOSPHORUS CONTAMINATION AND STORAGE IN BOTTOM SEDIMENTS OF THE JAMES RIVER ARM OF TABLE ROCK LAKE, SOUTHWEST MISSOURI

A Thesis

Presented to

The Graduate College of

Southwest Missouri State University

In Partial Fulfillment

Of the Requirements for the Degree

Master of Science, Resource Planning

By

Marc R. Owen

December, 2003

PHOSPHORUS CONTAMINATION AND STORAGE IN BOTTOM SEDIMENTS OF THE JAMES RIVER ARM OF TABLE ROCK LAKE, SOUTHWEST MISSOURI

Department of Geography, Geology, and Planning

Southwest Missouri State University, 2003

Master of Science, Resource Planning

Marc R. Owen

ABSTRACT

Eutrophic conditions in the upper James River Arm (JRA) of Table Rock Lake have been linked to phosphorus (P) inputs by wastewater treatment facilities and increasing urban development in the upper James River Basin (3,770 km^2). Since the majority of P in aquatic environments is bound to sediments, bottom sediment can function as both a source and sink of P in lake systems. This study evaluates the spatial distribution, physical and chemical characteristics, and storage of sediment-P in the active layer (<5 cm) of bottom sediments in the JRA. The JRA makes up about 20% of Table Rock Lake's surface area, contributes about 30% of the inflow, and has the poorest water quality of the entire lake. For this study, grab samples were collected in the main arm and tributary coves at the deepest part of the lake and at several shallow sites along the main arm. Concentrations increase in a down-lake direction in the main arm ranging from 5 to >2000 ppm P. However, water-column P concentrations show a decrease down-lake, indicating that sedimentation is removing P from the water. Trap efficiency of the JRA of both natural and anthropogenic P is estimated at 91%. In the main valley of the JRA, P correlates with depth and iron concentration where these variables account for both down-lake deposition, sediment focusing, and changes in dissolved oxygen important to the spatial distribution in bottom sediments. Tributary cove sediments show no correlation with land-use characteristics, suggesting concentrations are close to background levels. Higher enrichment of P in bottom sediments in the deeper areas suggests that the ability of the JRA to trap P is correlated with sediment at depths greater than 12-15 meters where dissolved oxygen levels are seasonally low. Less P is stored in the upper section of the JRA below Galena, however, this shallower area is the transition zone between the river and lake has high deposition rates.

KEYWORDS: phosphorus, sediment, contamination, geochemistry, Table Rock Lake

This abstract is approved as to form and content

_____

Robert T. Pavlowsky, Ph.D.
Chairperson, Advisory Committee
Southwest Missouri State University

PHOSPHORUS CONTAMINATION AND STORAGE IN BOTTOM SEDIMENTS OF THE JAMES RIVER ARM OF TABLE ROCK LAKE, SOUTHWEST MISSOURI

By

Marc R. Owen

A Thesis
Submitted to The Graduate College
Of Southwest Missouri State University
In Partial Fulfillment of the Requirements
For the Degree of Master of Science, Resource Planning

December, 2003

Approved:

_____
Robert T. Pavlowsky, Ph.D., Chairperson

_____
Rex G. Cammack, Ph.D.

_____
Erwin J. Mantei, Ph.D.

_____
Frank Einhellig, Graduate College Dean
Graduate College

ACKNOWLEDGEMENTS

I would like to begin by thanking Dr. Robert Pavlowsky (chairperson) for his guidance during my years at SMSU. I would also like to thank the other members of my committee Dr. Rex Cammack and Dr. Erwin Mantei. This project was funded under a United States Geological Survey Water Resources Grant to Dr. Pavlowsky entitled, *Spatial Distribution, Geochemistry, and Sources of Phosphorus and Metals in Bottom Sediments in the James River Arm of Table Rock Lake* and an SMSU Graduate College Thesis Grant. I would also like to thank Tricia Tannehill at the United States Army Corps of Engineers and Gary Krizanich at the USGS for providing GIS data for this project. Many thanks go to those who assisted me in the field and in the lab including John Horton, Susan Licher, Aidong Cheng, Amy Keister, John Kothenbeutal, Jian Yang, Ryan Wyllie, and Andrea and Chris Jones. Finally, I would like to thank my family, especially my wife Alana, for her patience and support.

TABLE OF CONTENTS

TABLE OF CONTENTS CONTINUED

TABLE OF CONTENTS CONTINUED

Page

LIST OF TABLES

Page

LIST OF TABLES CONTINUED

Page

LIST OF FIGURES

Page

LIST OF FIGURES CONTINUED

Page

CHAPTER 1

INTRODUCTION

Anthropogenic phosphorus (P) enrichment of surface and ground water can lead to algal blooms and eutrophication in aquatic ecosystems. Eutrophication is a biological process that occurs when nutrients, such as P and nitrogen, become available in the water column and increase primary production (Hem, 1985). Problems associated with the increased primary production include reduction of water clarity, taste and odor problems in drinking water, and fish kills associated with decreased dissolved oxygen in the water body. Over the last few years, the James River Arm (JRA) of Table Rock Lake has displayed the effects of eutrophication. Table Rock Lake is the receiving water body of the James River and is widely known for its recreational value, clear water and largemouth bass fishery. Thus, P pollution problems raised concerns by local government officials and citizens since the economy of the area, including the city of Branson, around Table Rock is heavily dependent on the tourist industry (MDNR, 1999).

Under the Clean Water Act, the Missouri Department of Natural Resources (MDNR) placed segments of the James River Basin, which flows in to the JRA, on the 303d list of impaired waters due to nutrient concentrations at unacceptable levels. Recently, Table Rock Lake has also been added to this list. This designation requires states to complete a Total Maximum Daily Load (TMDL) for waters on the 303d list. A TMDL is designed to assess the amounts of a particular constituent a water body can receive before it is impaired based on research aimed at restoring water quality (MDNR, 2001[a]). Identification of the sources of P and how they affect the reservoir is key to understanding where and how water quality management efforts should be focused.

Monitoring studies show that the JRA has the highest chlorophyll-a and total P concentrations in the entire lake and P has been identified as the limiting nutrient for eutrophication in Table Rock Lake (LMVP, 1998; MDNR, 2001[b]). While wastewater treatment facilities located in Springfield have been shown to be the chief emitters of P in the basin, the James River Basin is also home to a number of potential agriculture and urban non-point sources (Kiner and Vitello, 1997; MDNR, 2001[b]; Fredrick, 2001; Pavlowsky, 2001). Research indicates non-point sources such as septic systems, livestock grazing, and urban development in the basin probably do not have the impact that wastewater treatment facilities have on P loadings from the James River Basin (Pavlowsky, 2001). The main P source is believed to be the Southwest Wastewater Treatment Facility located along Wilson Creek in Springfield approximately 65 km above Galena, where the lake begins.

While much of the scientific work has focused on the James River Basin, a couple of questions remain unanswered as to what happens to P once it enters the lake environment. The first question is how P from the James River is distributed and stored in the JRA and how much gets to the main lake? The James River enters the JRA at Galena and flows 65 km to the confluence of the White River. Along that 65 km stretch, several smaller tributaries drain to coves of the JRA. This leads to question number two, what impact do potential P sources from the surrounding small developing tributaries have on the JRA? Some of these smaller tributary watersheds have agricultural land uses and contain wastewater treatment facilities for small municipalities. The relatively small size of the drainage area coupled with the karst topography and close proximity to the JRA make these watersheds a concern. In addition, septic systems and developments

located adjacent to the JRA may also be contributing significant amounts of P to the system.

SEDIMENT-PHOSPHORUS MONITORING IN THE JAMES RIVER ARM

Ongoing research stemming from the 303d designation and TMDL studies concentrate on monitoring nutrient levels in the water column to understand the summer algal blooms in the upper James River. Currently, data on water column P is available for the JRA at only a few locations. Several problems arise from this approach. First, water samples are highly variable and many samples are needed to objectively evaluate P trends. Second, while these monitoring stations do provide valuable temporal information, they lack a geographical component in identifying sources and their impacts. Third, there are few, if any, studies of the importance of bottom sediment sink/source dynamics in Table Rock Lake.

Sediments are an important component of nutrient cycling in aquatic ecosystems and have potential for use in pollution monitoring (Horowitz, 1991; Watts, 2000). Sediment samples can be gathered and analyzed more quickly and economically than water column data, while covering a larger geographic area. In contrast to water and biological samples, sediment samples can display a consistent local representation of aquatic pollution (Hakanson and Jansson, 1983). Since about 95% of P in aquatic systems tends to be absorbed by sediments as opposed to dissolved in water, sediment sampling provides an excellent way to locate pollution in a reservoir (Hem, 1985). Bottom sediments in particular have been identified as a good indicator of water quality for watersheds flowing to a lake or reservoir (Van Metre and Callender, 1996; Juracek, 1998).

Any study involving P in aquatic ecosystems needs to account for the mass stored in sediments. Although it is widely understood that the majority of P in rivers and lakes is associated with sediments, the amount of P stored in the bottom sediments of the JRA is unknown and may be an important source of P to the lake (Hem, 1985; Horowitz, 1991). Seasonal dissolved oxygen levels, water temperature and lake turn-over can cause P levels to increase in the water column in shallow areas of the lake (Baccini, 1985). However, when sediment settles in deep areas of the lake, P tends to remain in place in the sediments (Hakanson and Jansson, 1983). When water-column P concentrations fall below those in sediment pore waters, bottom sediments may become a source for P to the water column (Reddy et al, 1998).

PURPOSE AND OBJECTIVES

What effect does the James River, major tributaries, and local inputs have on the JRA in terms of the distribution and storage of sediment bound P? The purpose of this study is to measure the distribution of P in bottom sediments of the JRA. The specific objectives are:

1. To measure P, geochemistry, and physical properties of sediment in the JRA and its major tributary coves;
2. Quantify spatial and geochemical relationships using multiple regression modeling;
3. Evaluate the location and importance of anthropogenic P contributions;
4. Develop an annual P-budget for the JRA and determine the significance of sediment storage and P-cycling.

This study uses a bottom sediment survey to evaluate the spatial patterns of P stored in bottom sediments in order to assess the influence of P from the contributing

James River Basin, locate sources directly draining into the JRA from cove tributary watersheds and local inputs, and identify key geochemical relationships between P and sediments. This study quantifies the spatial distribution of P stored in bottom sediments rather than address specific chemical reactions and element phases that may be important to local P release to the water column. However, basic geochemical controls are investigated to help explain the spatial patterns. The P budget calculations involved the use of sediment-P data collected for this study and water-column P data from previous studies and water quality monitoring programs (references).

BENEFITS OF THIS STUDY

Results of this study may be beneficial to scientists. Since sediments are an important part of P-cycling in aquatic ecosystems, knowing the amount of P currently stored in sediments and where P is stored will give scientists a foundation to build from for future studies. Future studies may include depth-integrated water column sampling to look at P release from sediments, re-sampling of bottom sediments in 10 years to evaluate the effectiveness of P management in the James River and the JRA, and/or bottom sediment coring to examine sedimentation and P loading rates over time.

Currently, reductions in P concentrations from Springfield's Wastewater Treatment Facility are underway. Soon, other wastewater treatment facilities in the James Basin will be improving their plants to reduce P outputs. Recently, coordinated monitoring efforts are expanding to include local inputs from shoreline residences and hotels in order to improve their wastewater treatment effectiveness. However, little is known about where P is coming from and how much P is coming from these local sources at present.

CHAPTER 2

LITERATURE REVIEW

In general, little is known about the spatial distribution of P deposited and stored in the bottom of lakes affected by river pollution. Most studies use lake sediment cores to identify temporal sedimentation trends and estimate phosphorus loadings in lakes and reservoirs, often based on only a few cores (Uhlmann et al, 1997; Sanei et al, 2000). Furthermore, most of the studies that attempt to explain the spatial distribution of bottom sediment P are usually in relatively small bodies of water including detention/retention pond systems and other shallow impoundments (Johnson and Nicholls, 1989; Juracek, 1998; Brenner et al, 1999; Wilson and Van Metre, 2000). Larger reservoirs serve as sediment sinks and collect nearly all the fine-grain sediment delivered to them. Thus, bottom sediment characteristics reflect the water quality of the rivers that flow into it and are also useful for predicting P-loading patterns from surrounding watershed areas (Van Metre and Challender, 1996; Chalmers, 1998).

This chapter begins by describing recent water quality trends in the Ozarks, including how water quality in the Ozarks compares to national water quality trends, as well as water quality trends within the Ozarks region. The next three sections describe the P sources, transport and deposition in the lake environment. The first section will discuss P in aquatic systems in terms of sources and forms found in the environment. The second section reviews the importance of sediment in environmental investigations and provides a more detailed discussion of sediment-bound P and how it moves through the watershed. The final section focuses on describing the lake sedimentation processes

and understanding the factors that control the spatial distribution of P in bottom sediments.

WATER QUALITY RESEARCH IN THE OZARKS

Water quality has become a hot topic in the Ozarks both politically and culturally due to the dependence of communities on tourism and recreation which are fundamentally linked to water quality of streams and lakes in the region. Several regional water quality studies have been performed recently within the Ozarks. A National Water-Quality Assessment (NAWQA) performed by the USGS between 1992 and 1995 compared the Ozarks to other NAWQA areas around the country. The assessment discusses several water quality indicators including nutrients. Nutrient concentrations in the Ozarks are lowest in forested watersheds, while basins draining urban and agricultural land use rank high in nutrient concentrations compared to other regions in the U.S. (Petersen et al, 1998). Jones and Knowlton (1993) compared water quality of Missouri reservoirs and explain that reservoirs in the Ozarks have the lowest suspended solids and nutrient levels in the state.

Although the water quality in the Ozarks is generally good, the JRA of Table Rock Reservoir has some of the poorest water quality in the Ozarks. The Lakes of Missouri Volunteer Program (LMVP) performed a water quality study on Table Rock Lake in 1998. This study shows water column P-concentrations in the JRA are high for the region, with the upper JRA having P-concentrations up to 10 times higher than the regional average (LMVP, 1998). Knowlton and Jones (1989) found a steep down-arm gradient of total P (TP) in the epilimnion of the JRA during the summer. Concentrations ranged from >500 ug/L near Galena during base flow to <20 ug/L near the confluence

with the White River indicating that sedimentation and biological uptake may immobilize significant amounts of P in the JRA. The TMDL report for the James River estimates the P loading at Galena at 386 Mg/yr (MDNR, 2001[b]). This loading reflects the combined load from wastewater effluent, urban and agricultural nonpoint, and natural sources.

As a response to these studies, the Resource Planning Program at Southwest Missouri State University (SMSU) performed a basin-wide sediment study of the James River system to locate high P concentrations and identify P sources. Fredrick (2001) was able to use recently-deposited stream bed sediments collected throughout the James River Basin to show the mean and maximum P concentrations were highest in sediments below wastewater treatment facilities. In subwatersheds where no wastewater treatment facilities are located, a multiple regression equation approach was used to measure the influence of urban and agriculture uses on nonpoint P sources showing almost a doubling of sediment-P concentrations above background in urban and agricultural watersheds compared to forested ones.

PHOSHORUS SOURCES AND TRANSPORT

Phosphorus has been identified as the leading cause of eutrophic conditions in Table Rock Lake, therefore, it is necessary to understand where P originates and in what form it is found in the environment. Sources of P in water bodies can either be natural or anthropogenic. Phosphorus is a naturally occurring element that can be released into the environment via organic decomposition, weathering of bedrock, and by the atmosphere (Clark et al, 2000). Typically, anthropogenic produced P is associated with either point or non-point pollution sources.

Point-source pollution refers to pollution sources that can be traced back to a particular spot of output (Pierzynski, 1994). A major point source for P is wastewater treatment facilities. Humans and animals require P for metabolism and it is present in their waste material (Hem, 1985). Effluent from wastewater treatment facilities releases this P into the environment. Industrial discharge and concentrated animal feeding operation's (CAFO) effluent are also examples of point-source P pollution.

Nonpoint-sources of pollution are those that are not readily identifiable as coming from any particular point (Pierzynski, 1994). Usually, nonpoint-source P is related to different types of land use. Research shows that those areas with more urban land use and areas dominated by agricultural land use tend to have higher concentrations of nutrients, including P (Spahr and Wynn, 1997; Chalmers, 1998). Meals and Budd (1998) identified agriculture as a leading cause of nonpoint-source P pollution in the Lake Champlain watershed. Livestock waste and fertilizer application both on agricultural fields and urban lawns and gardens can contribute P to the environment in surface runoff. Improperly functioning septic systems are another important nonpoint-source for P when located in poor soils, steep terrain, and karst topography (Greene County, 2001).

Phosphorus can either be dissolved or sediment-bound (Sharpley et. al., 1999). Dissolved P occurs in only small concentrations and is available for biologic uptake (Hem, 1985, Sharpley et. al., 1999). Sediment-bound P is associated with organic matter and sediments suspended in the water column or deposited bed sediment (Sharpley et. al., 1999). In general, 95% of the total P in an aquatic environment is found in the sediment (Hem, 1985).

Phosphorus may be associated with sediments in several ways. Sediment-bound P can be incorporated into the matrix of a mineral such as Apatite ($Ca_{10}(PO_4)_6(OH)_2$), or it may co-precipitate with the mineral Calcite ($CaCO_3$) in lake sediments (Hakanson and Jansson, 1983). Phosphorus may also be absorbed on the surface of sediment particles. Surface charge density increases with decreasing grain size, so P tends to concentrate in fine-grained sediments (Horowitz, 1991). For example, clay will generally bind more P then sand. Phosphorus may also be absorbed to sediment particles by oxides of iron (Fe), manganese (Mn), and aluminum (Al) found as coatings on sediments (Davison, 1985; Logan, 1995). Finally, P is incorporated in the organic matter fraction by biological decomposition as well as absorbed to the surface of organic matter (Horowitz, 1991).

SEDIMENTS AND WATER QUALITY

Sediment is an important component of water quality. For constituents, such as P and many trace metals, sediments can act like a sponge absorbing these pollutants at potentially high concentrations (Horowitz, 1991). The spatial patterns of these sediments, the characteristics of these sediments, and the pollutants attached to these sediments provide a way to identify sources of pollution (Combest, 1991). However, sediment sources, which are typically basin-wide, and pollution sources, which can come from a single point source, may not always correlate (Novotny and Chesters, 1989). Understanding the location and intensity of sediment sources, transport, and depositional storage areas within a watershed is important to assessing the nature and scope of these sediment-borne pollutants. The following section will discuss sediments in terms of erosion, storage, and delivery from a watershed and describe the use of sediment as an

environmental management tool. Finally, a short review of using sediment monitoring to locate areas of P enrichment is discussed.

Sediment Erosion, Transport, and Storage

Sediments enter surface waters via natural soil erosion as well as from anthropogenically enhanced soil erosion. Natural soil erosion can be high in areas that are steep, semiarid, or when soil morphology or bedrock is less resistant to weathering (Shumm and Harvey, 1982). Anthropogenically induced soil erosion is typically associated with agriculture land use practices and construction sites in urban areas (Pierzynski et al, 1994). The removal of vegetation from the landscape causes soil to be subjected to the erosive force of the raindrop, increases runoff, and causes flooding (Elliot and Ward, 1995).

During European settlement, initial land clearing was responsible for high rates of soil erosion, altering stream channels from increased flooding and deposition. In the Turner Creek watershed in Georgia, Magilligan and Stamp (1997) show that the two-year storm discharge more than doubled from rapid land clearing in the mid 1800s. Geomorphic readjustment to increased discharge and sediment waves has left its mark on the landscape that can still be observed today in many regions. Knox (1977) found headwater tributaries in Wisconsin's Platte River are wider and shallower due to higher and more frequent flooding since the 1830s, while downstream channel reaches have become narrower and deeper due to the deposition of this eroded sediment. In the Ozarks, Carlson (1998) recorded high sedimentation rates during the period of initial settlement of the Elm Branch and Honey Creek of the Spring River Basin near Aurora, Missouri in the late 1800s. Similarly, Owen (1999) found increased overbank

sedimentation due to land clearing in the Pearson Creek and James River floodplain near Springfield, Missouri.

Agricultural land clearing is not the only cause of streambank erosion and re-adjustment from altered flows and more frequent flooding. Urban areas can also cause streams to readjust to increased runoff from high impervious surfaces within the watershed. Pizzuto et. al. (2000) compared and contrasted urban and rural watersheds in southeast Pennsylvania and showed urban streams have a higher bankfull discharge per unit drainage area than the rural counterparts. These increased discharges can cause streams to become wider by eroding the banks and deeper by scouring the bed, transporting these sediments downstream.

Complicating the process, current sediment delivery rates may not necessarily be linked to present erosion rates. Geomorphic studies suggest historical land use practices have increased the amount of sediments in fluvial systems to which streams and rivers are still adjusting and that most of these sediments are stilled stored in floodplain deposits in upper reaches of large watersheds (Trimble, 1977; Meade, 1982). Trimble (1993) shows that the upper main valley of streams in the Upper Midwest can be significant sediment source due to adjustments to soil erosion brought on by agricultural practices of the early 1930s, and that lower main valleys are still receiving this sediment. Faulkner and McIntyre (1996) show that erosion reduction efforts in the Buffalo River watershed did not translate to sediment reduction in Riecks Lake in west central Wisconsin, thus underscoring the long-term effects of poor agricultural practices.

Sediment Assessment as an Environmental Management Tool

Sediments can be beneficial to environmental managers as both assessment and monitoring tools. Two methods used to do this are sediment budgets and sediment monitoring. Sediment budgets are used to assess sediment input, storage, and output of watersheds. Sediment budgets may be used for watershed management by analyzing the effectiveness of conservation and erosion control measures to achieve desired outputs (Philips, 1986). A sediment survey can be used to identify high levels of a sediment-borne pollutant, calculate a mass balance for that pollutant, and to research processes (Forstner, 1989). The use of sediment for this study is as a monitoring tool to identify sources and illustrate the influences of these sources, but understanding spatial distribution of sediment-P in reservoirs may be helpful in completing sediment budgets using reservoir sedimentation as a temporal check on delivery rates.

Linking sediment delivery rates with pollution sources is a particularly difficult problem faced by environmental managers. Novotny and Chesters (1989) consider the enrichment of sediments by pollutants during sediment transport to be critical in water quality management efforts. Sediment budgets can be very effective in understanding the link between upland erosion rates and water quality. Phillips (1986) displayed how a sediment budget on the Tar River in North Carolina helped show that agricultural erosion control efforts meant to lower P loadings would not be enough to accomplish a major reduction. Sediment budgets are also valuable in understanding how eroded sediment is moving through a watershed and displaying the potential of this sediment to induce future water quality problems. Beach (1994) used a sediment budget to estimate the spatial distribution of floodplain sediment storage in three Minnesota watersheds,

concluding that the majority of sediments from these basins has not moved more than 3 to 4 km in the last 137 years.

These findings illustrate the role floodplains have in storage of sediments is fairly consistent for watersheds in the upper Midwest. This suggests sediments, as well as sediment-associated pollutants such as P, can be stored in floodplain sediments and have the potential to be released at a later time. Walling (1999) explains that linking P fluxes, land use, and sediment delivery is difficult because of the ability of watersheds to buffer land use effects and the influence of floodplains as a temporary and long-term storage site for sediment phosphorus.

Sediments can also be used in environmental monitoring and have long been discussed as valuable in the environmental field to monitor contaminants in aquatic ecosystems and to identify pollution sources (Horowitz, 1991; Combest, 1991; Mantei and Sappington, 1994; Graf, 1996). Other studies have used trace elements, such as Cs-137, Pb-210, and historical mining contamination as stratigraphic markers in sediments to address environmental questions such as estimating floodplain sedimentation rates and reservoir sedimentation rates in addressing sediment delivery and storage (Lewin et al, 1977; Calcagno and Ashley, 1984; Knox, 1987; Walling et al, 1992, Leece and Pavlowsky, 1997; Van Metre et al, 1997; Hyatt and Gilbert, 2000).

Spatial Distribution of Sediment-Bound Phosphorus

The spatial distribution of pollutants in fluvial sediments is typically described as it relates to the source of the pollution. In many instances, a spike in the concentrations of a pollutant is noted at the source and those concentrations decrease downstream in a

negative exponential decay trend due to dilution, decomposition and biologic uptake. This phenomenon has been recorded recently in sediment studies in the James River and Chat Creek in southwest Missouri (Fredrick, 2001, Trimble, 2002). This is commonly known as the distance decay model. However, this model is too general and does not accurately describe the distribution of all sediment-borne pollutants in a fluvial system. Graf (1996) explains that fluvial processes, such as stream power and sediment sorting, may account for the variability of concentrations of pollutants in sediments that do not necessarily follow distance decay models. The distribution of sediment-bound P in a watershed is related to a variety of environmental and cultural factors. Environmental factors include sediment composition and hydrology, and cultural factors include land use and location of point-source discharge.

The spatial variability of P-concentrations in sediments can be used to identify sources and correlate with land use practices. Chalmers (1998) found that P tends to be concentrated in fine-grained sediments as opposed to coarse-grain sediments in the Winooski River Watershed of Vermont. Variability of sediment delivery processes reflects in the geography of contaminated sediments. White (2001) used recently deposited bed sediment to quantify elevated P-loadings from sub-watersheds with high numbers of poultry houses within the drainage area. The processes that deliver polluted sediments to a depositional environment, such as a lake, are complex. Identifying the source areas can prove to be difficult. Sediment characteristics affect enrichment potential, land use activities and point sources supply contaminants, however, high sediment delivery rates and pollution sources may not always correlate because sediment sources may not be where the pollutant is originating (Novotny and Chesters, 1989).

This is true in the James River Basin where it is believed the main P source is a wastewater treatment facility.

LAKE SEDIMENTS AND PHOSPHORUS

Once sediment reaches the river mouth, lake processes control the fate of the sediment. However, due to seasonal variations in lake levels, the boundary of where the river ends and where the lake begins is fuzzy. It is at this boundary where lake processes and fluvial processes can overlap. After reviewing how P enters the environment and is transported downstream, the next step is to look at how sediment behaves in a lake environment. The first section will discuss sedimentation processes in lakes and reservoirs. The next section examines bottom sediment chemistry of lakes and reservoirs. The final section looks at P distribution in lake bottom sediments.

Lake Sedimentation

Lakes are complicated systems and sedimentation patterns can involve many processes. Generally, lake deposits can be a result of both river action at the mouth, as well as wind/wave action, turbidity action, and turnover resuspension in deeper areas (Hakanson and Jansson, 1983; Eadie et al, 1990). When flowing water enters the lake and flow velocity declines, bed load and coarse sediments begin to deposit, forming a delta, and in pelagic areas where there is no flowing water, fine grain sediments dominate the lake bottom (Morris and Fan 1998).

Longitudinally, sediment size tends to increase with increasing distance upstream of a dam (Berkas, 1989, Wilson and Van Metre, 2000). This increase is because fine grain sediment takes longer to settle out of suspension. Wind/wave and turbidity action transport these sediments further downstream, and toward the deeper portions of the lake

(Hakanson and Jansson, 1983). This sorting phenomenon was also found by Calcagno and Ashley (1984) who explained the spatial distribution of sediments in a small reservoir in New Jersey by showing grain size decreases with lake depth, while sorting is better at greater depths. Hilton et al. (1986) suggest that of all the mechanisms controlling sediment distribution in a shallow lake in the U.K., intermittent complete mixing is the most responsible for the relationship between accumulation and depth. Intermittent complete mixing occurs during seasonal turnover, where mixing waters churn up bottom sediments and carry them to the deepest portion of the lake (Hilton et al, 1986). Basin morphology can also influence how wind and waves affect lake sedimentation (Brenner et al, 1999). In some cases, the presence of aquatic vegetation can act as sediment traps causing increased sedimentation near the shore in the photic zone (Brenner et al, 1999; Sanei et al, 2000).

Bottom Sediment, Water, and Phosphorus Interaction

Once sediments have reached the lake bottom, water chemistry conditions can influence the fate of P in sediments. Besides grain size, the most critical aspect in the ability of sediments to retain P is dissolved oxygen content. The redox boundary is often used to describe the boundary between aerobic or oxic and anaerobic or anoxic/reduced waters and sediments. The location of the redox boundary, whether in the water column or in the sediments, controls P release and uptake upon settling. Davison (1985) states when the redox boundary is located in the water column, iron (Fe) and manganese (Mn) will move to the sediments, and when the redox boundary is located in the sediment, Fe and Mn tend to become soluble. This is an important concept for two reasons. First, P behaves much the same way as Fe and Mn in sediments. Second, P can be absorbed or

co-precipitated in Fe and Mn oxides. So, in deeper areas of the lake where there is little dissolved oxygen in bottom sediments, a strong relationship between Fe, Mn, and P would be expected to exist. On the other hand the Fe, Mn, and P relationship would be more variable in shallower areas where the redox boundary is in the sediments since Fe and Mn can be redistributed within and released from bottom sediments.

Several chemical and biological processes are involved in the release and uptake of P by lake bottom sediments at the redox boundary. In deep lakes, such as Table Rock, seasonal thermal stratification in the summer creates a redox boundary at approximately 15 m deep in the water column (USACE, 1985). Once sediment and associated P are deposited, several factors can cause P to detach from sediments and be released to the water-column. Seasonal bottom sediment to water column release of P due to turn over can be caused factors such as decreasing pH due to high biological activity, decreased dissolved oxygen after algal blooms from degraded organic matter, and depletion of dissolved oxygen during summer stratification (Baccini, 1985; Graneli, 1999). However, barriers to the transfer of P from being sediment bound to being dissolved include the presence of Fe oxides and the aerobic decomposition of organic matter, which act as sponges for P (Baccini, 1985).

All sediment-bound P is not released into the water column under these changing aerobic conditions. Klump et al (1997) found that 70% to 90% of sediment-borne P entering Green Bay may be buried by fresh sediment, suggesting the long-term retention by sediments. Due to this long-term retention, even after external P-loading is reduced, eutrophic conditions can persist since sediments can release P back to the water-column (Uhlmann et al, 1997). The upper layer of sediment that is affected by the water-column

above it is referred to as the active layer. Researchers suggest that the depth of the active layer can be from 20 cm deep in sediments to as deep as 40 cm depending on hydrologic conditions (Klump et al, 1997; Reddy et al, 1998).

SPATIAL PATTERNS OF PHOSPHORUS IN LAKE BOTTOM SEDIMENTS

The combination of both sedimentation patterns and water chemistry influences the spatial distribution of P in bottom sediments. Using this knowledge, the spatial distribution of P can be described using geographic criteria that can easily be measured. These criteria basically simplify the sedimentation and chemical processes responsible for P distribution in bottom sediments. In a lake, the longitudinal, vertical, and horizontal location of sediments can be described using depth and distance from the river mouth.

An important factor in the distribution of P in bottom sediments is lake depth, which affects sediments in two ways. First, shallow lake sediments release more P into the water than deep lake sediments, which retain more P (Hakanson and Jansson, 1983). Second, P tends to absorb to fine-grain sediment, which is found in higher proportions in the deeper areas of the lake. A variable of lake depth may account for the variability of sediment P since it is expected that higher P will be in the old channel rather than shallow floodplains and terrace areas adjacent to it. Juracek (1998) found higher mean P concentrations in bottom sediment cores from the deeper in-channel sites as opposed to out-of-channel sites.

Increasing P concentrations with depth can explain variations at cross-sections, but the positive relationship between depth and P contradict the downstream decay trend because mean lake depth usually increases down-lake, however, studies show that down-

lake decay may not always occur in reservoirs. Juracek (1998) found no up-lake or down-lake relationships with P in sediments in a Kansas reservoir, and Wilson and Van Metre (2000) showed P concentrations in sediments increase going down-lake towards the dam of a reservoir in New Mexico.

Ultimately, the spatial distribution of P in bottom sediments can be used to answer environmental questions concerning eutrophic conditions. By quantifying the spatial distribution of P in sediments the relative influences of inputs from different basins can be compared. Johnson and Nicholls (1989) estimated over 50% of P entering Lake Simcoe from two separate watersheds is deposited in the main lake sediments, while high P in lake outflows suggests P contributions from direct drainage from shoreline sources. Information such as this is useful in directing management efforts, where in the above case shoreline management efforts concentrated on keeping P from entering the lake.

SUMMARY

Water quality in the Ozarks is generally good compared to other areas in the United States. However, the JRA of Table Rock Lake has some of the poorest water quality of reservoirs in the Ozarks. The eutrophic conditions in the JRA have been linked to P inputs to the lake. The Southwest Wastewater Treatment Plant in Springfield has been identified as the main source of P within the James River Basin. Therefore, water quality has economic benefits to tourism and recreation in the region.

Sediment is the transportation vehicle for P in watersheds and is responsible for concentrating it in the aquatic environment. In fact, 95% of P in the aquatic environment is associated with sediments as opposed to dissolved in water. This phenomenon allows sediments to be used as a source monitoring/identification tool for P in lakes and rivers because samples reflect a more consistent representation of local pollution. In contrast, water and biological samples are highly variable and expensive to collect.

Fine-grain sediments and organic matter can absorb and concentrate P at high levels. In a lake environment, chemical and physical processes are responsible for the spatial distribution of P in bottom sediments. Fine-grain sediment and organic matter will accumulate in the deeper areas of the lake where dissolved oxygen is low. At these depths, P is trapped and essentially taken out of the biological cycle.

CHAPTER 3

STUDY AREA

Table Rock Lake is a United States Army Corps of Engineers (USACE) reservoir on the White River in the Ozark Plateaus region of southwest Missouri. Construction of the dam was completed in August 1958, and the lake was built for flood control, hydroelectric power generation, and recreation (USACE, 1985). At the powerpool depth of 915 feet above sea level, the lake covers 167 km^2 of Barry, Stone, and Taney counties in Missouri with some areas of the lake extending into northern Arkansas.

This study focuses on the James River Arm (JRA) of Table Rock Lake and the James River Basin which covers Webster, Greene, Barry, Lawrence, Christian, Stone, and Taney counties in Missouri (Figure 3.1). The JRA flows to the White River from the north and is the largest tributary to Table Rock Lake covering 34 km^2 or 20 % of the total area of the lake surface and contributes approximately 30% of the total inflow to the lake with a mean annual residence time of 147 days (Knowlton and Jones, 1989). This chapter will begin by describing the James River Basin in general terms and then cover the Lower James River Basin with direct drainage into the JRA in more detail.

THE JAMES RIVER BASIN OF THE MISSOURI OZARKS

The James River Basin (3,770 km^2) is located in the Ozark Plateaus region of southwest Missouri. Generally, the town of Galena is considered the point where the James River ends and the James River Arm of Table Rock Lake begins. For the purposes of this study, Upper James Basin will refer to the James River Basin above Galena, and

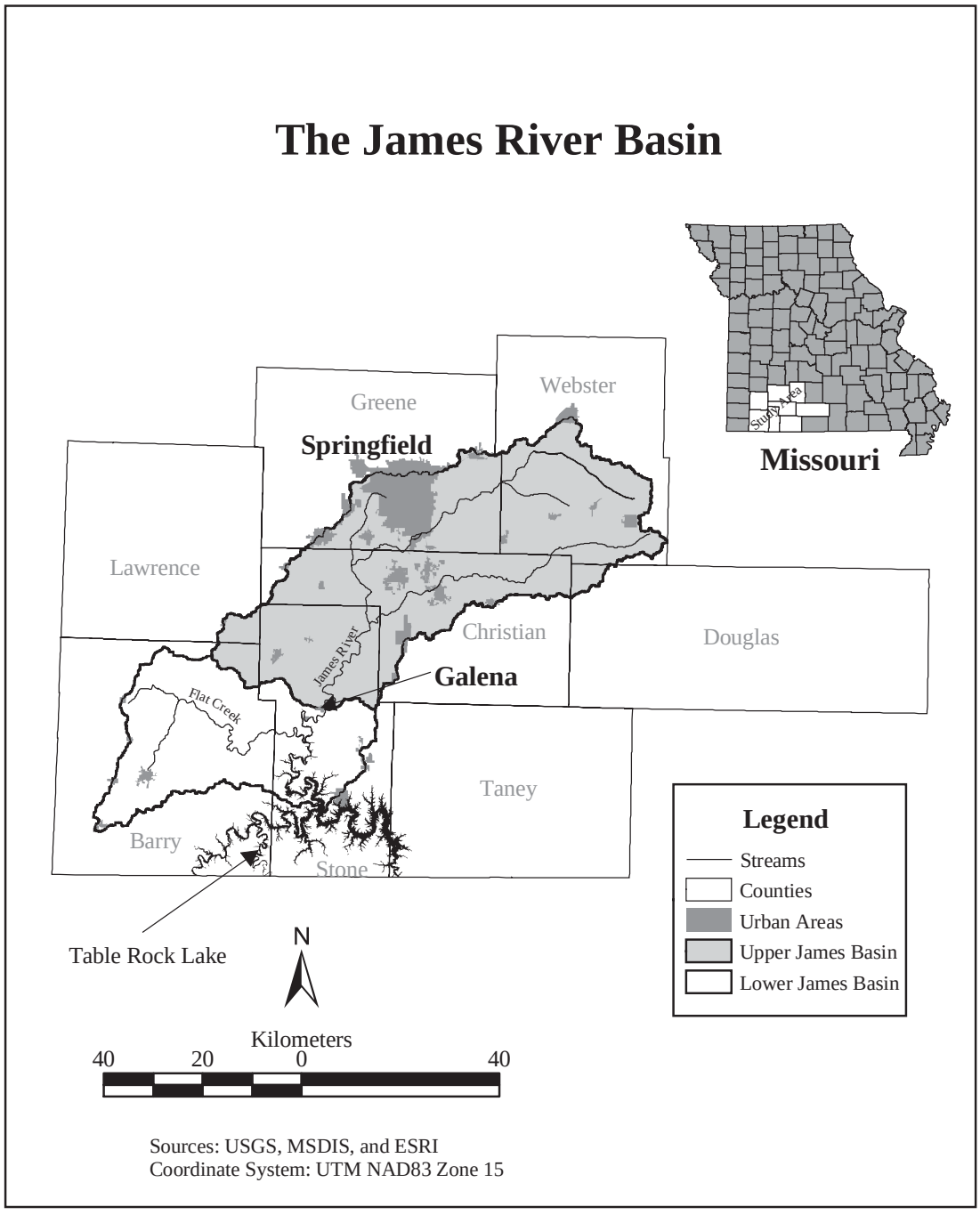

Figure 3.1 Location of the James River Basin

Lower James River Basin will refer to the James River Basin below Galena, including the JRA and Flat Creek.

The James River Basin covers two Ozark Plateaus physiographic regions, including the Springfield Plain and the White River Hills of Missouri and Arkansas (Figure 3.2). Climate for these regions is considered temperate, with an average annual temperature of 15^{o} C and average precipitation of around 105 cm per year (Adamski et al., 1995). Both physiographic regions are underlain by horizontal limestone, dolomite, and shale bedrock (Aldrich and Meinert, 1994). These bedrock units are of differing ages with the White River Hills (Ordivician) being older and more dissected than the Springfield Plain (Mississippian) (Adamski et al, 1995). The karst topography accounts for the numerous springs, losing streams, and sinkholes common in the areas which act as a conduit between surface runoff and groundwater (Petersen et al, 1998). The steepness of the White River Hills is responsible for differences between the two regions in terms of soils, pre-settlement land cover, and historical land-use.

The Springfield Plain

The Springfield Plain extends from southwest Missouri into parts of northwest Arkansas, northeast Oklahoma, and southeast Kansas. Soils are mostly mollisols and alfisols with approximately 20 to 35 cm of loess over cherty limestone residuum and fragipans are typical on uplands approximately 75 to 100 cm below the surface (Hughes, 1982). Prior to European settlement, land cover was mostly prairie with some forested areas where larger waterways carved valleys (Sauer, 1920). This area was first settled in

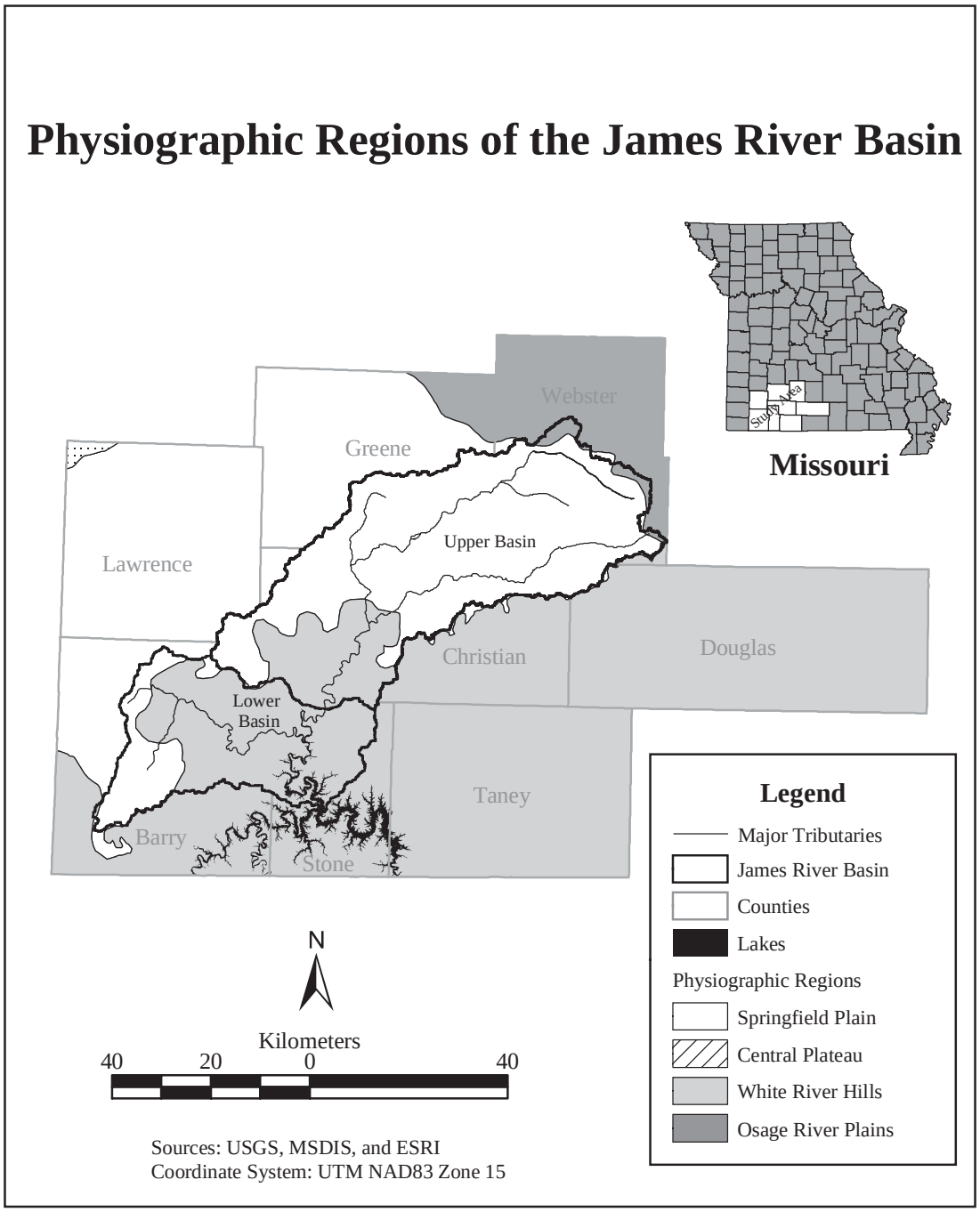

Figure 3.2 Physiographic Regions of the Ozark Plateaus in the James River Basin
(Physiographic regions are based on the work of C.O. Sauer in 1920)

the 1820s but immigration did not expand very rapidly until the railroad arrived in the1870s (Rafferty, 1980). The prairie lands were converted into arguably the finest agricultural area in the Ozarks with heavy production of row crops extending into the 1930s. Today, the Springfield Plain is still a major agricultural area with counties in the region having some of the highest numbers of both dairy and beef cattle within the state (Rafferty, 1980). The city of Springfield is also located here and is the largest metropolitan area in the Ozarks. According to the 2000 Census, the Metropolitan Statistical Area (MSA) had a population over 300,000.

The White River Hills

The White River Hills region of the Ozarks follows the course of the White River through northern Arkansas and southwest Missouri. Upland soils are deep, excessively drained, and gravelly, while soils on the steep hillslopes are shallow, well drained, and gravelly (Aldrich and Meinert, 1994). Forests covered much of the region until the timber boom of the late 1800s when much of the area was logged for railroad ties (Rafferty, 1980). In the early 1900s row crop agriculture was unsuccessfully attempted on the uplands causing major erosion of gravelly soils that eventually made its way to streams, where large gravel waves are still pulsing through larger streams (Jacobson, 1998). Today, this area is dotted by small cattle farms, weekend retreats, and the Mark Twain National Forest. Regions within the James River Basin have important physical and cultural differences. Table 3.1 is a generalized summary of the environmental and cultural setting of these two regions in the study area. These differing regions offer a

Table 3.1. James River Basin Environmental Setting

The Springfield Plain and the White River Hills Physiograpic Regions

Feature	Springfield Plain	White River Hills
Climate	Annual Average Temperature = 15^{o}C Annual Average Precipitation = 105 cm	
Geology (age)	Limestone (Mississipian)	Limestone, Dolomite, and Shale (Ordivicain)
Topography (highest relief)	Rolling Hills (300 ft)	Steep Hills (500ft)
Soils	Mollisols and Alfisols	Alfisols and Ultisols
Pre-settlement land-cover	Prairie	Forest
Major historic land use	Agriculture	Timber Industry

(from Adamski et al, 1995).

challenge in meshing environmental, historical, and cultural characteristics to the needs of everyone living in the watershed.

THE JAMES RIVER ARM AND MAJOR TRIBUTARIES

Since this study is focused on the lower James River Basin and the JRA, a little more detailed look at this area is needed. This section describes in detail the JRA and the tributary coves looked at in this study. The JRA of Table Rock Lake stretches 65 km from Galena to the main lake and holds approximately 15% of Table Rock Lake (Figure 3.4). The JRA is split into three sections: the upper (10-25 km), middle (26-45 km), and lower (46-63 km) sections.

Geology of the area around the JRA is similar for all the tributary watersheds (Figure 3.5). The majority of the area is dolomite, limestone, and shale with small areas of sandstone. The Burlington-Keokuk, Elsey-Reed Springs, and Jefferson City-Cotter formations have major affects on soil conditions (Aldrich and Meinert, 1994). Minor

formations, consisting of shales and sandstones, exist between these major formations. The geography of topography, soils, and vegetation are all a derivative of these geologic formations (Table 3.2).

Major Tributaries

The largest tributary to the JRA is Flat Creek, which has a drainage area of 840 km^2 and has several small communities located there. Land use in the Flat Creek watershed is mostly agricultural. Two other larger tributaries are Aunts Creek and Piney Creek which have much smaller drainage areas of 64 km^2 and 45 km^2 respectively. Aunts Creek, located in the lower JRA, is the most developed watershed but is still mostly forested. Piney Creek watershed is mostly forested and the Piney Creek Wilderness Area takes up most of the drainage area. Consequently, no urban areas and very little agriculture exist within the drainage area. Smaller tributaries including Wooly Creek, Bears Den Creek, Peach Orchard Creek, Jackson Hollow, Cape Fair, and Swift Shoal Creek have drainage areas of less than 20 km^2 and varying land uses. Table 3.3 shows drainage area and land use characteristics for each cove tributary watershed in the JRA. Several other small tributaries exist but were not able to be sampled. Details on sampling are explained in the methods chapter.

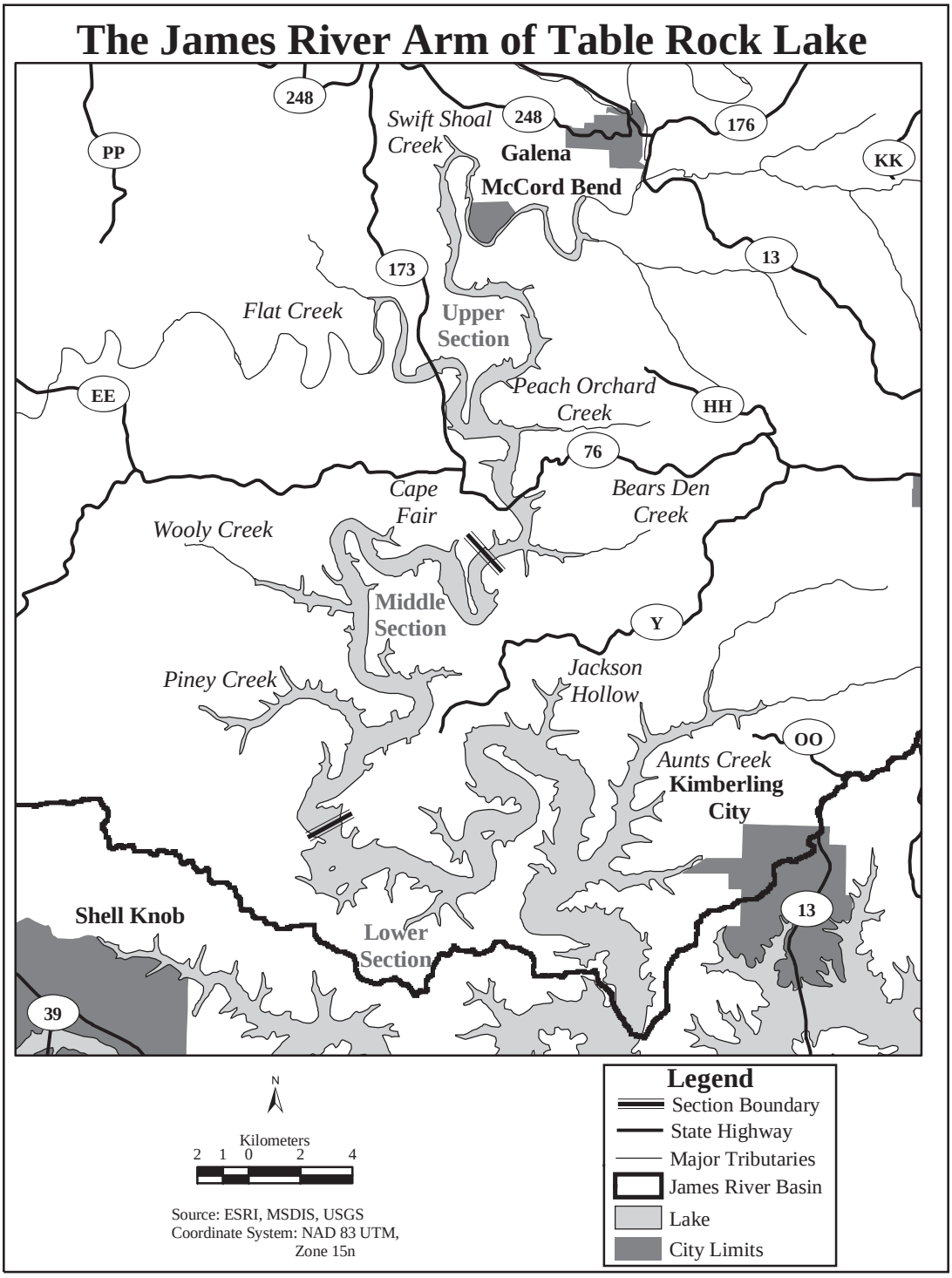

Figure 3.3 General Reference Map of the James River Arm

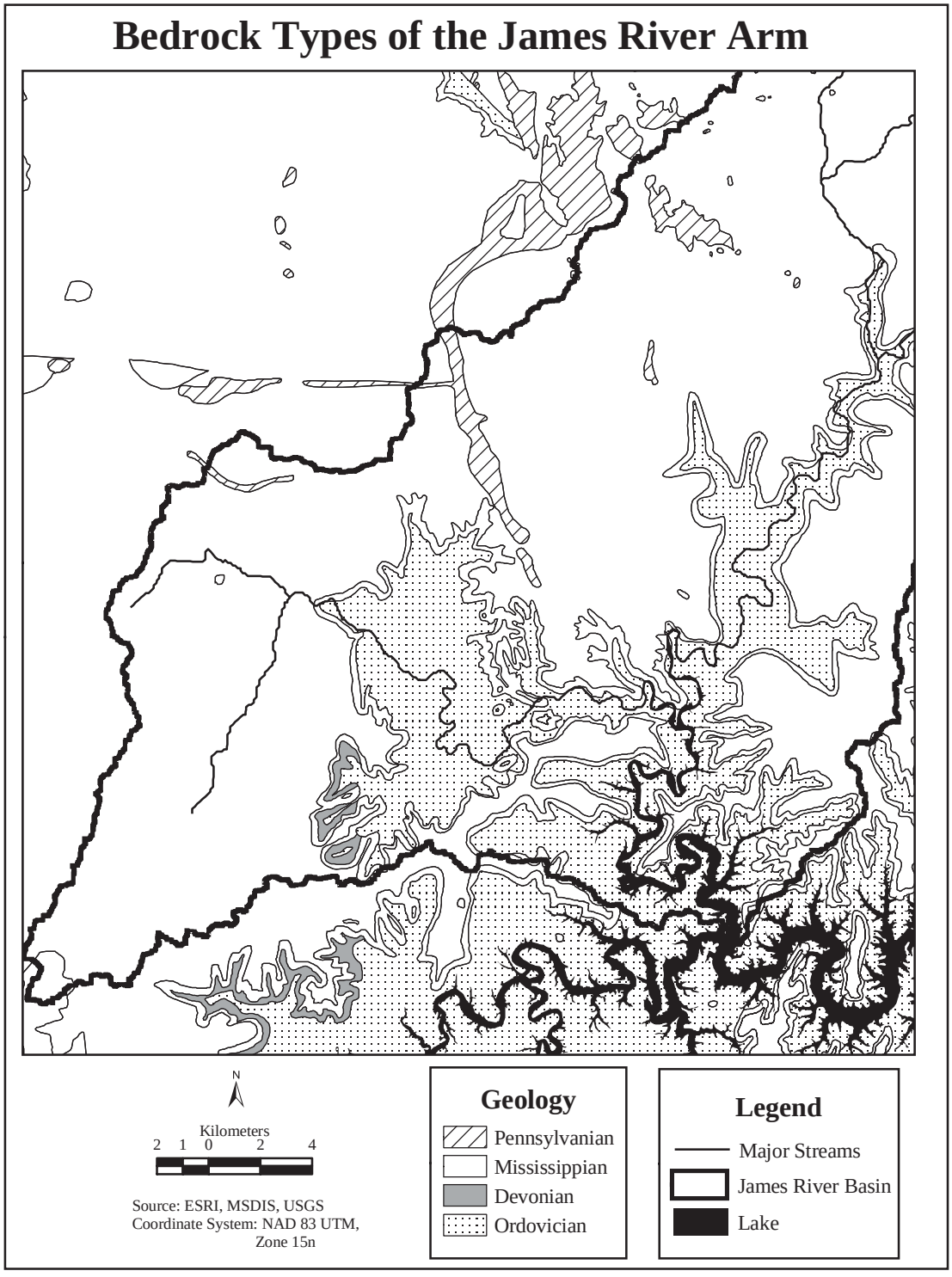

Figure 3.4 Geology of the Lower James River Basin
(See Table 3.2 for a description of the bedrock units)

Table 3.2. Tributary Watershed Bedrock Formations and Soil Characteristics

Age	Formation	Slopes (%)	Soils
Pennsylvanian	Hale Sandstone	2-20	Alfisols Ultisols
Mississippian	Fayetteville Shale		
Mississippian	Batesville Sandstone		
Mississippian	Hindsville Limestone		
Mississippian	Burlington-Keokuk Limestone	1-60	Ultisols
Mississippian	Reed Springs-Elsey Limestone	5-14	Inceptisols Ultisols
Mississippian	Pierson Limestone	2-95	Mollosols Alfisols
Mississippian	Compton Limestone		
Devonian	Chattanooga Shale		
Ordovician	Jefferson City-Cotter Dolomite		

(from Aldrich and Meinert, 1994)

Table 3.3. James River Arm Tributary Watershed Drainage Areas and Land-Use

Watershed	Drainage Arm (km^2)	% Agriculture	% Forest	% Urban
Flat Creek	840	56.5	41.4	1.3
Aunts Creek	64	11.8	79.9	3.3
Piney Creek	45	1.1	95.6	0
Wooly Creek	17	0.1	89.4	7
Bears Den Creek	15	23.4	73	1.8
Peach Orchard	9	41.8	56.4	0.3
Jackson Hollow	4	4.1	88.1	0.1
Cape Fair Cove	3.5	30.6	63.7	1
Shift Shoal Creek	2	19.9	78.9	0.4

CHAPTER 4

METHODOLOGY

Methods for this study included field methods, laboratory methods, GIS data collection techniques, statistical analysis methods, bottom sediment storage estimates, and annual P-budget/sedimentation methods. Field methods included, lake bottom sediment sampling and locating using a Global Positioning Systems (GPS) receiver. Laboratory methods include sediment sample preparation, chemical analysis, grain size analysis, and organic matter content analysis. Spatial data collection techniques include making measurements from historical maps and GIS analysis such as watershed delineation and overlaying-clipping spatial data. Statistical methods included descriptive statistical production and visualization through box-plots, comparative statistical methods using scatter-plots and Pearson correlation, and producing spatial process multivariate regression models. Storage estimates used a bulk density equation based on texture, transect data, and average P concentrations to calculate total P storage in the top 5 cm of bottom sediment, which is in the upper portion of the active layer with the water column (Klump et al, 1997; Reddy et al, 1998). Finally, an annual P-budget was developed from discharge and average water-column P concentrations by section and compared with storage in top 5 cm.

FIELD METHODS

Sediment samples (n=105) were collected off the lake bottom sediment surface using an Ekman spring-loaded grab sampler, which sampled approximately the top 10 cm of sediment. Using a sonar-style depth finder, samples were collected in the old channel

of the JRA at the deepest point of the cross-sectional area. These samples were collected approximately every 1-2 km (1 mile) from Galena to the confluence of the main lake, a distance of approximately 65 km (40 miles). Samples were also collected in the Main Lake above and below the confluence of the JRA and Main Lake. For comparison purposes, grab samples were collected from streams entering the JRA including Piney Creek, Flat Creek, Aunts Creek, and the James River. Stream samples were collected in low energy areas at the tails of gravel bars where fine grain sediment accumulates during seasonal flooding.

Sampling sites are distinguished by geographic area and are classified based on the location and method of sampling. The "S" and "JR" classifications represent grab samples collected at tails of gravel bars in tributary streams (S) and the James River (JR) above the last riffle of the James River. The "AS" and "AD" classifications represent samples collected in the main stem of the JRA in the deepest portion of the old channel and from shallower areas on the submerged valley floor of the channel at several cross-sectional locations. These samples are separated at the 12-meter mark classified as arm shallow (AS) and arm deep (AD) samples. The "C" classification is for samples collected in the tributary coves of the JRA. Finally, the "WU" and "WD" classifications represent samples taken in the main lake of Table Rock upstream (WU) and downstream (WD) of the confluence with the JRA. Table 4.1 shows the distribution of samples to their geographic classification and Figure 4.1 is a map displaying sampling sites by their geographic classification.

Table 4.1 Summary of Sediment Sampling Geographic Classifications

Classification	n	ID	Sampling Technique
Stream	7	S	tail of gravel bars above lake
James River	6	JR	tail of gravel bars above lake
Cove	38	C	channel and valley floor
Arm Shallow	38	AS	<12 meters channel and valley floor
Arm Deep	37	AD	>12 meters channel and valley floor
Main Lake upstream of JRA	3	MU	channel
Main Lake downstream of JRA	3	MD	channel

The 12-meter mark represents the upper limit of potentially anoxic conditions and was chosen due to field experiences and is backed up by published lake stratification data. In the field, a very evident change in sediment color and temperature was recorded for samples taken below 12 meters in depth. Locally, it is widely known the thermocline is around the 40-50 foot (12-15 meters) range where summer time fishing is at its best. United States Army Corps of Engineers (1985) data shows the average depth of the thermacline for the entire lake is near 15 meters.

Each sediment sample was placed into a plastic bag and labeled. At each sampling point, an accurate location was recorded using a Garmin 12x GPS receiver. In addition, water depth was recorded off the depth finder reading in feet and eventually converted to meters. Triplicate samples were taken at a channel and a valley floor site along several transects to account for sampling variability. Appendix A show UTM coordinates, depth, distance from Galena or tributary stream, and valley width of each sample site.

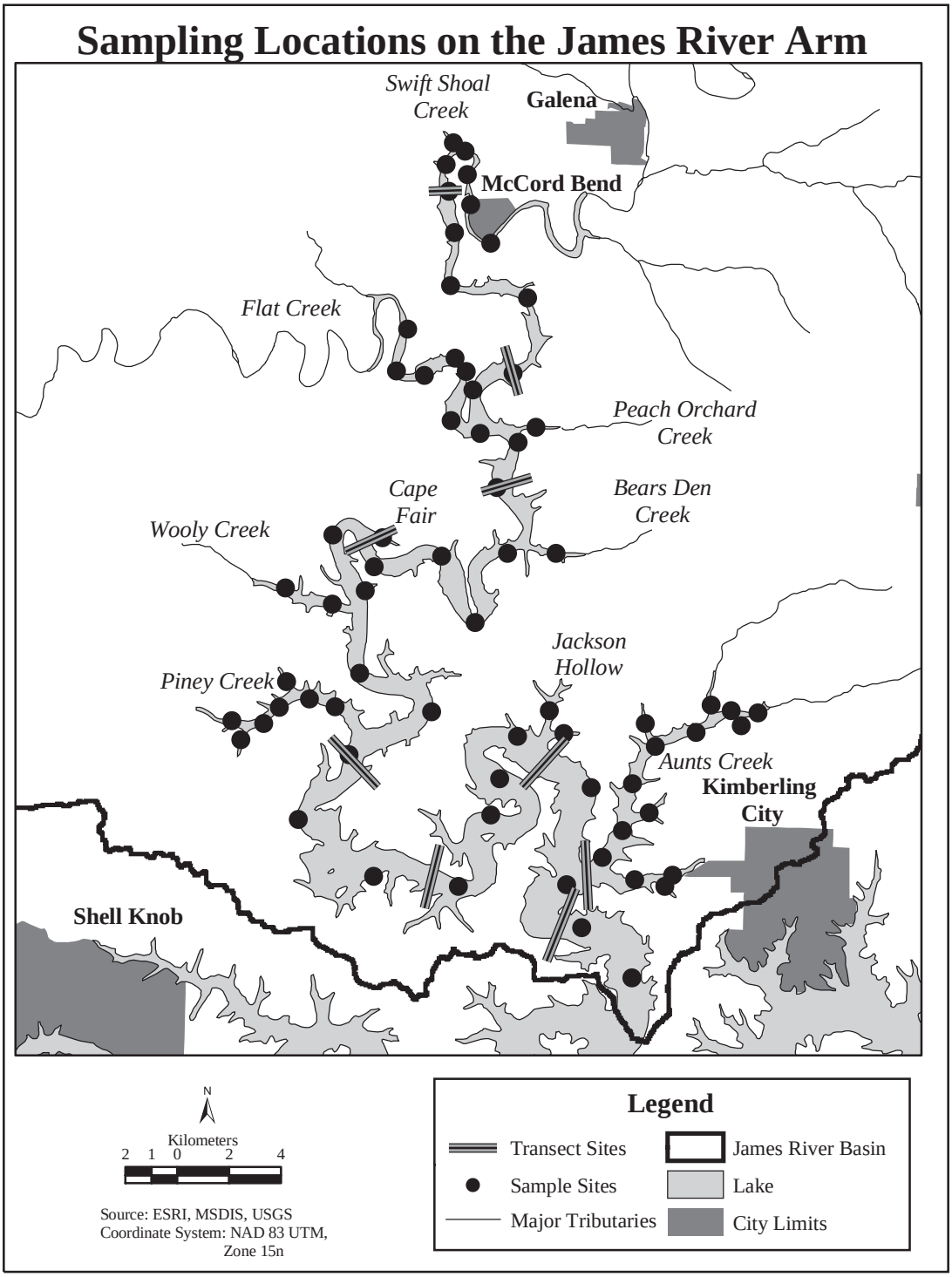

Figure 4.1 Channel and Transect Bottom Sediment Sampling Locations

LABORATORY METHODS

Sample Prep and Chemical Analysis

Sediment samples were dried in a 60 ^{0}C oven for 3-7 days until completely dry. After they were dry, they were disaggregated using mortor and pestle and passed through a 2 mm sieve. Sediment samples were sent to Chemex Labs for ICP chemical analysis. Using a 3:1 Hydrochloric:Nitric Acid extraction method, a total P concentration was derived from the sediment in parts per million (ug/g). In addition, 31 other elements were analyzed including Al, Ca, Fe, and Mn. Appendix B displays the concentrations of P, aluminum (Al), calcium (Ca), Fe, and Mn and metals copper (Cu), mercury (Hg), lead (Pb), and zinc (Zn) at each site. Several sediment samples distributed throughout the JRA were analyzed three times for P to see variability within a sample to test the reliability of the chemical analysis. Appendix D shows triplicate analysis data that assessed sample variability with the chemical analysis method used for this study.

Grain Size Analysis

Textural analysis of sediment samples was assessed in the Geomorphology Laboratory at SMSU using standard methods (Pavlowsky, 1995). Textural analysis was performed using the hydrometer method measuring the percentage of sand, silt, and clay. For each sample, approximately 40 grams of sediment was weighed out for analysis.

Organic matter was removed from the sample by digestion in 1% acetate acid and 30% H_2O_2 for 8 hours. Then, the sample was heated to 90 ^{o}C for 1 hour to make sure the reaction was complete. If the liquid was clear, the sample went to the next step. If the liquid was still dark, the digestion processes was repeated until the liquid was clear. The

supernatant liquid was decanted and the samples were placed into a 110 ^{o}C oven to dry and the post digestion weight was recorded.

The dry samples were mixed with 125 ml of 10% sodium-hexametaphosphate in a blender for 10 minutes to disperse clay particles. After blending, samples were loaded into 1-liter cylinders and topped off with distilled water. The samples were allowed to sit overnight to come into equilibrium with the lab's temperature and humidity.

Samples were then suspended in the cylinders and a standard soil hydrometer was used to record specific gravity of the solution for the 63 *um*, 32 *um*, 16 *um*, 8 *um*, 4 *um*, and 2 *um* size fractions. Before and after each set of readings, temperature and a reading was recorded for a "blank" cylinder, with no sediment, to account for temperature and humidity changes between sets of readings. After the last reading, the samples were wet sieved for sand and dried for validation of the 63 *um* reading. Appendix B shows hydrometer procedure data for each sample, and Appendix D shows grain-size triplicate analysis data that assessed sample variability with the grain-size analysis method used for this study.

Organic Matter Analysis

Organic matter analysis of sediment samples was assessed in the Geomorphology Laboratory at SMSU using standard methods (Pavlowsky, 1995). Organic matter content was measured using the loss on ignition (LOI) technique. This procedure is commonly used to analyze organic matter content in sediments. Samples were dried in a 105 ^{o}C oven for 2 hours to remove moisture. A 5-gram sample was placed in a porcelain crucible and the pre-burn weight was recorded. These samples were placed in a 600 ^{0}C muffle furnace for 6 hours to incinerate the organic matter in the sediment. After 6 hours

the samples were re-weighed and the difference was recorded. The difference was used to calculate organic matter content in percentage by weight. Appendix B shows organic matter analysis data.

SPATIAL ANALYSIS METHODS

Spatial data for this study was collected three ways. First, depth measurements were conducted in the field using a sonar type depth finder as described in the field collection methods portion of this section. Second, a 1947 United States Army Corps of Engineers topographic map for this portion of the White and James rivers was used to take valley width measurements at the 915 ft elevation for each sample site. Finally, distance measurements were collected from the mouth of the James River and tributaries to coves. A watershed data was collected above sampling locations in coves. This section describes these data collection methods used for this study in more detail.

Elevation Data and Watershed Delineation

For the tributary watershed analysis portion of this study, watershed delineation is extremely important to be able to use drainage area characteristics in explaining the distribution of pollutants in lake sediments. In order to delineate above each sample location, elevation data and bathymetric data were merged to make this process possible. The final product was a seamless DEM that included both the upland and lake bottom elevations.

Elevation data merge. Digital elevation models (DEMs) of the area around the JRA and the watershed above the lake were obtained from the Missouri Spatial Data Information Service (MSDIS) at the University of Missouri. MSDIS has merged 30-meter USGS DEMs and have them available for each county in the state. These county

DEMs were downloaded, unzipped, and converted from ArcInfo interchange files (.e00) to grids. The county DEMs do not have elevation values below the lake surface level at 915 feet. The lake bottom elevation data came from a bathymetric triangulated irregular network (TIN) obtained from the USGS Mid-Continent Mapping Center in Rolla, Missouri.

The first step in this process was to mosaic the county DEM together into one large DEM. All elevation data in the DEM was standardized as integer data. Once the elevation data was integer, all elevation data $\geq$ 915 feet were converted to "no data". The bathymetric TIN was converted into a 30–meter grid.

The next step involved overlaying the county DEM data with the TIN derived grid of the lake. This process created a new DEM with the lake elevation data replacing the "no data" in the county DEMs. This created a seamless DEM of the lake bottom and the upland areas of the watershed.

Delineation and clipping. Using the county boundary vector data as an overlay, the overall DEM was clipped. This process removed the dam elevation located in Taney County creating an uninterrupted terrain and a pour point so the sinks in the DEM could be filled for watershed delineation. Watershed delineation involves filling sinks, calculating flow direction and calculating flow accumulation. The James River Basin was delineated from the point it entered the main lake. The James River Basin was then clipped from the overall DEM. This created a DEM of the entire James River Basin from the point it enters the main lake.

GIS Watershed Analysis

This section describes the methods used to assess watershed characteristics of the cove tributary watersheds. One of the biggest challenges for sediment and water research is linking the terrestrial environment with the aquatic environment. This study uses a Geographic Information System (GIS) to analyze watershed characteristics above sampling locations to attempt to make this terrestrial-aquatic connection. Watershed assessment methods include land use analysis, road density analysis, and dock density analysis using a GIS.

Land use analysis. Land use for drainage areas was derived from National Land Cover Data (NLCD) produced by the USGS and revised in July of 2000. These data were created from a collection of satellite data from the late 1980s and early 1990s from different times of the year during "leaf on" and "leaf off" conditions. These data are classified using the standard Anderson Level One classification system (Anderson et al, 1976). For the purposes of this study, this classification system was generalized into urban, agriculture, forest, and water classifications (Table 4.2). These data were clipped using the drainage area polygons for all of the cove samples. The number of pixels in each category were summed and divided by the total number of pixels to give a percentage of each land use for that drainage area.

Road density analysis. Road density was calculated to have a more detailed look at development for each cove's tributary watershed. Since the land use data used for the analysis was created back in the early 1990s, a better development assessment approach was desired to account for that shortcoming in the dataset. Road density was calculated by using a 1998 Missouri Department of Transportation road coverage downloaded from MSDIS by county, and the drainage basins that were delineated above each cove sample

site. The road network for the counties was merged and then clipped using the drainage area. A total length of roads (L_R km) was determined for each basin and divided by drainage area (A_D km^2) to give a road density (D_R).

Dock density analysis. In order to account for the density of local shoreline development, a dock density variable for each cove sample site was developed. A private dock point file was obtained from the United States Army Corps of Engineers at Table Rock Lake. This file contained the location of every private dock on the lake. For each cove sample site the drainage area was used to select and calculate the number of docks (D) located within that area. This number was then divided by the drainage area (A_D km^2) and lake surface area (A_L km^2) within the drainage area to give docks per drainage area ratio (DA_D) and docks per lake area ratio (DA_L).

STATISTICAL ANALYSIS TECHNIQUES

Statistical analysis for this study involves descriptive statistics, comparative statistics, and multivariate spatial process regression modeling. Descriptive statistics for sediment composition and geochemical data is displayed using box-plots and charts

Table 4.2 Land-Use Generalizations From National Land Cover Data (NLCD)

NLCD #	Description	New Classification
11	Open Water	Water
12	Perennial Ice /Snow	
91	Woody Wetlands	
92	Emergent Herbaceous Wetlands	
21	Low Intensity Residential	Urban
22	High Intensity Residential	
23	Commercial/Industrial/Transportation	
31	Bare Rock/Sand/Clay	
32	Quarries/Strip Mines/Gravel Pits	
33	Transitional	
85	Urban/Recreational Grasses	
41	Deciduous Forest	Forest
42	Evergreen Forest	
43	Mixed Forest	
51	Shrubland	
61	Orchards/Vineyards/other	Agriculture
71	Grasslands/Herbaceous	
81	Pasture/Hay	
82	Row Crops	
83	Small Grains	
84	Fallow	

showing the variability and spatial distribution of these variables. Comparative statistics uses a Pearson Correlation matrix and simple regression to isolate correlated variables to understand geochemical and spatial relationships between variables. This was performed in SPSS statistical software. Finally, stepwise linear regression models are used to explain the spatial trends of sediments and constituents attached to them. This was also performed in SPSS statistical software using a 0.05 significance level for the variables.

PHOSPHORUS STORAGE AND ANNUAL BUDGET TECHNQUIES

Sediment-P Storage

Sediment-P storage was estimated for the main valley of the JRA by using the bottom sediment volume, an average bulk density of the sediment, and a mean P concentration from the samples collected. The specific steps used to gather this information are described below.

Sediment volume. Sediment volume was estimated using data gathered during grab sediment sampling. The sediment cross-sectional area (CSA) for each transect site was calculated and plotted versus distance from Galena. The average width of fine-grain sediment at each transect site was calculated for the upper, middle, and lower sections of the main valley. A sediment depth of 5 cm was used because this is the layer that comes into contact with the overlying waters and represents a portion of the probable P pool available for remobilization into the water column (Klump et al, 1997; Reddy et al, 1998). Sediment volume was calculated in this manner:

$$Volume\ (m^3) = SW \times SL \times SD$$

Where *SW* is the average sediment width (m) sediment length *SL* (m) and *SD* is sediment depth (m).

Sediment mass. To estimate the mass of the top 5 cm of bottom sediment, a reservoir sediment bulk density equation based on particle size and a time after deposition, estimated at ten years, was used (Petersen, 1986).

$$Wt = Wi + 0.43K \left[\frac{T}{T\text{-}1} (\log_e T) - 1 \right]$$

In the equation, *Wt* is the bulk density for given average deposits in *T* years in Mg/m^3, *Wi* is the initial unit mass weighted on the basis of particle-size gradation in Mg/m^3 , *K* is a constant weighted on the basis of particle-size gradation in Mg/m^3 , and *T* is time after deposition in years. This equation was used for all JRA main valley sediments, and averaged based on upper, middle, and lower sections described above. Sediment mass was then calculated:

$$Sediment\ Mass\ (Mg) = Bulk\ Density\ (Mg/m^3) \times Volume\ (m^3)$$

Sediment P-mass. Average P concentrations for the upper, middle, and lower sections of the main valley were taken from all sediment samples in those respective areas. Total P-mass for recent sediments for each section of the main valley of the JRA was then calculated:

Sediment P-Mass (Mg) = Sediment Mass (Mg) x [P (g/Mg) / 1,000,000 (g/Mg)]

Water column-P mass

Water column-P was calculated by first estimating the water volume of the main valley of the JRA and taking the average P concentration of each geographic section to yield a total water column-P concentration for each section. The specific steps for this process are outlined here.

Main valley volume. Volume was calculated by estimating the cross-sectional area (CSA)(m^2) from an average depth reading gathered at transect sites during sampling and width measurements coming from the USACE 1945 pre-dam map used previously. The CSA for each transect was plotted versus distance from Galena. A best-fit curve was used to find the average CSA at ten equally spaced locations for the upper, middle and lower sections of the main valley of JRA.

Water column-P concentration. Water column-P concentrations are from USGS depth integrated total-P concentration data from 1984-1995 at two locations along the JRA and a mean P concentration at Galena from 1993 to 2001 (Fredrick, 1999; Pavlowsky, 2001; USGS, 2003). Average concentrations at these sites were plotted against distance from Galena and a best-fit curve was used to calculate concentrations at ten equally spaced locations for the upper, middle and lower sections and a mean concentration was obtained for each section.

Total Water Column-P Mass (Mg) = Volume (m^3) x [P (mg/m^3)/ 1,000,000,000 (mg/m^3)]

Annual Budget Calculations

Annual loading was calculated for the James River at Galena, each section of the main valley of the JRA, and the major cove tributary watersheds entering the JRA. The mean water column-P concentration method explained above was used for each section of the main valley. Mean P concentrations at the USGS gaging station at Galena (07052500) were used to estimate loading to the JRA. Flow estimates for each watershed were based on a regional regression equation. Annual load for each section was determined. The annual P budget was completed by estimating annual storage and P accumulation rates. The specific steps used to gather this information is described here.

Water column-P concentrations. Phosphorus concentrations for each section of the main valley were estimated using the water column-P regression equation described above. For the tributary coves, a water-column P concentration of 16 ug/L was used, which is an average based on work by Knowlton and Jones (1989) for small tributary coves around the entire lake. Phosphorus inputs to the JRA were based on mean concentrations at the USGS gaging station at Galena prior to treatment plant upgrades at Springfield explained above.

Flow estimates. Flow estimates were estimated using a regional linear regression equation for drainage area versus mean discharge for the White River and the Arkansas River based on data collected at 24 USGS stations the southern Missouri Ozarks (Pavlowsky, 2002).

Mean Q (cfs) = 1.05 Ad ($miles^2$)

Drainage areas for the James River at Galena, the tributary coves, and the three sections along the main valley were calculated using the GIS methods described above.

Annual load. Using the discharge estimates for the James River at Galena, the tributary coves, and the upper, middle, and lower sections of the main valley of the JRA with average water-column P concentrations, an annual loading for each area was calculated using the equations below.

Annual Load (Mg/yr) = Q (m^3/s) x C (mg/l) x 31.536 (constant)

In this equation, *Q* is the mean annual discharge and *C* is the mean water column-P concentration. The constant is derived as the product of 31,536,000 seconds per year times 0.000001 Mg/mg.

Annual P storage and trap efficiency. The annual loads for each section of the main valley were used to estimate annual storage and export. Annual P budget for the main valley of the JRA and trap efficiency of the JRA were calculated using the annual storage estimates in the calculations detailed below (units = Mg):

Upper Section Storage $= (L_G + L_{UC}) - L_U$

Middle Section Storage $= (L_U + L_{MC}) - L_M$

Lower Section Storage $= (L_M + L_{LC}) - L_L$

Trap Efficiency $= (L_G + L_{UC} + L_{MC} + L_{LC}) - L_L / L_G)*100$

Where L_G is the load at Galena, L_U is the upper section load, L_M is the middle section load, L_L is the lower section load, L_{UC} is the upper section cove load, L_{MC} is the middle section cove load, and L_{LC} is the lower section cove load. The annual P storage was used to estimate sedimentation rates in each section of the JRA.

$$\textit{Sedimentation Rate (cm/year)} = \frac{\textit{P deposition rate (Mg / yr)}}{\textit{Stored P in top layer (Mg / 5 cm)}}$$

CHAPTER 5

RESULTS AND DISCUSSION

The results and discussion chapter of this study is described in four sections. The first section describes the physical and chemical properties of the JRA bottom sediments. The second section displays down-lake patterns of bottom sediment P in the arm for channel and transects and compares these trends to cove samples. The third section shows results of multivariate regression analysis to quantify and evaluate the spatial distribution of P concentrations in the JRA and estimates an enrichment ratio based on those models. The final section estimates P storage in bottom sediments of the JRA and relates P storage to an annual P budget for the JRA.

PHOSPHORUS CONCENTRATIONS AND SEDIMENT PROPERTIES

This section generally describes the distribution of sediment P concentrations in the JRA with descriptive statistics. Box-plots are used to evaluate concentration trends by geographic location. The physical and chemical properties of bottom sediments in the JRA are evaluated in the same way.

Sediment-P and Geochemistry

The spatial distribution of P in the JRA can be visualized using a map showing the location of each sampling site and the concentration of P in bottom sediments of each site (Figure 5.1). Generally, sediment-P concentration increases down-lake from Galena where the James River loads enter the JRA and tend to be lower in the tributary coves than in adjacent main arm locations. However, due to the meandering pattern of the JRA, changing lake depth, the variations in sediment composition and cove contributions make this map difficult to analyze. To resolve this problem, P concentrations are broken down

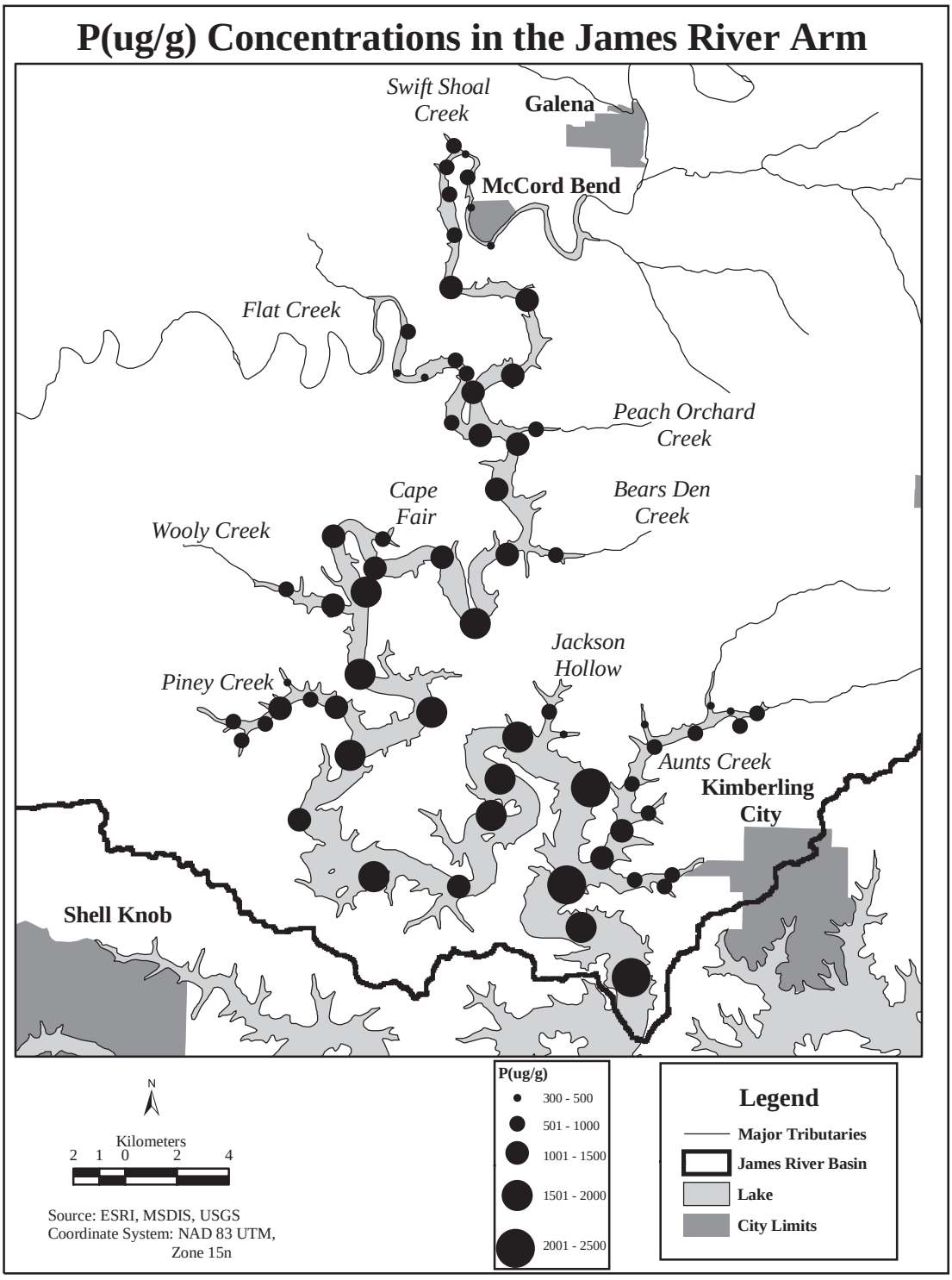

Figure 5.1. Phosphorus concentrations (ug/g) at Sampling Locations

by geographic area and depth and are compared using a box-plot with P concentrations stratified according to geography and sedimentation characteristics (Table 5.1, Figure 5.2). This format is also used to display other physical and chemical characteristics of bottom sediment in the JRA.

Phosphorus. Phosphorus concentrations in all JRA bottom sediments have a mean of 969 ug/g and a range from 5 ug/g to 2,520 ug/g. The variability of sediment-P concentrations in lake sediments decrease with depth as CV% ranges from 65% in shallow sediments to 20% in deep sediments. The CV% for tributary coves, which represent shallow and deep areas, fall between CV% in the main valley at 40%. The higher CV% for shallow samples suggests the influence of mixing and more variable sedimentation conditions in the shallower areas.

Comparison of P concentrations in tributary streams with cove sediments shows an increase of P from stream sediments as they empty into the lake cove environment (Figure 5.2). This is also true for P concentrations from the James River to the JRA as they increase with depth in the main valley. Also, P sediment concentrations are slightly higher in the White River below the confluence with the JRA than above indicating an approximate 25% increase from the JRA.

Cove sediment-P concentrations are similar between coves and do not change measurably down-arm. Table 5.2 shows descriptive statistics for sediment P concentrations for each cove. Mean P concentrations in cove range from 585 ug/g to 1000 ug/g, and CV% values are fairly consistent ranging from 38% to 49%.

Table 5.1. Descriptive Statistics for Sediment P ug/g by geographic area

Location	n	mean	median	min	max	sd	cv%
Streams (S)	7	361	390	220	460	87	24
Cove (C)	38	758	705	300	1670	305	40
James River (JR)	6	392	310	210	850	231	59
Arm Shallow (AS)	38	625	535	5	1480	404	65
Arm Deep (AD)	37	1559	1570	600	2520	429	20
White River Down (WD)	3	2377	2377	2210	2460	144	6
White River Lake Up (WU)	3	1890	1890	1720	2090	87	5
All Lake Bottom Samples	119	1034	900	5	2520	606	59

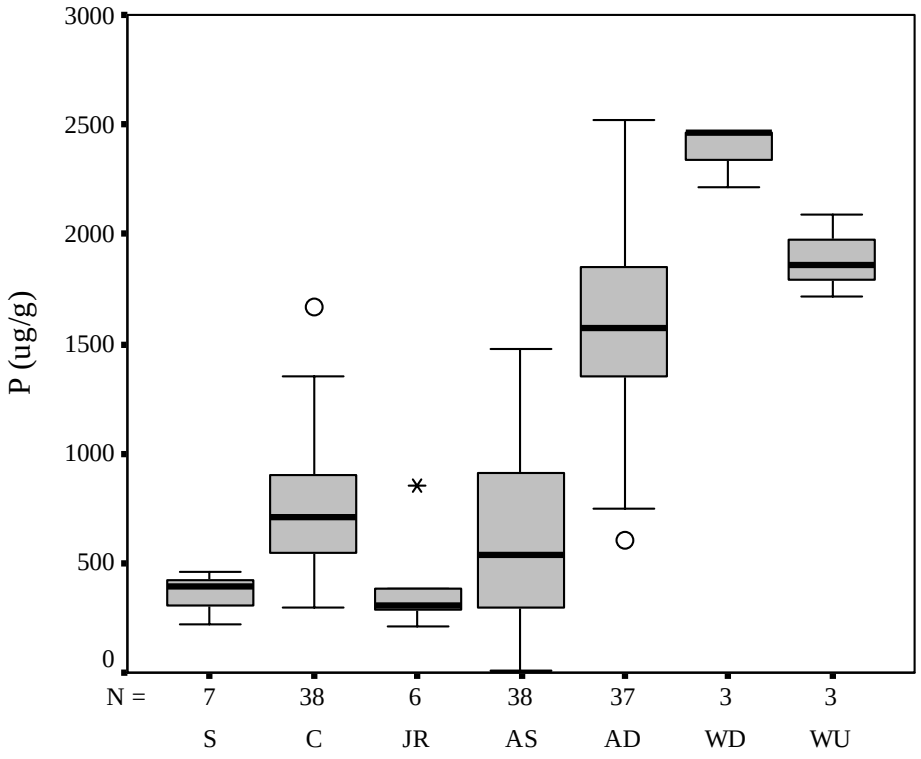

Note: middle value is median value, O = outlier value, and * = extreme value.

Figure 5.2. Sediment-P concentrations by geographic area
(Data grouped by cove tributary streams (S), tributary coves (C) the James River above Galena (JR), the JRA main valley shallow (AS), deep (AD), and the White River down-lake (WD) and up-lake (WU) of the JRA.)

Table 5.2. Descriptive Statistics for sediment P ug/g for coves
Names of coves appear in the order they enter the JRA

Location	n	mean	median	min	max	sd	cv%
Swift	1	890	-	-	-	-	-
Flat	6	585	625	300	810	223	38
Peach	1	710	-	-	-	-	-
Bear	1	870	-	-	-	-	-
Cape	1	710	-	-	-	-	-
Wooly	2	1000	1000	650	1350	495	49
Piney	7	740	630	490	1270	293	40
Jackson	2	745	745	500	990	346	47
Aunts	17	792	720	400	1670	351	44

Aluminum. The distribution of aluminum (Al) in the JRA bottom sediments mirrors P (Figure 5.3). Concentrations increase coming from streams and the James River as sediments enter the JRA. Cove concentrations fall between the deep and shallow samples in the main valley. Concentrations of Al will have a positive relationship with clay, indicating sorting and fining of sediment down-arm (Aslan and Autin, 1998). Also, the JRA appears to be adding additional clay-size particles to the White River due to the increase of Al in samples located down-lake of the JRA compared to those samples up-lake. Again, Al concentrations tend to increase in clayey sediments so a positive relationship with clay% would be expected.

Calcium. Calcium (Ca) concentrations are distributed much the same way as Al and P in the main valley but are much lower in the White River samples (Figure 5.4). While this distribution is perhaps the hardest to explain, data suggests Ca is related to clay particles. Soils in this area are derived from limestone, dolomite, and shale residuum, which are high in Ca. Concentrations of Ca that correlate with Al would suggest Ca is entering the JRA from the erosion and deposition of soil particles from the drainage area. Distribution and sources of Ca is important to this study because of the relationship between P and Ca in sediments. Phosphorus can be related to Ca naturally in

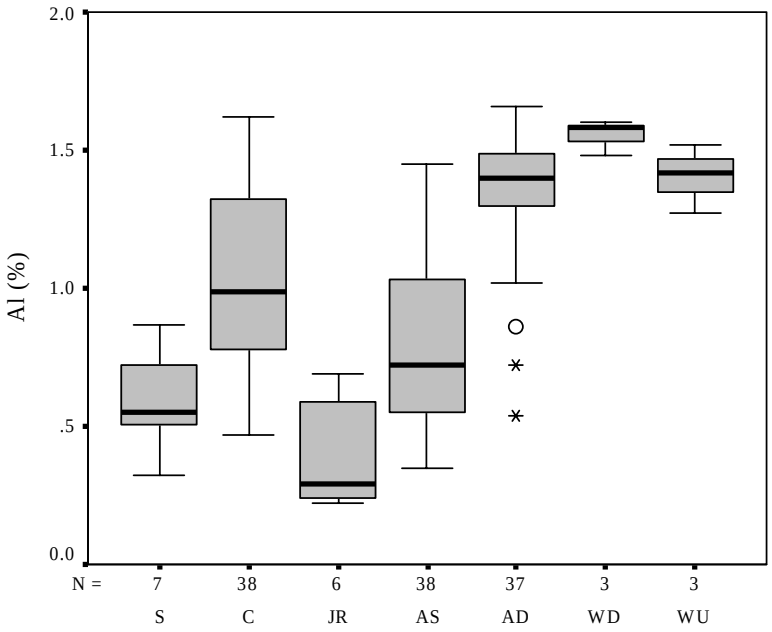

Note: middle value is median value, O = outlier value, and * = extreme value.

Figure 5.3. Distribution of Al by geographic area

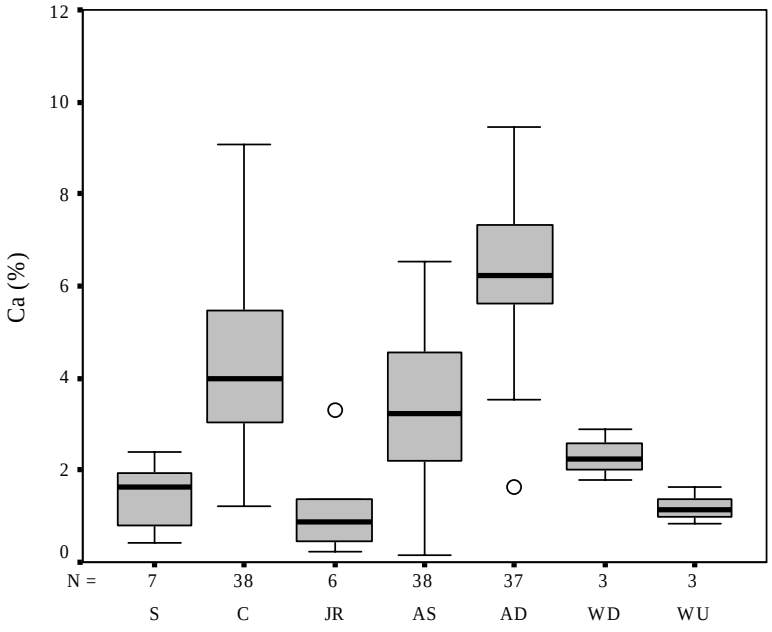

Note: middle value is median value, O = outlier value, and * = extreme value.

Figure 5.4. Distribution of Ca by geographic area

the mineral Apatite ($Ca_{10}(PO_4)_6(OH)_2$), and co-precipitated with calcium carbonate ($CaCO_3$) in limestone and through evaporation at the lake surface. Knowlton and Jones (1989) suggest that during low flow when the majority of P entering the JRA is in the dissolved form, the majority P sedimentation is due to organic matter accumulation and the precipitation of calcite. Another possible source of Ca could be from shell fragments of mollusks and plankton that have settled to the lake bottom.

Iron. Iron (Fe) distribution in bottom sediments is different from Al, Ca, and P (Figure 5.5). Concentrations of Fe decrease from the streams and James River to the coves and to the shallow areas of the main valley of the JRA. However, Fe increases again in the deep main valley sediments. This distribution can be explained by understanding the physical and chemical mobility of Fe in sediments. As with Al and Ca, Fe concentrations should increase with clay in sediments. In this case, this relationship is not seen due to lake chemistry. In the presence of oxygen, Fe changes to its oxidized form, which is very insoluble and has the ability to absorb or coprecipitate pollutants, however, in the absence of oxygen Fe changes to its reduced form and becomes soluble (Hakanson and Jansson, 1983). In the coves and shallow main valley where sediments have lower amounts of clay, lower amounts of Fe oxides are expected (Horowitz, 1991). In deep sediments, where the redox boundary is in the water column, reduced conditions and low dissolved oxygen move pore water Fe to the top layer of sediment where it can become concentrated (Davison, 1985). In the White River, Fe concentrations dilute the sediments below the JRA compared to Fe concentrations above the JRA. Again, Fe accumulation in bottom sediments is due to limited physical mobility in the deeper portions of the White River.

Manganese. Spatial patterns of manganese (Mn) in the JRA bottom sediments are very similar to Fe concentrations (Figure 5.6). Like Fe, Mn will form oxide coatings on sediment which absorb P and other pollutants (Horowitz, 1991). In a similar manner as Fe, Mn oxidation state phase changes also occur due to seasonal dissolved oxygen fluctuations.

Sediment Composition

The distribution of sand as a percentage of bulk sediment by weight indicates the overall sedimentation patterns of the JRA (Figure 5.7). Sand percentage decreases drastically from the tributary streams and the James River flowing to the coves and main valley. When fluvial inputs enter the lake system, flow velocities decrease and coarser material is deposited. Sediments thus fine longitudinally away from the mouth, with sediment focusing also concentrating finer material in the deepest part of the channel (Morris and Fan, 1998). The coarsest sediment in the JRA is found in the shallower areas in the upper portion of the main valley and along the shoreline. Very little sand is found in the deeper areas of the main valley. The higher sand content in deeper sediments is probably due to proximity of deep areas to bluffs, which supply sand by surface wash and erosion of steep slopes and exposed rock outcrops. An example is at the Virgin Bluff, which is the nearly 360^{o} bend in the lake between Bears Den and Cape Fair coves. Main lake sand percentage is not different above and below the JRA.

Distribution of silt also reflects sedimentation patterns (Figure 5.8). Silt as a percentage of sediment composition increases from the tributary streams and the James River to the coves and shallow areas of the main valley. Then, silt percentage drops back down in the deep areas of the main valley as clay increases in the deepest portion of the

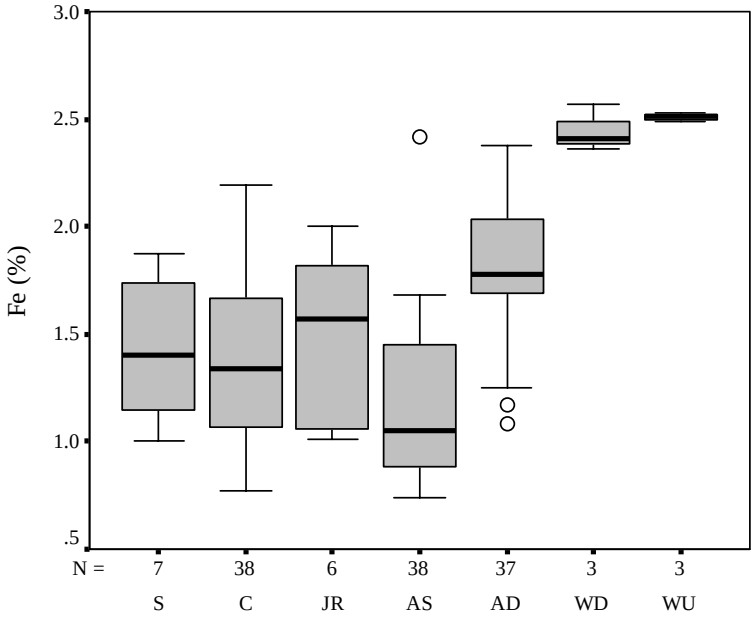

Note: middle value is median value, O = outlier value, and * = extreme value.

Figure 5.5. Distribution of Fe by geographic area

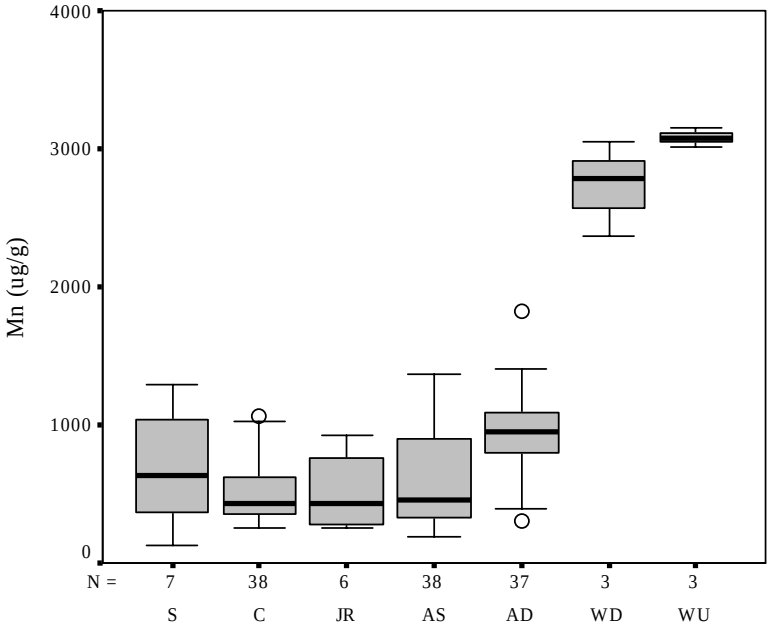

Note: middle value is median value, O = outlier value, and * = extreme value.

Figure 5.6. Distribution of Mn by geographic area

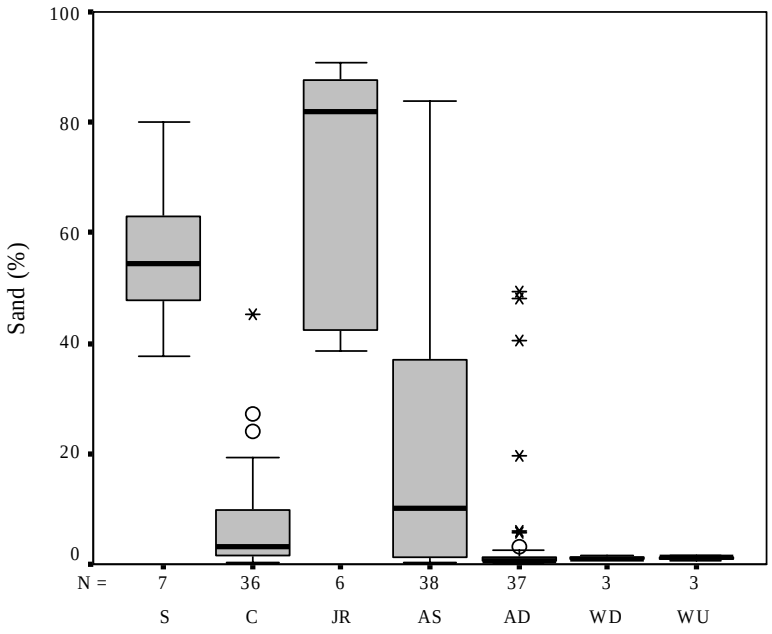

Note: middle value is median value, O = outlier value, and * = extreme value.

Figure 5.7. Distribution of sand by geographic area

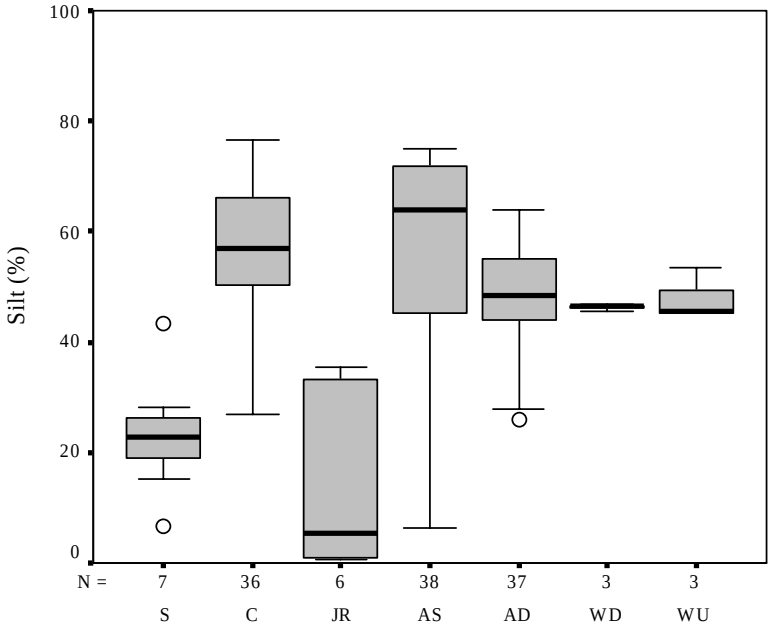

Note: middle value is median value, O = outlier value, and * = extreme value.

Figure 5.8. Distribution of silt by geographic area

lake. This trend shows an accumulation of silt-sized material in the shallow areas of the main valley and coves. As with sand, silt does not change in the White River above and below the JRA.

Just like sand and silt trends, variability in the accumulation of clay size particles throughout the JRA reflects the influence of depth on sedimentation patterns (Figure 5.9). Also, as with P, Al, and Ca, clay percentage increases from the tributary streams and the James River to the main valley. Clay then also increases from the shallow areas in the upper JRA and along the shoreline to the deeper areas of the lake. Again, this increase in clay is the result of longitudinal and lateral fining of sediments. This shows the majority of sediments in areas of the lake >12 meters in depth are composed of clay size material. Unlike Al, Ca, and P, clay content is not different above and below the JRA in the White River.

Organic matter (OM) shows the same spatial pattern as clay, indicating sedimentation as a major factor in explaining its variability within the JRA (Figure 5.10). As a percentage by weight, OM increases from the streams and the James River into the cove and main valley. Within the main valley, OM increases from the shallow environment to the deep environment showing similar longitudinal and lateral sedimentation patterns previously discussed. Sedimentation cannot explain the OM distribution completely, since lake chemistry also controls decomposition rates under different aerobic conditions. In the presence of oxygen, bacteria can decompose OM relatively quickly compared to OM deposited in anaerobic areas of the lake (Baccini, 1985). Therefore, OM accumulates in the deeper areas of the lake where decomposition is relatively slow. The White River does not display a difference in OM concentrations

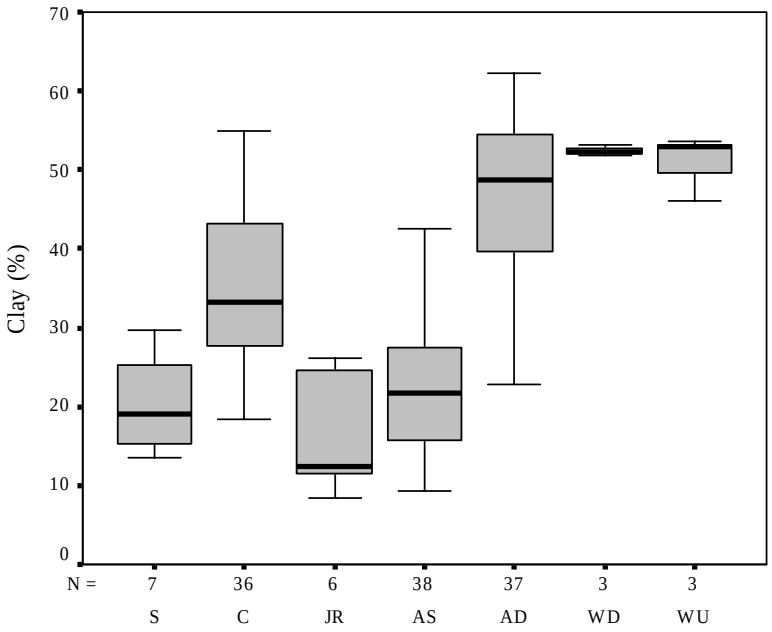

Note: middle value is median value, O = outlier value, and * = extreme value.

Figure 5.9. Distribution of clay by geographic area

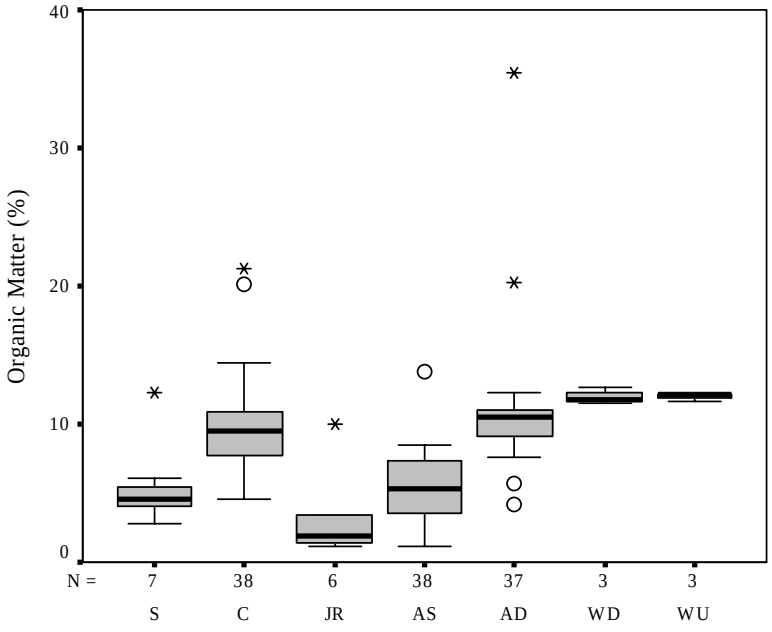

Note: middle value is median value, O = outlier value, and * = extreme value.

Figure 5.10. Distribution of organic matter by geographic area

above and below the confluence with the JRA, suggesting a maximum depth limit where OM concentrations do not increase beyond a threshold.

SPATIAL DISTRIBUTION OF PHOSPHORUS IN THE JRA

Understanding the spatial distribution of P in sediments and comparing these concentrations can give information on pollution sources and P-cycling processes in lake bottom sediments. This section describes the spatial patterns of P down-arm from Galena to the main lake in channel sediments and valley floor samples. A P/Al ratio is used to standardize samples to locate anthropogenic P in sediments. Also, variability at sample sites will be discussed to account for sampling error.

Down-Arm Trends

Generally, P increases down-arm in channel sediments with increasing distance and depth from the mouth of the James River at Galena compared to P concentrations in cove sediments (Figure 5.11). JRA main valley channel concentrations range from approximately 800 ug/g in the upper arm area to about 2500 ug/g near the main lake. Channel sediments samples were collected from the deepest part of the channel at a particular location or lake cross-section. The increase in P concentrations in bottom sediments down-arm of Galena is an especially important trend because water column P concentrations decrease in the same direction, showing an opposite trend (LMVP, 1998).

The positive relationship between P concentrations and depth and distance again expresses the importance of physical sedimentation patterns of the reservoir and the ability of sediments to retain P in deep areas of the lake that experience seasonal dissolved oxygen changes and limited upward mobility of water in the deep environment. The aim of this study is not to directly measure sink/source dynamics of bottom

sediments, but to use what is already known about the sink/source dynamics of bottom sediments to explain these spatial patterns. The accumulation of P in the deep zones of the lower JRA indicates that bottom sediments are acting as a sink for P. Shallower sediments, which can be a source for P under seasonal low dissolved oxygen levels, display lower concentrations indicating these areas are not experiencing long-term P retention. With the exception of Swift Shoal Creek Cove, main valley channel P concentrations are consistently higher than cove sediments (Figure 5.11). None of the mean cove P concentrations exceed 1000 ug/g despite the differences in drainage area, land use, and local development patterns. The main lake samples do show an increase in P concentration below the JRA compared to concentrations above the confluence. This indicates that P is moving from the JRA into the main lake.

Cross-Valley Trends

Longitudinally, P concentrations increase down-lake in channel sediments and the pattern also holds true across the valley floor. Valley floor transects taken approximately every 7-8 km from Galena show the "3-dimensional" spatial distribution of P (Figure 5.12). The first dimension is the down-arm trend of P concentrations which increase at transect sites just as channel samples. The second dimension is laterally across the valley floor where P concentrations are variable due to the third dimension, depth.

With the exception of the transect at 12 km, sediment P concentrations increase with increasing depth longitudinally and laterally where river processes shift to more lake dominated regions below Galena. The points at the far right of each transect represent the channel or deepest sample at that distance from Galena. As previously discussed,

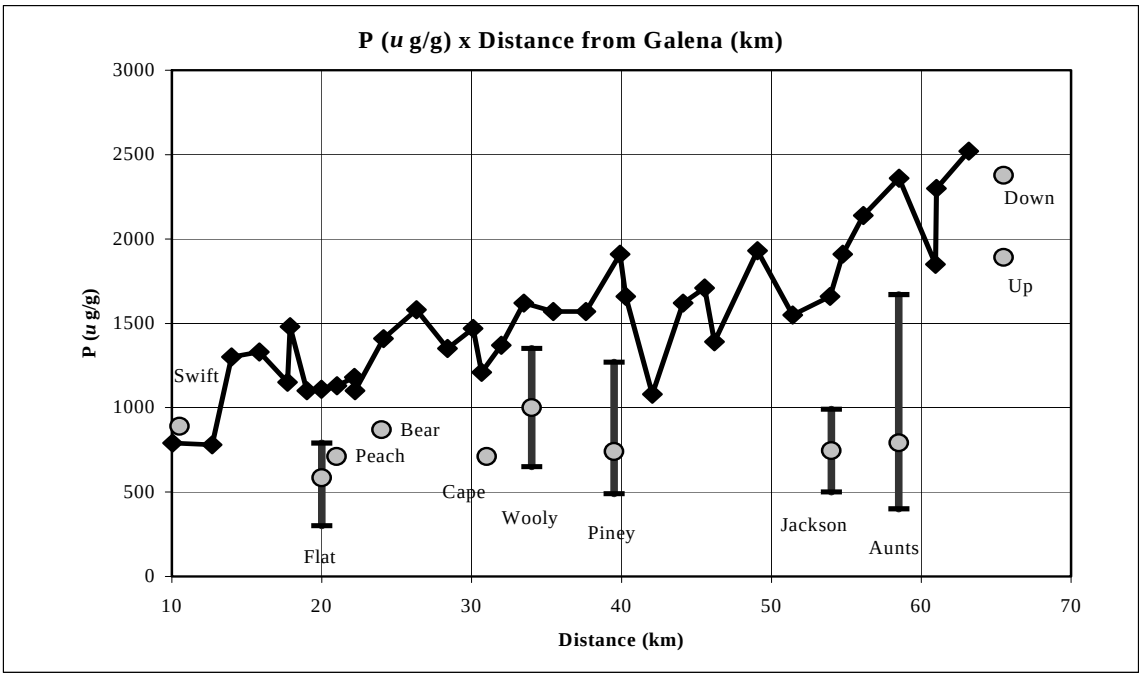

Figure 5.11. Down-lake sediment-P ug/g
(Channel sample sites from Galena to main lake with mean-max-min P(ug/g) for cove samples where they enter the JRA.)

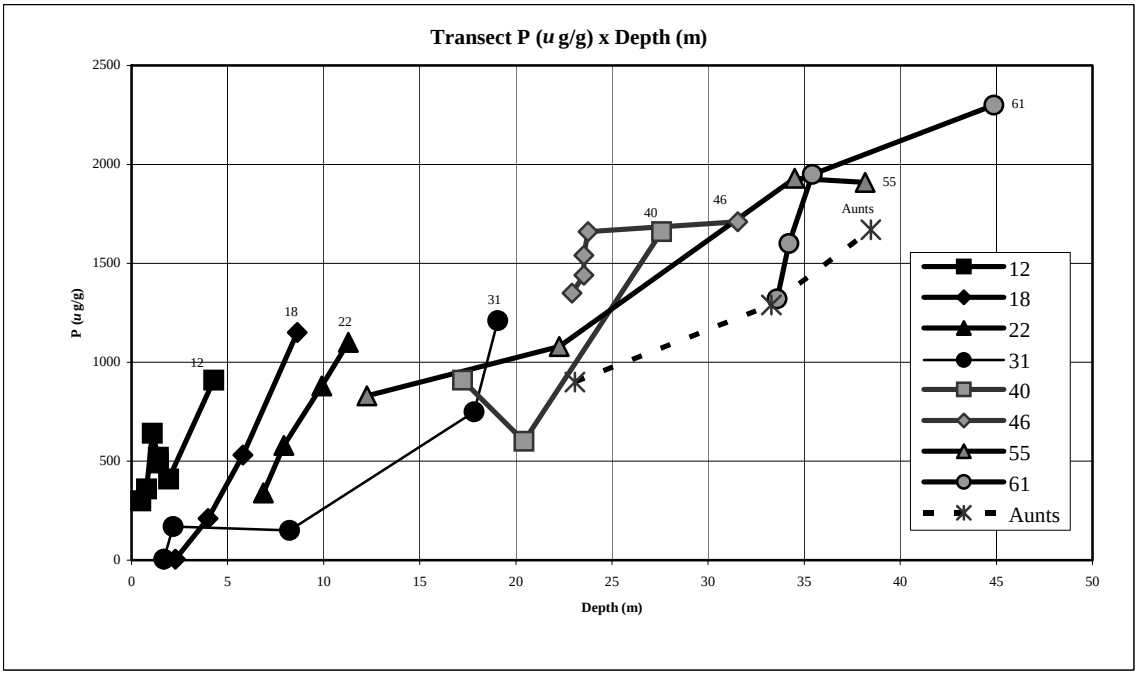

Figure 5.12. Valley floor P(ug/g) vs. Depth (m) for transect sites.
(Numbers next to transect lines represent distance (km) from Galena.)

depth can be used to estimate P because it can be used to account for sedimentation changes as well as changing aerobic conditions. Basically, the trend here shows sediment-P concentrations are roughly equal to depth (m) times 50.

Another interesting aspect is the slope of the lines representing transects at depths below 12 meters are much steeper than at transects in the deeper areas. This suggests there is higher variation in P concentrations along a transect in the upper section of the JRA along a transect. Going down-arm, mean depth increases to the point where the designation between channel and valley becomes less important. This supports a chemical as well as sedimentation rationale for using the 12 meter mark for a changing aerobic environment in the lake. The transect site taken at Aunts Creek Cove shows P concentrations at that location are a little lower than the main valley concentrations even at similar depths.

P:Al Ratio

The P:Al ratio is a commonly used and widely accepted method of identifying anthropogenic pollutant concentrations by standardizing samples to account for differences in grain size since higher Al concentrations are found in the clay fraction (Horowitz, 1991). From Galena going down-arm, the P:Al ratio in channel sediments stays fairly constant until the last 10 km when there is a spike in the P:Al ratio (Figure 5.13). Possible reasons for this are; changes in sediment composition, changes in organic matter type, or changes in geological contribution of the sediment. Cove P:Al ratios show mixed results plotted with the arm channel ratio. Samples from larger coves, such as Piney Creek, Aunts Creek, and Flat Creek, plot below the arm channel samples. Most of the smaller coves plot with the arm channel concentrations indicating these smaller

coves could be enriched with P from catchment sources or P-laden sediments from the main arm valley are being transported into and settling in these small cove areas. These tributary coves probably do not have the discharge to flush sediment out or deliver "clean" low-P sediments the lake environment.

Comparing the P:Al ratio with depth at transects shows some interesting trends (Figure 5.14). At transects located 12, 18, 22, and 31 km from Galena, P:Al ratios increase with depth at a transect and there is little change in P enrichment moving down-arm. Transect sites located further down-arm have a slightly elevated P:Al ratio compared to up-lake areas. Furthermore, transects located at 40, 46, and 55 km have the highest P:Al ratios in the shallowest areas of the transect, indicating a possible enrichment from shoreline developments located nearby. The Aunts Creek transect P:Al ratio is slightly lower than the arm transect sites.

Site and Sample Variability of P Concentrations

Table 5.3 shows the results of triplicate analysis of sites at transect locations. Three samples were collected at channel and valley floor sites to assess the variability of P, Fe, clay, and OM at a particular distance down-arm along a transect. Evaluation of CV% values shows that sampling error is $\leq$ 20% for P. The highest variation in P concentration occurs at the valley site at 18 km from Galena where CV% for P is 20%, which is only based on two samples because P data for one sample was <10 ug/g. Plotting the standard deviation of the triplicate sites versus depth (m) shows P is more variable within channel sites for three out of the five channel and valley sites (Figure 5.15). For triplicate sites at 18 and 61 km from Galena, the valley sites displayed higher variability. The site at 10 km is only represented by a valley triplicate, due to the lack of

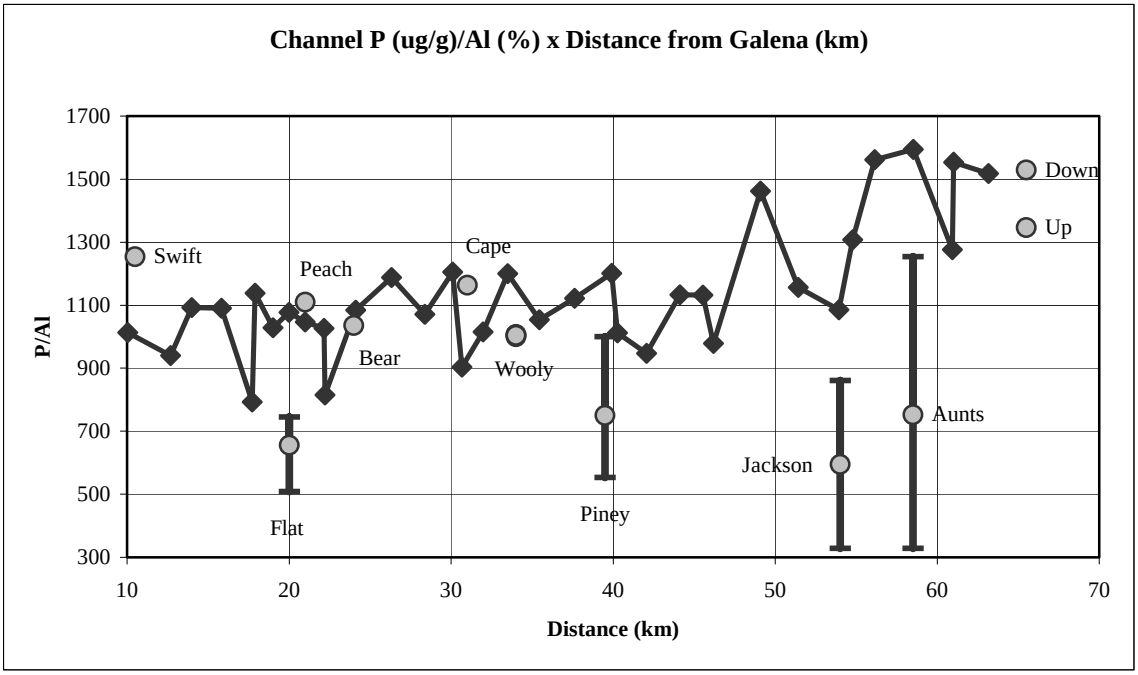

Figure 5.13. Channel Sediment P:Al ratio vs. Distance (km) from Galena
(Mean-min-max cove P:Al ratio where they enter the JRA.)

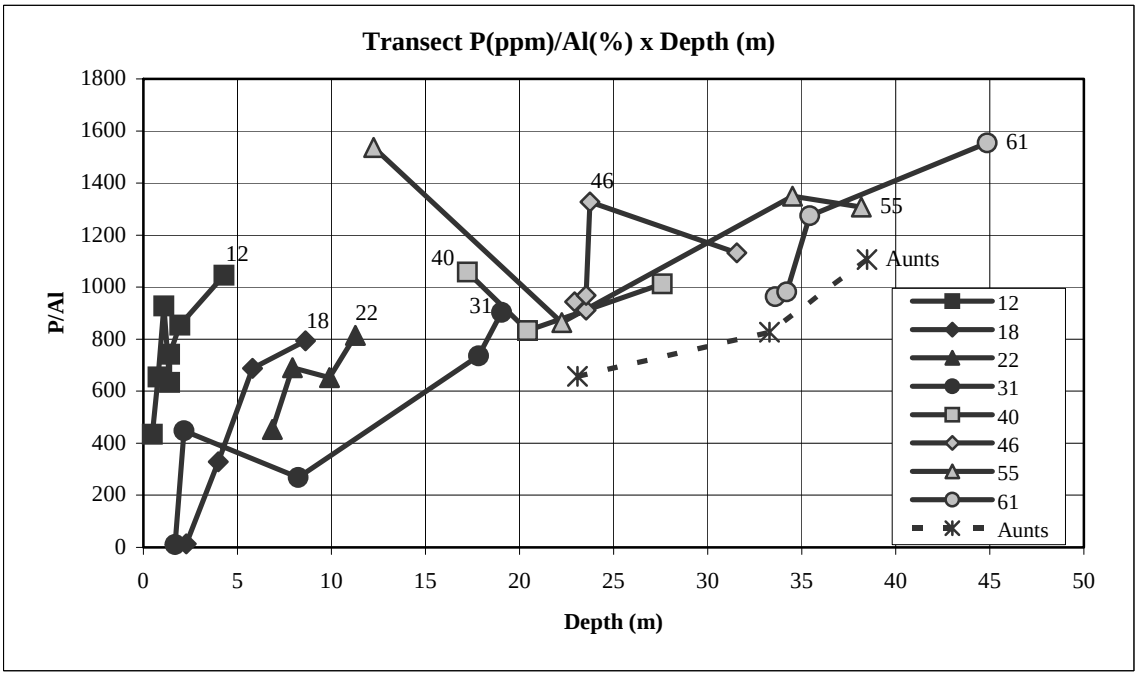

Figure 5.14. Valley Floor Sediment P:Al Ratio vs. Depth (m) at Transects
(Numbers on transect line represent distance site is from Galena.)

Table 5.3. Down-Lake Site Variability for P, Fe, Clay, and Organic Matter

Dist[1] (km)	Site	Depth (m)	P (ug/g)			Fe (%)			Clay (%)			OM (%)		
			Mean	Sd[2]	cv%[3]	Mean	Sd[2]	cv%[3]	Mean	Sd[2]	cv%[3]	Mean	Sd[2]	cv%[3]
10	V	5.8	670	115	17	1.01	0.02	2	20.03	3.23	16	5.42	1.17	22
12	Ch	3.5	537	45	8	0.98	0.15	16	17.78	2.54	14	4.80	1.40	29
	V	1.4	410	10	2	0.85	0.04	5	18.30	0.64	4	4.95	0.14	3
18	Ch	8.6	1173	32	3	1.70	0.02	1	41.67	0.84	2	8.55	0.25	3
	V	4.0	245	49.5	20	0.86	0.03	3	23.36	1.13	5	5	0.02	0.4
31	Ch	19.1	1247	188	15	1.83	0.17	9	50.29	2.34	5	9.01	0.17	2
	V	8.2	160	17	11	0.76	0.04	5	20.07	1.32	7	3.72	0.32	9
46	Ch	31.5	1800	108	6	2.04	0.05	2	55.76	5.99	11	10.45	0.48	5
	V	23.5	1423	15	1	1.87	0.03	1	51.23	0.78	2	9.29	0.13	1
61	Ch	44.9	2307	70	3	2.32	0.07	3	42.47	1.87	4	12.10	0.34	3
	V	35.4	1740	187	11	2.16	0.04	2	48.59	2.34	5	11.27	0.71	6
Mean	Ch	21.5	1412.67	88.67	6	1.77	0.09	5	41.60	2.72	7	8.98	0.53	6
	V	13	774.72	65.79	8	1.25	0.03	2	30.26	1.57	5	6.61	0.42	6

Note: Ch = channel samples and V = valley floor samples

1. Dist = Distance from Galena (km)
2. Sd = Standard deviation
3. cv% = Coefficient of variation % = sd/mean * 100

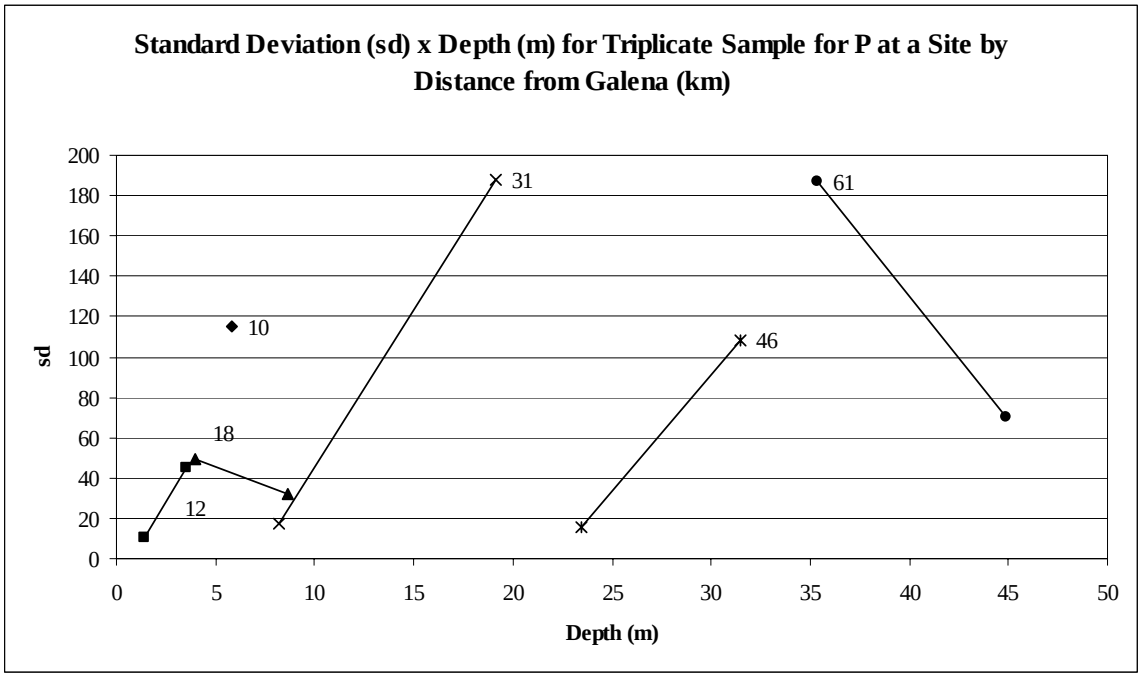

Figure 5.15. Standard Deviation (sd) vs. Depth (m) for Triplicate Samples
(Deeper sample represents channel site and shallower site is from the valley.)

accumulation of fine-grained sediment in the channel. Plotting the CV% versus depth shows no clear trends in the variations in samples from one site to the next for channel and valley sites (Figure 5.16). For the majority of sites, differences in variations between the channel and valley areas were within 5%, with the exception at the 18 km site discussed above. Variability within a particular sample site is less than 20% for the majority of the study area indicating the variability at a site is due to physical and chemical processes, not errors.

Sample variability determined by triplicate analysis of 16 samples shows very low variability of P concentrations (Table 5.4). Mean concentrations of the three times the single sample was analyzed ranged from around 240 ug/g to around 2,100 ug/g. The highest CV% for the triplicate samples was 6.2 % and the low was 1.3. %, indicating methodology in the chemical analysis was fairly consistent for samples despite the sample location or P concentration of the sample.

ANALYSIS OF GEOGRAPHIC AND GEOCHEMICAL INFLUENCES

The spatial distribution of P in the JRA has been shown and preliminarily discussed in the previous section. This section aims at explaining this distribution by comparing P concentration to sediment characteristics at sites and comparing P concentrations with spatial characteristics of sampling sites. Also, as discussed previously, cove sample P concentrations will be compared to watershed characteristics of the contributing areas above sample locations. These relationships will then be used to model concentrations for bottom sediments to explain the spatial distribution of P and identification of P sources in more detail and estimate enrichment.

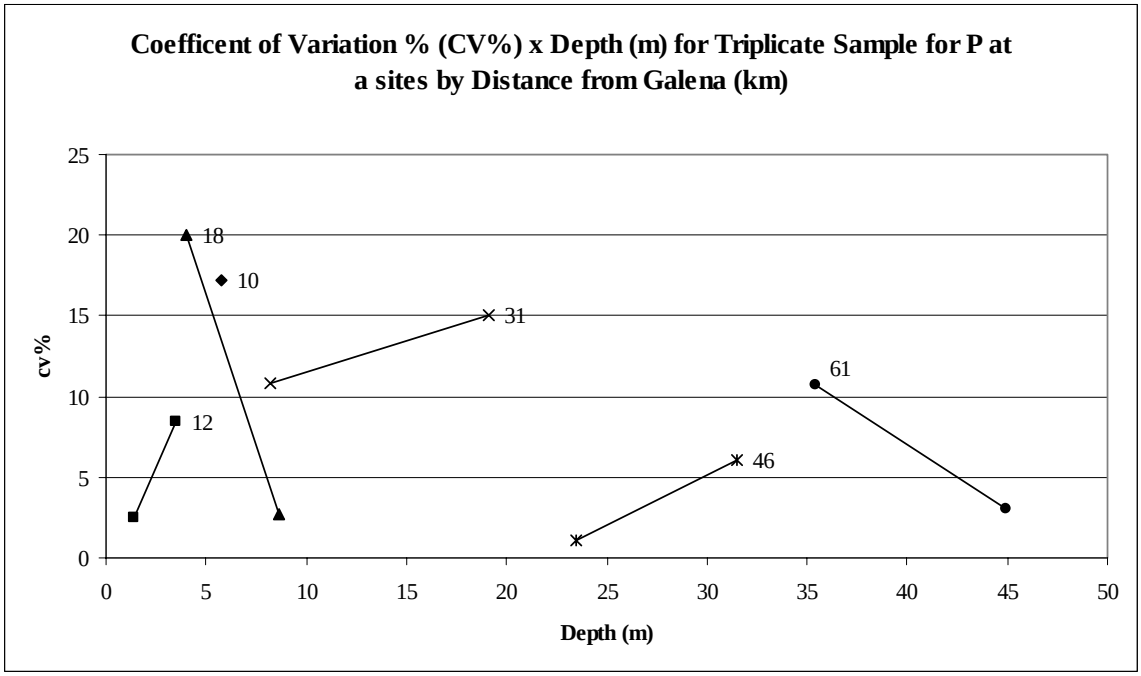

Figure 5.16. Coefficient of variation percentage (cv%) vs. depth (m) for triplicate samples (Deeper sample represents channel site and shallower site is from the valley.)

Table 5.4. Within Sample Sediment-P Variability

Site	Channel Location	Mean P (ug/g)	sd	cv%
2	Channel	1113.33	15.28	1.4
8	Channel (Flat)	246.67	15.28	6.2
13	Channel	1490.00	87.18	5.9
19	Channel	1506.67	80.83	5.4
23	Channel (Piney)	993.33	30.55	3.1
34	Valley	346.67	15.28	4.4
41	Channel	1500.00	52.92	3.5
54	Channel (Aunts)	1080.00	20.00	1.9
104	Valley	523.33	11.55	2.2
108	Channel	1263.33	50.33	4.0
117	Valley	423.33	20.82	4.9
121	Channel	1206.67	37.86	3.1
127	Valley	1266.67	51.32	4.1
131	Channel	1583.33	40.41	2.6
142	Channel	2113.33	70.95	3.4
145	Valley	1596.67	20.82	1.3
Mean	Channel	1281.52	45.60	3.56
Mean	Valley	831.33	23.95	2.88

Phosphorus and Sediment Relationships

An understanding of P relationships with sediment composition and geochemistry can be used to better understand absorption and sedimentation processes important in the spatial distribution of P in bottom sediments. Table 5.5 contain Pearson Correlation coefficients (R) for relationships between P and the sediment composition variables organic matter, sand, silt and clay, and sediment geochemical variables Al, Ca, Fe, and Mn. These relationships are displayed in different groupings of samples. Some outlier samples were removed from the arm (n = 4) and cove (n = 4) samples due to high organic matter and Fe, as well as P concentrations below detection level.

Including all JRA bottom sediments, P has significant correlation (0.01 level) with all variables except silt. High correlation exists between P and clay, Al, and Mn with R-values >0.80. To a lesser extent, P correlates positively with organic matter, Ca, and Fe and negatively with sand. As with the "all samples" example, arm samples show significant correlation (0.01) with all variables except silt. However, in the main valley P correlates well with OM, clay, Al, Fe, and Mn with R-values >0.85. Again, P has a negative correlation with sand.

Table 5.5 Correlation between P and Sediment Composition and Geochemistry
Sediment-P reported with Pearson Correlation coefficient (R)

Geographic Location	n	OM	Sand	Silt	Clay	Al	Ca	Fe	Mn
All	105	**.421**	**-.561**	-.053	**.810**	**.836**	**.663**	**.791**	**.830**
Arm (all depths)	71	**.900**	**-.641**	-.049	**.885**	**.906**	**.668**	**.954**	**.870**
Arm (Shallow)	36	**.864**	**-.589**	.394	**.816**	**.870**	**.540**	**.889**	**.921**
Arm (Deep)	35	**.666**	**-.595**	.067	**.640**	**.719**	.030	**.898**	**.818**
Coves	34	**.596**	**-.447**	**-.226**	**.674**	**.731**	**.553**	**.655**	**.582**

Bold = significant at 0.01 level
Underline = significant at 0.05 level

Splitting the arm samples to shallow (<12 m) and deep (>12 m) shows a much different correlation and shows there is a difference in P process and possible sources in the cove and arm geographic areas. Strong correlations exist between shallow arm P and OM, clay, Al, Fe, and Mn. This suggests the variability in P concentrations in the samples is due to a combination of sedimentation patterns, which is a physical process, and the presence of Fe-Mn oxides, which reflects a chemical process in sediments. However, when looking at the deep samples strong correlation between P only exists with Fe and Mn. In deep sediments OM, clay, and Al levels are high in all sediments and do not vary much, so changes in P concentrations do not necessarily follow sedimentation patterns, but lake chemistry in concentrating Fe-Mn oxides are much more important at these depths.

Cove samples show a much different pattern than any of the previously discussed areas. Significant correlations exist between cove sediment P and all variables with clay, Al, and Fe having the only R-values over 0.60. Other positive correlations exist with OM, Ca, and Mn with R-values between 0.50 and 0.59. Negative correlations exist between P and sand and silt. This indicates that different source and sedimentation factors drive P accumulation in coves than the main valley.

In summary, sediment-P correlates well with a wide variety of sediment composition and geochemical variables in the entire JRA. In shallow areas, P correlates well with both sediment composition and geochemical variables. This suggests that physical processes such as sedimentation and chemical processes associated with changing aerobic conditions control P distribution in the upper portions of the arm and other shallow areas around the JRA. In deeper areas, P correlates very well with Fe and

Mn showing anaerobic conditions there is the major factor in P distribution. In the coves however, P correlates poorly in comparison with the rest of the JRA with these variables suggesting different source and sedimentation driving distribution.

Phosphorus and Spatial Relationships

For this study, spatial characteristics of sediment sampling sites were used to help explain distribution of P in bottom sediments and show how these variables can be used to estimate P concentrations without having to run expensive sample analysis. Table 5.6 contains Pearson Correlation coefficients between sediment P and sample depth in the lake, distance the sample is from the mouth at Galena or the stream mouth of the tributary watershed, and width of the lake at the sample site. The depth variable represents the combined influence of down-lake sedimentation, sediment focusing, and different aerobic conditions. Distance from the stream mouth for coves and from Galena for the arm is also used as a way to look at longitudinal sedimentation as well as distance decay from a source. Valley width is used to account for sedimentation and dilution due to the reservoirs morphological influence on flow velocity and sedimentary environment.

Table 5.6 Correlation between P and Spatial Relationships
Sediment-P reported with Pearson Correlation coefficient (R)

Geographic Location	n	Depth	Distance from Stream Mouth	Valley Width
All	105	**.861**	**.689**	**.727**
Arm (all depths)	71	**.877**	**.788**	**.736**
Arm (Shallow)	36	**.727**	.182	.215
Arm (Deep)	35	**.746**	**.548**	**.468**
Coves	34	**.796**	**.433**	**.711**

Bold = significant at 0.01 level
Underline = significant at 0.05 level

Of these spatial variables, depth shows the highest correlation with P concentration with R-values ranging from 0.70 to 0.90 for every geographic category. This is important to identify since lake depth is such an easy variable to collect with a simple sonar depth finder or from bathymetric maps. Distance and valley width work well overall in models including all sediments and arm sediments, but correlations weaken in the shallow arm, deep arm, and cove categories. These spatial variables also have a lot of covariation with depth as well as with each other.

Phosphorus and Watershed Relationships for Coves

Since one of the objectives of this study is to identify nonpoint P sources within the cove tributary watersheds, characteristics of these areas were assessed using GIS watershed analysis methods. Characteristics of contributing areas above sampling locations were compared to P concentrations of the sediment samples and displayed as Pearson Correlation R-values (Table 5.7). These variables are explained in the methods chapter of this study.

Correlations exist between P and lake area, number of docks, and dock density with R-values between 0.55 and 0.66 for these variables. Correlations between lake area and P suggest that the more lake area above sampling sites the more accumulation of P and fine sediments. However, further investigation shows lake area and docks are highly correlated. A P-correlation matrix for all cove variables will be displayed in the regression model section (Table 5.17). The relationship between dock/drainage area shows a slight relationship between sediment-P and shoreline development in the coves. The other variables have poor to no correlation with P concentrations in bottom sediments.

Table 5.7 Correlation between P and Tributary Cove Watershed Characteristics
Above cove sample sites and sediment P reported with Pearson Correlation coefficient (R) (n=34)

Watershed Variable	R Value
Drainage Area (A_D)	-0.24
Lake Area (A_L)	**0.66**
Road Density (D_R)	0.06
Urban Land Use (U)	0.01
Forest Land Use (F)	0.20
Agriculture Land Use (A)	-0.24
Docks (D)	**0.63**
Dock/Drainage Area (D_{AD})	**0.55**
Docks/Lake Area (D_{AL})	0.36

Bold = significant at 0.01 level
Underline = significant at 0.05 level

Spatial Process Regression Models for Phosphorus

Now that location of P is known and correlations between P and geochemical, sediment composition, spatial, and watershed analysis variables have been made, the next step is to model P concentrations using these variables to explain the spatial distribution. This will be accomplished by displaying a variety of P regression models for several geographic areas of the JRA. These different models are first shown as an all inclusive set of models for all areas together. Then, arm and cove models are created to better predict P concentrations within these areas.

For each area, a Pearson Correlation matrix is shown for all the variables used to predict P concentrations. Stepwise linear regression models were used to predict P concentrations in ug/g. Variables that correlated with each other having R-values higher than 0.70 were not used together to avoid inaccuracy of models due to co-variation. A model summary is provided to explain R^2, standard error (SE), % error, model

significance (Sig.), the constant slope (b_0), and each variable slope and significance for each model.

All JRA bottom sediments. The first set of models uses all bottom sediment samples from the arm and coves to predict P(ug/g). Table 5.8 is a Pearson Correlation matrix displaying the R-value between variables at the 0.01 and 0.05 significance levels. Table 5.9 is a summary of several models organized from 1 to 3 parameters using spatial and geochemical variables or combinations of these variables to get the "best" model in terms of lowest % error and highest R^2 value. The best model for the entire JRA was the 3 parameter depth-geochemical model. This model uses depth, Mn concentration, and Ca concentration to predict P(ug/g). Depth accounts for both sedimentation patterns and changing aerobic conditions. Concentrations of Mn account for the presence of oxides capable of absorbing P. The correlation with Ca reflects the complex nature of the particulate P in the JRA, where P can be in the mineral matrix of Apatite or can co-precipitate with $CaCO_3$.

This model has an R^2 value of 0.91 and a standard error (SE) of 158(ug/g). Plotting the standardized residual versus the standardized predicted value shows an R^2 value of 0.00, emphasizing the models predicted value's variability is similar to the original data (Figure 5.17). Comparing actual P(ug/g) with predicted P(ug/g) from the model shows an R^2 value of 0.91, which displays the model is fairly accurate in predicting P concentrations (Figure 5.18). However, this modeling technique can predict P for the entire JRA bottom sediments using only the spatial variable depth while accounting for 74% of the variance. This is important to note because depth is an easy variable to collect using bathymetric maps or sonar readings.

Table 5.8 Pearson correlation for all JRA sediments
(n=105)

	OM	Sand	Silt	Clay	Al	Ca	Fe	Mn	Dist	Depth	VW
OM	1	**-.322**	-.051	**.486**	**.352**	**.428**	**.295**	.194	.237	**.372**	**.366**
Sand		1	**-.676**	**-.637**	**-.702**	**-.605**	**-.374**	**-.497**	-.149	**-.443**	**-.255**
Silt			1	-.137	.040	.201	**-.292**	.037	**-.284**	-.228	**-.280**
Clay				1	**.902**	**.602**	**.808**	**.630**	**.498**	**.835**	**.636**
Al					1	**.591**	**.865**	**.752**	**.486**	**.784**	**.604**
Ca						1	**.405**	**.407**	**.503**	**.597**	**.549**
Fe							1	**.742**	**.575**	**.781**	**.654**
Mn								1	**.567**	**.617**	**.533**
Dist									1	**.734**	**.858**
Depth										1	**.868**
VW											1

Bold = correlation is significant at the 0.01 level (2-tailed).
Underline = correlation is significant at the 0.05 level (2-tailed).

Table 5.9 Linear Regression Model Summaries for all JRA sediments
Mean P = 976 ug/g (n=105)

Model	R^2	SE	% Error	Sig.	b_0	b_1	b_2	b_3
Depth	0.74	286	29	0.00	401.13	Depth(m) 38.58 (0.000)*		
1 parameter Geochemical	0.73	293	30	0.00	-362.04	Al(%) 1286.60 (0.000)*		
2 parameter Geochemical	0.84	231	24	0.00	-297.62	Mn(ug/g) 0.91 (0.000)*	Clay(%) 19.42 (0.000)*	
3 parameter Geochemical	0.87	203	21	0.00	-382.53	Mn(ug/g) 0.89 (0.000)*	Ca(%) 64.95 (0.000)*	Clay(%) 13.31 (0.000)*
2 parameter Depth-Chemo	0.89	190	19	0.00	64.68	Depth(m) 24.77 (0.000)*	Mn(ug/g) 0.82 (0.000)*	
3 parameter Depth-Chemo	0.91	158	16	0.00	-93.05	Depth(m) 19.68 (0.000)*	Mn(ug/g) 0.80 (0.000)*	Ca(%) 53.00 (0.000)*

* Number in parentheses is significance of parameter.

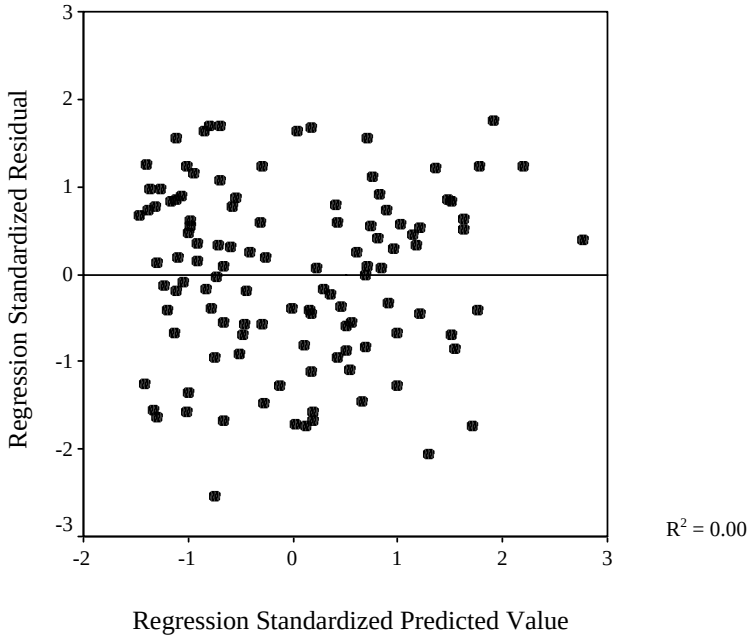

Figure 5.17. Residual Plots for All JRA Model

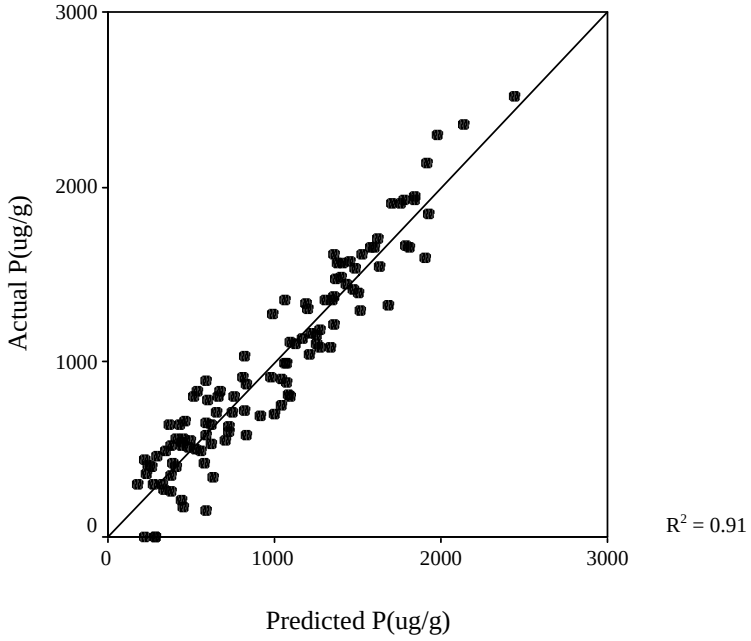

Figure 5.18. Predicted P (ug/g) vs. Actual P (ug/g) for All JRA Model

Main valley sediments. This set of models is for the main arm and uses all bottom sediment samples from the main valley to predict P ug/g. Table 5.10 is a Pearson Correlation matrix displaying the R-value between variables at the 0.01 and 0.05 significance levels. Table 5.11 is a summary of several models organized using spatial, sediment composition, and geochemical variables to get the "best" model in terms of lowest % error and highest R^2 value.

The best model for the main arm only was the 1 parameter geochemical model. This model uses only Fe concentration to predict P ug/g. Iron (Fe) works well for a couple of reasons. First, Fe oxides form coatings on sediments and can absorb P in aerobic conditions. Reoxidized Fe can form a gel complex with fractions of Al and silica that has a high absorption capacity for P in bottom sediments (McCallister and Logan, 1978). This model has an R^2 value of 0.91 and a standard error (SE) of 185 ug/g. Plotting the standardized residual versus the standardized predicted value shows an R^2 value of 0.00, emphasizing the models predicted value's variability is similar to the original data (Figure 5.19). Comparing actual P ug/g with predicted P ug/g from the model shows an R^2 value of 0.84, which displays the model is fairly accurate in predicting P concentrations (Figure 5.20). Depth accounts for 77% of the variance in the main valley, again displaying the utility of using spatial characteristics to explain P concentration patterns.

Main valley shallow arm sediments. The set of models in Tables 5.12 and 5.13 describe sediment P distribution in the shallow arm using bottom sediment samples collected at <12 meter lake depths. Table 5.12 is a Pearson Correlation matrix displaying the R-value between variables at the 0.01 and 0.05 significance levels. Table 5.13 is a

Table 5.10 Pearson correlation for main valley sediments
(n=71)

	OM	Sand	Silt	Clay	Al	Ca	Fe	Mn	Depth	Dist	VW
OM	1	**-.684**	-.002	**.897**	**.901**	**.780**	**.896**	**.740**	**.873**	**.830**	**.786**
Sand		1	-.649	**-.691**	**-.769**	**-.683**	**-.590**	**-.681**	**-.506**	**-.487**	**-.441**
Silt			1	-.101	.081	.137	-.141	.155	-.225	-.187	-.180
Clay				1	**.929**	**.763**	**.905**	**.743**	**.876**	**.815**	**.748**
Al					1	**.784**	**.939**	**.853**	**.808**	**.768**	**.704**
Ca						1	**.706**	**.500**	**.682**	**.746**	**.666**
Fe							1	**.844**	**.884**	**.829**	**.768**
Mn								1	**.648**	**.564**	**.526**
Depth									1	**.960**	**.910**
Dist										1	**.940**
VW											1

Bold = correlation is significant at the 0.01 level (2-tailed).
Underline = correlation is significant at the 0.05 level (2-tailed).

Table 5.11 Linear Regression Model Summaries for main valley sediments
Mean P= 1116 ug/g (n=71)

Models	R^2	SE	% Error	Sig.	b_0	b_1
Depth	0.77	297	27	0.00	452.58	Depth(m) 39.24 (0.000)*
1 parameter Sediment Comp	0.81	270	24	0.00	-379.31	OM(%) 195.58 (0.000)*
1 parameter Geochemical	0.91	185	17	0.00	-742.32	Fe(%) 1263.55 (0.000)*

* Number in parentheses is significance of parameter.

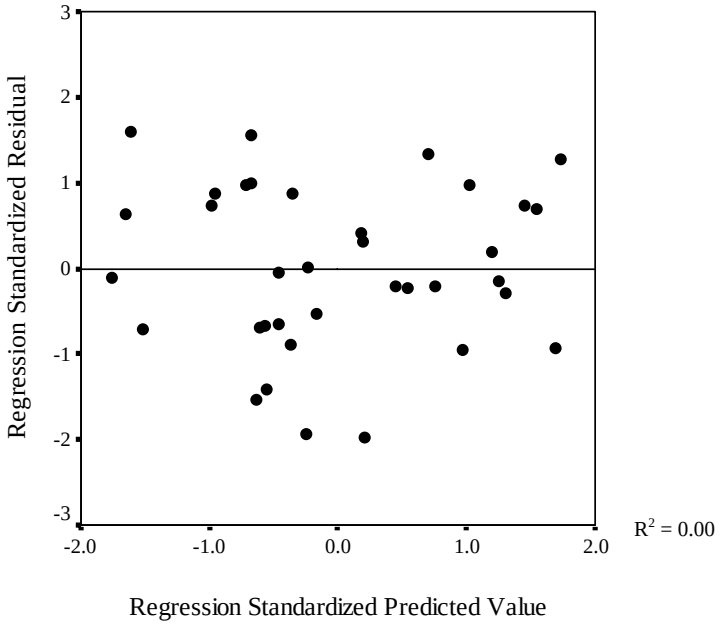

Figure 5.19. Residual Plots for Main Valley Bottom Sediment Model

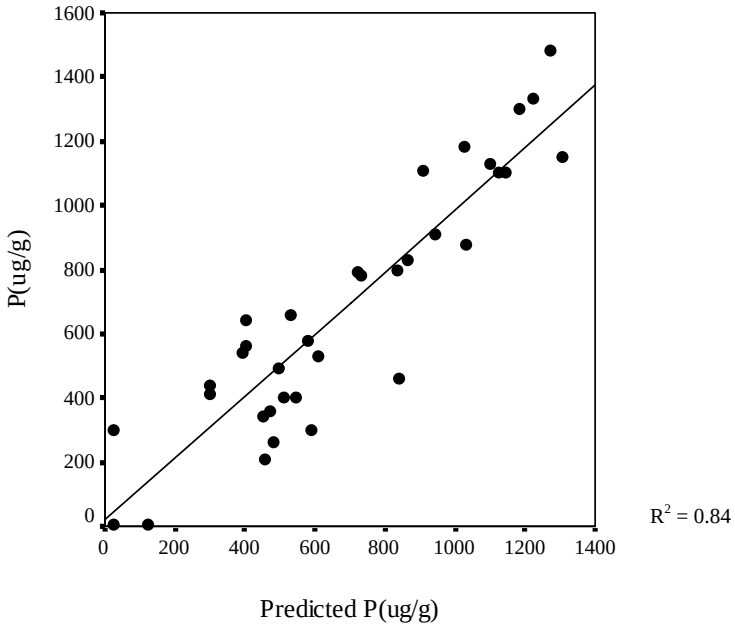

Figure 5.20. Predicted P(ug/g) vs. Actual P(ug/g) for main valley model

summary of several models organized from 1 to 3 parameters using spatial and geochemical variables or combinations of these variables to get the "best" model in terms of lowest % error and highest R^2 value.

The best model for the shallow (<12 meter) sediments of the main arm was the 3 parameter geochemical-spatial model. This model uses Fe concentration, distance from Galena, and silt % to predict P ug/g. The potential role Fe plays in P absorption hasalready been discussed. Distance correlates negatively with P concentrations in the shallow areas suggesting distance decay at these depths, or that P concentrations in shallow areas of transects are not affected as much by inputs at Galena. Silt % is probably a good predictor due to the fact changes in silt in the shallow zones can effect P concentrations more than sand because sand % are so low. This model has an R^2 value of 0.88 and a standard error (SE) of 143 ug/g.

Plotting the standardized residual versus the standardized predicted value shows an R^2 value of 0.00, emphasizing the models predicted value's variability is similar to the original data (Figure 5.21). Comparing actual P ug/g with predicted P ug/g from the model shows an R^2 value of 0.88, which displays the model is fairly accurate in predicting P concentrations (Figure 5.22). Depth does not explain variability in P concentrations as well in the shallow areas accounting for only 53% of the variance compared to the 77% using depth for all sediments in the JRA. Depth as a variable is weaker here because it is negated by only using shallow samples. However, when using both depth and distance, 73% of the variance is explained.

Main valley deep arm sediments. The models in Table 5.14 and 5.15 describe sediment P distribution in the deep arm using bottom sediment samples collected at >12

Table 5.12 Pearson correlation for shallow (<12m) sediments
(n=36)

	OM	Sand	Silt	Clay	Al	Ca	Fe	Mn	Depth	Dist	VW
OM	1	**-.661**	**.485**	**.827**	**.829**	**.665**	**.727**	**.799**	**.683**	**.297**	**.323**
Sand		1	**-.956**	**-.774**	**-.756**	**-.780**	**-.463**	**-.651**	**-.624**	**-.592**	**-.497**
Silt			1	**.553**	**.550**	**.681**	.224	**.433**	**.440**	**.530**	**.433**
Clay				1	**.954**	**.742**	**.830**	**.910**	**.817**	**.534**	**.476**
Al					1	**.676**	**.882**	**.945**	**.778**	**.461**	**.453**
Ca						1	**.496**	**.617**	**.791**	**.785**	**.702**
Fe							1	**.922**	**.750**	.301	.310
Mn								1	**.792**	*.420*	*.386*
Depth									1	**.694**	**.654**
Dist										1	**.814**
VW											1

Bold = correlation is significant at the 0.01 level (2-tailed).
Underline = correlation is significant at the 0.05 level (2-tailed).

Table 5.13 Linear Regression Model Summaries for Shallow (<12m) Sediments
Mean P= 664 ug/g (n=36)

Models	R^2	SE	% Error	Sig.	b_0	b_1	b_2	b_3
Depth	0.53	272	41	0.00	221.66	Depth(m) 83.31 (0.000)*		
2 parameter Spatial	0.73	210	32	0.00	642.67	Depth(m) 132.63 (0.000)*	Dist(km) -45.35 (0.000)*	
1 parameter Geochemical	0.79	182	27	0.00	-642.18	Fe(%) 1174.25 (0.000)*		
3 parameter Geo-Spatial	0.88	143	22	0.00	-790.20	Fe(%) 1180.17 (0.000)*	Silt(%) 7.59 (0.000)*	Dist(km) -19.28 (0.001)*

* Number in parentheses is significance of parameter.

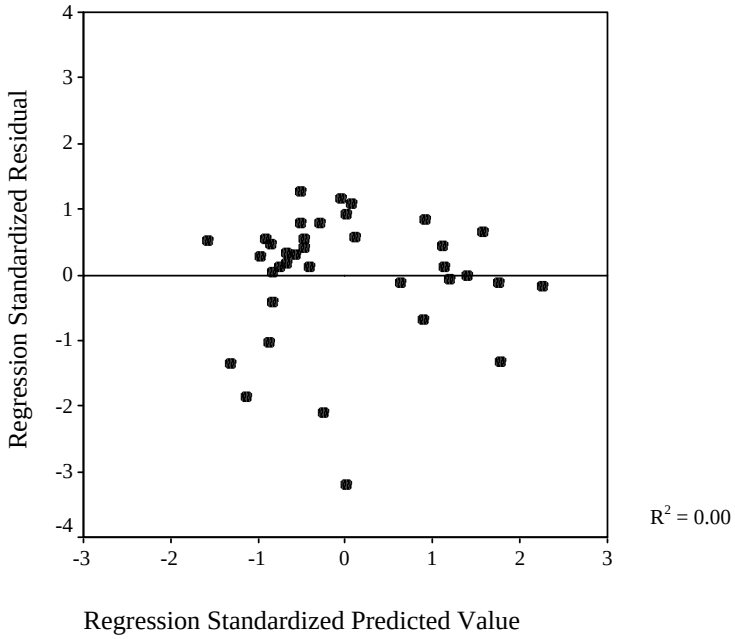

Figure 5.21. Residual Plots for Shallow Main Valley Model

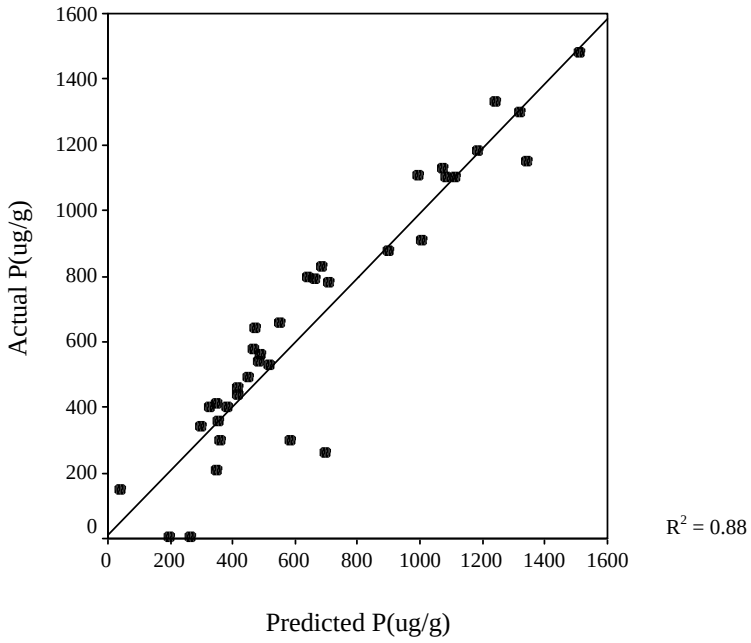

Figure 5.22. Predicted P (ug/g) vs. Actual P (ug/g) for Shallow Main Valley Model

meter lake depths. Table 5.14 is a Pearson Correlation matrix displaying the R-value between variables at the 0.01 and 0.05 significance levels. Table 5.15 is a summary of several models using 1 to 2 parameters including spatial and geochemical variables or combinations of these variables to get the "best" model in terms of lowest % error and highest R^2 value.

The best model for the deep (>12 meter) sediments of the main arm was the 1 parameter geochemical model. This model uses Fe concentration to predict P ug/g. The correlation between Fe and P concentrations has already been explained. This model has an R^2 value of 0.81 and a standard error (SE) of 189 ug/g. Plotting the standardized residual versus the standardized predicted value shows an R^2 value of 0.00, emphasizing the models predicted value's variability is similar to the original data (Figure 5.23). Comparing actual sediment P with predicted sediment P from the model shows an R^2 value of 0.79, which displays the model is fairly accurate in predicting P concentrations (Figure 5.24). As in the shallow model, depth does not predict as well because only deep, anaerobic samples were used in this model.

Cove sediments. Along with the variables used in previous models, cove sediment models use several watershed variables to predict P (ug/g). Table 5.16 is a summary of the abbreviations used for these spatial variables used to predict P in bottom sediments in the JRA coves. Table 5.17 is a Pearson Correlation matrix displaying the R-value between variables at the 0.01 and 0.05 significance levels. Table 5.18 is a summary of several models organized from 1 to 3 parameters using spatial and geochemical variables or combinations of these variables to get the "best" model in terms of lowest % error and highest R^2 value.

Table 5.14 Pearson Correlation for Deep (>12m) Sediments
(n=35)

	OM	Sand	Silt	Clay	Al	Ca	Fe	Mn	Depth	Dist	VW
OM	1	**-.651**	.115	**.663**	**.700**	.349	**.752**	.414	**.749**	**.690**	**.611**
Sand		1	**-.568**	**-.661**	**-.808**	**-.439**	**-.565**	**-.509**	-.328	-.163	-.083
Silt			1	-.242	.209	.346	-.007	.194	-.215	-.182	-.221
Clay				1	**.762**	.203	**.673**	*.423*	**.583**	.357	.298
Al					1	.357	**.849**	**.600**	**.502**	.408	.292
Ca						1	.133	-.244	-.050	.167	.067
Fe							1	**.734**	**.725**	**.620**	**.506**
Mn								1	**.472**	.278	.222
Depth									1	**.873**	**.778**
Dist										1	**.861**
VW											1

Bold = correlation is significant at the 0.01 level (2-tailed).
Underline = correlation is significant at the 0.05 level (2-tailed).

Table 5.15 Linear Regression Model Summaries for Deep (>12m) Sediments
Mean P= 1580 ug/g (n=35)

Models	R^2	SE	% Error	Sig.	b_0	b_1	b_2
Depth	0.56	286	18	0.00	599.33	Depth(m) 34.03 (0.000)*	
2 parameter Sed. Comp-Spatial	0.69	242	15	0.00	830.75	Depth(m) 28.16 (0.000)*	Sand(%) -14.32 (0.001)*
1 parameter Geochemical	0.81	189	12	0.00	-951.36	Fe(%) 1376.81 (0.000)*	

* Number in parentheses is significance of parameter.

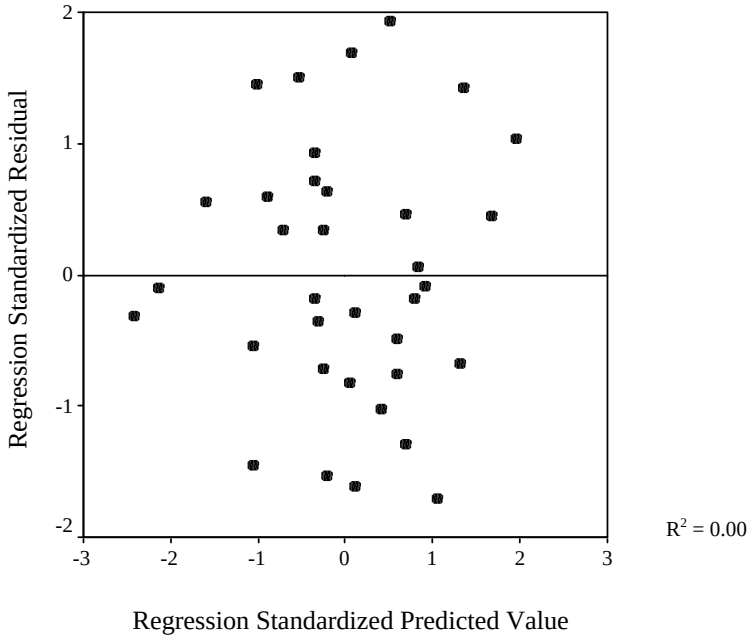

Figure 5.23. Residual Plots for Deep Main Valley Model

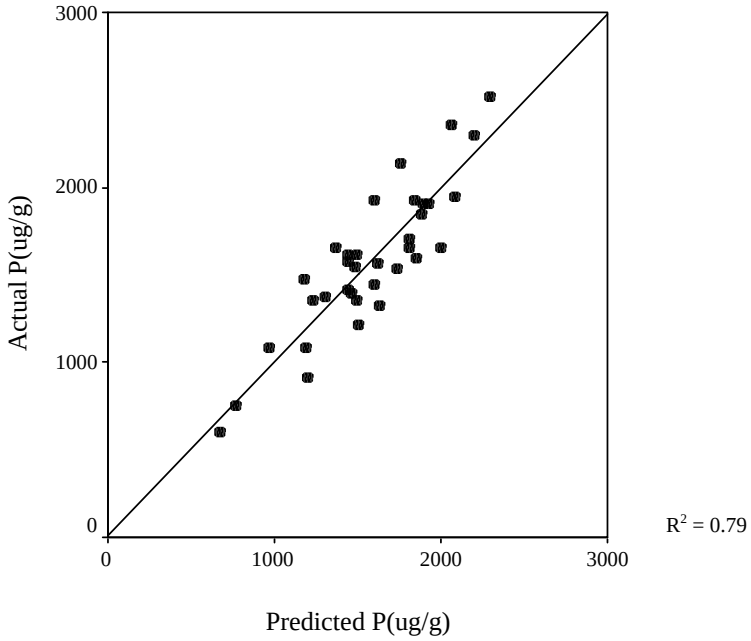

Figure 5.24. Predicted P(ug/g) vs. actual P(ug/g) for Deep Main Valley Model

Table 5.16 Description Abbreviations for Cove Watershed Characteristics

Abbreviation	Description
A_D	Drainage Area
A_L	Lake Surface Area
D_R	Road Density
U	Urban Land-Use Percentage
F	Forested Land-Use Percentage
A	Agriculture Land-Use Percentage
D	Number of Docks
D/A_D	Number of Docks / Drainage Area
DA_L	Number of Docks / Lake Surface Area

The model that accounts for the most variability in the tributary coves of the JRA was the 2-parameter geochemical model. This model uses Ca concentration and Fe concentration to predict P(ug/g). Correlation between Fe and P reflects the association between these variables in different aerobic conditions, while the association of Ca and P displays the co-precipitation with calcite. This model has an R^2 value of 0.86 and a standard error (SE) of 125 ug/g. Plotting the standardized residual versus the standardized predicted value shows an R^2 value of 0.01, emphasizing the models predicted value's variability is similar to the original data (Figure 5.25). While several outlier values seem to influence the model. However, comparing actual P ug/g with predicted P ug/g from the model shows an R^2 value of 0.75 and removing those values does not significantly change the predictability of the model (Figure 5.26). Depth explains about 65% of the variance of P concentrations in the coves due to the variety of depths sampled.

More interesting is the 3-parameter sediment composition and spatial model incorporating depth, urban area, and % sand. The negative correlation with sand accounts for increasing grain size of sediments. The positive correlation with depth

Table 5.17 Pearson Correlation for Cove Sediments

(n=34)

	OM	SND	SILT	CLY	Al	Ca	Fe	Mn	DTH	DIST	VW	A_D	A_L	D_R	U	F	A	D	D/A_D	D/A_L
OM	1	**-.470**	-.148	**.607**	.412	.346	.380	.172	**.565**	-.025	.335	**-.585**	.270	.027	.154	**.472**	**-.507**	.425	**.524**	**.499**
	SND	1	**-.550**	-.305	**-.501**	***-.384***	-.407	-.322	-.291	-.020	-.127	.296	-.167	-.202	-.207	-.146	.185	-.253	-.311	-.376
		SILT	1	**-.628**	-.335	.297	**-.454**	-.120	-.437	-.265	-.425	.070	-.279	.201	.091	-.285	.283	-.246	-.212	-.132
			CLY	1	**.849**	.019	**.897**	.437	**.770**	.321	**.603**	-.356	**.474**	-.041	.089	**.460**	**-.495**	**.516**	**.531**	**.501**
				Al	1	.056	**.963**	**.550**	**.745**	**.449**	**.646**	-.183	**.600**	.012	.032	.268	-.299	**.595**	**.529**	**.451**
					Ca	1	-.087	.091	.226	-.047	.205	-.283	.140	.158	-.106	.071	-.087	.144	.120	-.006
						Fe	1	**.551**	**.708**	.419	**.591**	-.181	**.539**	-.097	-.026	.292	-.307	**.542**	**.462**	**.432**
							Mn	1	.392	**.710**	.430	.431	**.585**	-.040	-.020	-.399	.377	**.438**	.263	.162
								DTH	1	.463	**.880**	-.347	**.780**	.115	.253	.322	-.400	**.830**	**.771**	**.555**
									DIST	1	**.671**	**.572**	**.815**	-.077	.019	-.495	.462	**.600**	.357	.181
										VW	1	-.138	**.934**	.010	.127	.132	-.192	**.908**	**.718**	**.458**
											A_D	1	.065	.008	-.119	**-.878**	**.894**	-.189	-.283	-.307
												A_L	1	-.020	.144	-.087	.025	**.924**	**.659**	.384
													D_R	1	**.602**	-.134	.024	.028	**.462**	.235
														U	1	-.020	-.127	.232	**.488**	.351
															F	1	**-.987**	.091	.175	.215
																A	1	-.162	-.277	-.274
																	D	1	**.792**	**.602**
																		D_DA_D	1	**.785**
																			D_DA_L	1

Bold = correlation is significant at the 0.01 level (2-tailed).
Underline = correlation is significant at the 0.05 level (2-tailed).

Table 5.18 Linear Regression Model Summaries for Cove Sediments

Mean P= 773 ug/g (n=34) * Number in parentheses is significance of parameter.

Models	R^2	SE	Sig.	% Error	b_0	b_1	b_2	b_3
Depth	0.65	194	0.00	25	394.50	Depth(m) 28.95 (0.000)*		
2 Parameter Spatial	0.70	182	0.00	24	428.57	Depth(m) 31.01 (0.000)*	Urban(%) -31.90 (0.035)*	
3 Parameter Sed. Comp-Spatial	0.77	164	0.00	21	530.78	Depth(m) 28.52 (0.000)*	Urban(%) -37.26 (0.008)*	Sand(%) -9.08 (0.009)*
1 Parameter Geochemical	0.65	193	0.00	25	-27.78	Al(%) 790.71 (0.000)*		
2 Parameter Geochemical	0.86	125	0.00	16	-484.90	Ca(%) 93.48 (0.000)*	Fe(%) 626.77 (0.000)*	

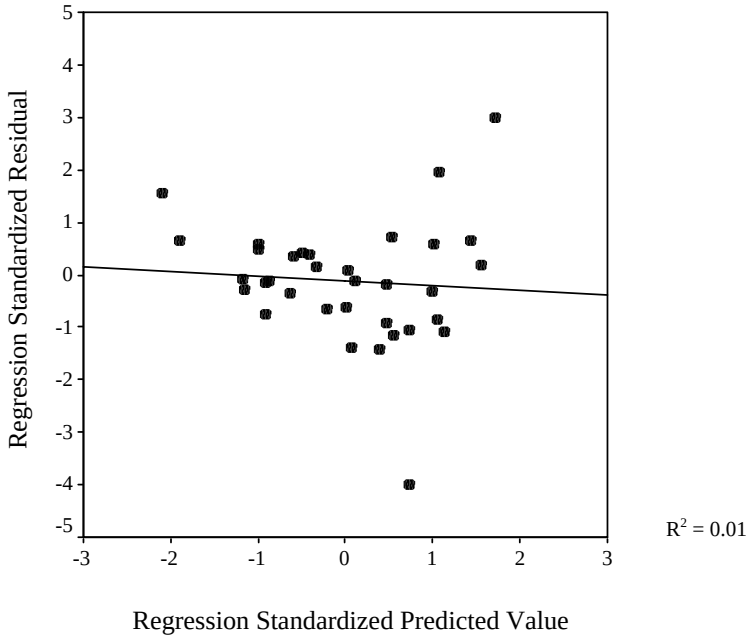

Figure 5.25. Residual Plots for Cove Model

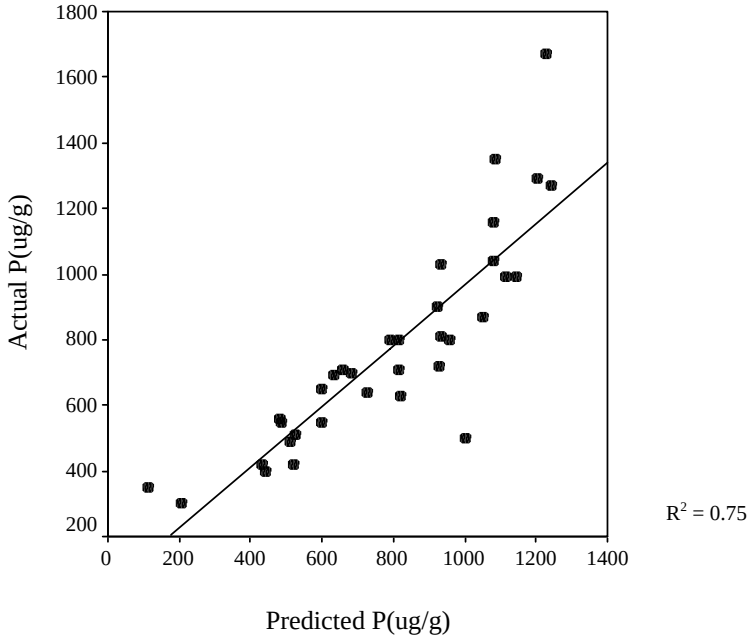

Figure 5.26. Predicted P(ug/g) vs. Actual P(ug/g) for Cove Model

accounts for sedimentation processes and changing aerobic conditions. The negative correlation between P and urban area in the cove watershed suggests development is not a source for P, however, this model does not account for size of cove or watershed which may dilute the P concentration.

Estimated Background P and Enrichment

As discussed earlier, P concentrations in coves generally are lower than P concentrations in arm sediments. Sediments in coves represent the less-polluted area of the JRA. Assuming that coves are not subjected to diffusional or current-driven inputs from the main valley of the JRA, and cove samples can be used to estimate a background P concentration at least removing the influence of P loading from the James River. Cove bottom sediments probably do not truly represent a completely uncontaminated sample. However, most cove samples are comparable to samples in Piney Creek cove, which is the most pristine area of the JRA, entirely draining forest lands. The combination of these factors coupled with the lack of understanding of background concentrations for bottom sediments in Table Rock Lake, cove samples were used to estimate a conservative background P concentration for bottom sediments.

Background P was estimated using the depth cove model and is compared to predicted P from the all arm sediment depth model. The cove depth model only accounts for 65% of the variance, which is low compared to other cove models. In this case however, the goal is to figure an enrichment factor and depth is the only common model between the arm and coves that had a relatively high correlation with P. Table 5.19 shows a comparison of the two models. These two models were run using depth data from the main arm and an enrichment ratio was calculated on the difference.

Table 5.19 Summary of models used to Develop Enrichment Ratio

Location	Model	R^2	Mean P ug/g	SE	Sig.	% Error	b_0	b_1
Cove (n=34)	Depth	0.65	773	194	0.00	25	394.50	Depth (m) 28.95 (0.000)*
Arm (n=71)	Depth	0.77	1116	297	0.00	27	452.58	Depth (m) 39.24 (0.000)*

Results of the two depth models are compared with distance from Galena (Figure 5.27). From 10 to 25 km from Galena, the two models are fairly close being within the standard error of the models. Between 25 and 63 km the enrichment is higher than the standard error of the arm model, which is about 300 ug/g. At distances less than 25 meters, which are shallow, concentrations are similar different between coves and the main valley. The enrichment increases with increasing depth after 25 meters, which is about 15 meters deep, which again illustrates how P is tied to sedimentation patterns and the ability of the lake to trap P in deeper areas.

The P-enrichment ratio is calculated by dividing the main valley predicted depth model P concentrations by the estimated background-P concentration. Enrichment of P in sediments ranges from a maximum of around 1.31 (24%) down-lake, in deeper areas and a minimum of about 1.15 (13%) up-lake, in shallower areas (Figure 5.28). Since the background concentrations are based on cove sediments, these comparisons indicate that coves sediments and shallow sediments of the main valley may be similar in P storage. While in deeper areas of the main valley, enrichment is higher where much of the P has settled out and is trapped in deeper sediments. The enrichment ratio seems to level out in the deepest areas of the main valley. The accuracy of the enrichment ratio at these depths

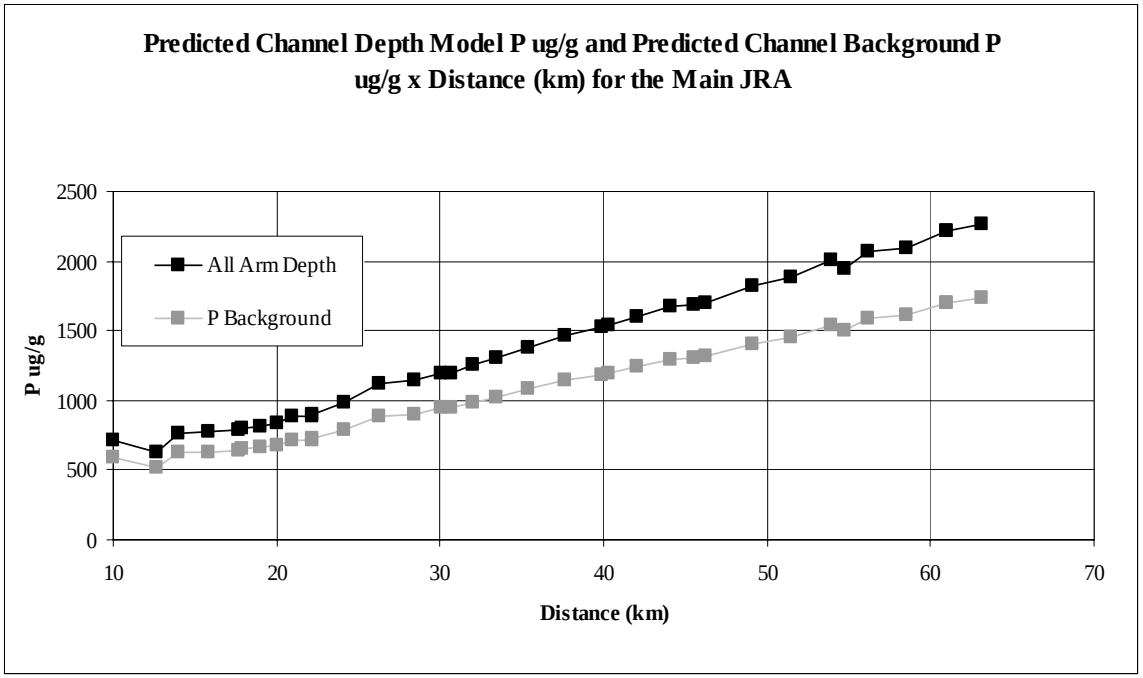

Figure 5.27. Comparison of Modeled P(ug/g) vs. Distance (km) from Galena

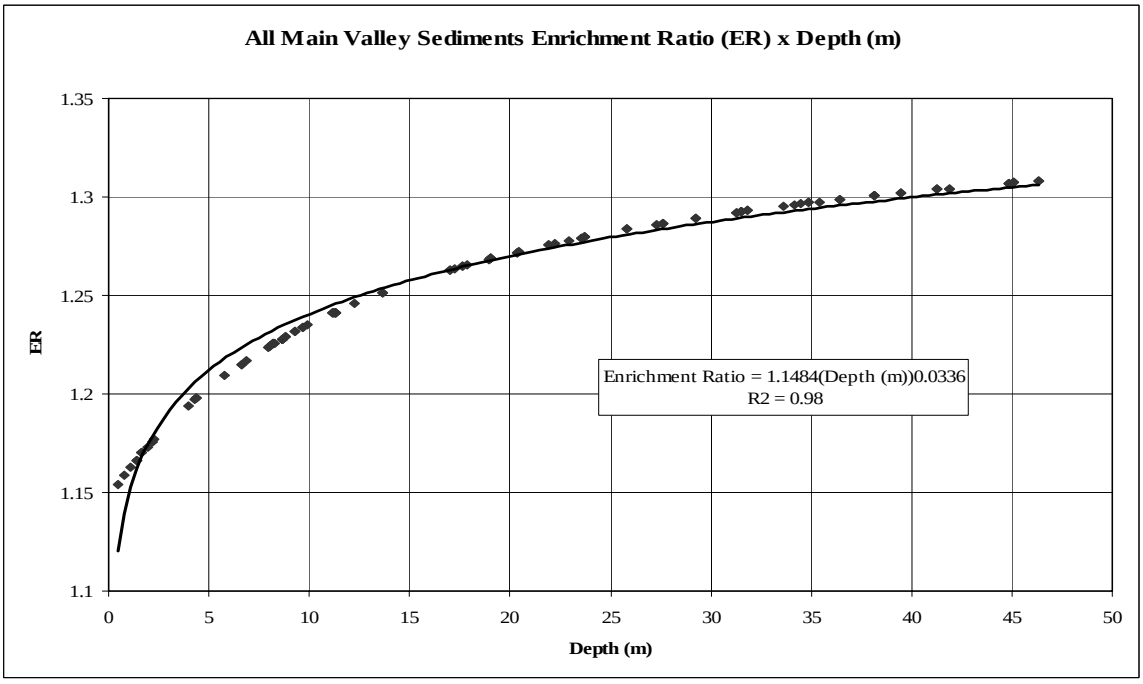

Figure 5.28. Enrichment Ratio versus Depth (m)

is lower because representative samples from coves do not go this deep. However, the data indicates enrichment of main valley sediments compared to cove sediments is not as drastically different as might be expected.

TOTAL P-STORAGE, LOADING, AND ANNUAL BUDGET

This section describe the estimated total-P stored in the top 5 cm of sediment and in the water-column by section, annual loading by section, and an annual P budget by section in the main valley of the JRA. Using these estimates a total-P accumulation rate was calculated.

P-Mass Storage in Recent Arm Sediments

Using the sediment mass and the average P concentration (ug/g) for each section of the main valley, a stored P-mass for the upper 5 cm of bottom sediment was estimated (Table 5.20). Sediment volume and mass increase down-lake, but density decreases. This density decrease is probably due to the increasing percentage of organic matter in sediments in deep areas and the accumulation of course-grain sediments from the James River being stored up-lake in the JRA. Stored P-mass also increases down-lake with 93.14 Mg in the upper section, 366.05 Mg in the middle section, and 820.66 Mg in the lower section (Table 5.21).

Mass Water-column P

The CSA's and the best-fit line used to estimate water-column P are found in Table 5.22 and Figure 5.29. The best-fit line used to estimate water-column P by section is shown in Figure 5.30. The original water-column data is shown in Appendix E. A summary of these results is provided in Table 5.23. Water column P concentrations decrease down-arm from upper, middle, to the lower main valley of the JRA. The

Table 5.20. Estimation of Bottom Sediment Mass

Section	Distance (km)	Avg. Sediment Width (m)	Length (m)	Depth (m)	Volume (m3)	Density (Mg/m3)	Sediment Mass (Mg)
Upper	10-25	147	15,000	0.05	110503.61	1.06	116999.51
Middle	26-45	330	19,000	0.05	313442.35	1.00	314498.18
Lower	46-63	614	17,000	0.05	521938.25	0.90	469618.17

Table 5.21. Estimated P-Storage in Bottom Sediments

Section	Sediment Mass (Mg)	Avg P(g/Mg)	Stored P-Mass (Mg)
Upper	116999.51	796	93.14
Middle	314498.18	1164	366.05
Lower	469618.17	1748	820.66

average estimated concentration in the upper section is 219 (ug/L). This decreases to 105 (ug/L) in the middle section and 47 (ug/L) in the lower section. While P concentrations decrease lake volume increases from about 8,600,000 m^2 in the upper section to 80,700,000 m^2 in the middle section and to 189,900,000 m^2 in the lower section. So, while concentrations decrease down-lake, actual P-mass increases down-arm in the water column. Estimated water column-P mass in the upper main valley of the JRA is 1.9 Mg, 8.5 Mg in the middle main valley, and 8.9 Mg in the lower main valley of the JRA (Table 5.24). Total P held in the water column for the main valley of the JRA is 19.3 Mg.

Total mass-P in the main valley of the JRA represents both the amount of P dissolved and suspended in the water column, as well as the potentially available P in the top 5 cm of sediment. Totals from the estimated sediment mass and water column P calculations show the upper section of the main JRA valley has the lowest amount of mass P with 94.9 Mg (Table 5.24). The middle section total P mass is 374.9 Mg, while the lower section P mass is 829.9 Mg.

Table 5.22. Summary of CSA (m^2) Estimates

Transect	Distance (km)	Average Depth (m)	Width (m)	CSA(m^2)
A	11.6	1.26	83.8	105.63
B	17.7	3.19	91.4	291.97
C	22.2	5.99	304.8	1827.09
D	30.7	6.99	221.0	1545.31
E	40.3	13.05	472.4	6162.67
F	45.5	17.90	419.1	7500.26
G	54.8	17.86	723.9	12929.78
H	61.0	24.68	685.8	16924.61

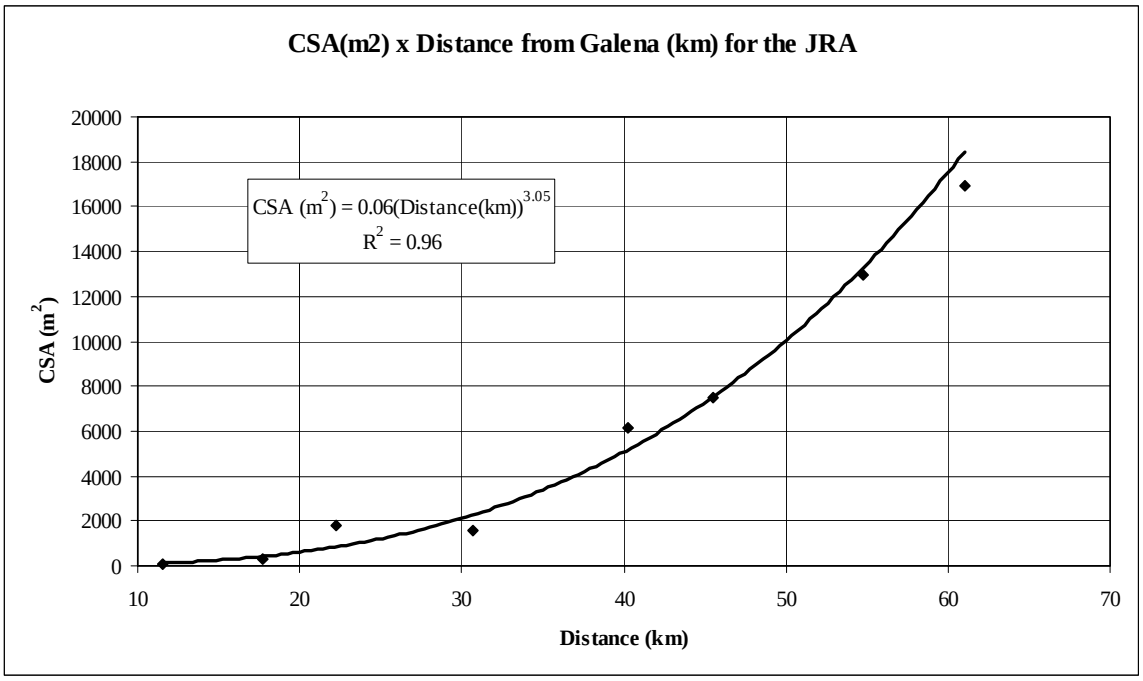

Figure 5.29. Cross-Sectional Area (m^2) vs. Distance from Galena (km)

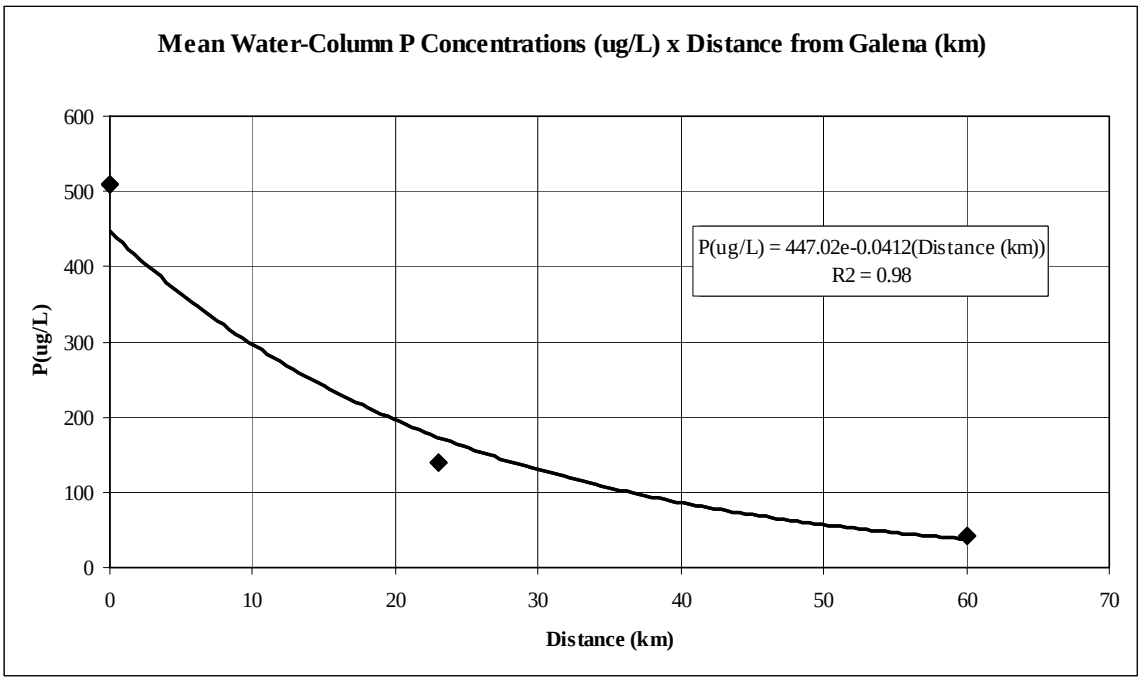

Figure 5.30. Water-column P (ug/L) vs. Distance from Galena (km)
(See data set in Appendix E.)

Table 5.23. Summary of Water-Column P Estimates

Location	Average CSA (m^2)	Total Distance (km)	Volume (m^3)	Average Water Column P (ug/L)	Water Column P(Mg)
Upper	541	16	8,660,269	219	1.9
Middle	4,039	20	80,775,880	105	8.5
Lower	12,662	15	189,934,474	47	8.9
Totals	-	51	279,370,623	-	19.3

Table 5.24. Total Mass-P Stored in the Main Valley

Location	Sediment Mass P (Mg) Top 5 cm	Water Column P (Mg)	Total P Storage (Mg)
Upper	93	1.9	94.9
Middle	366	8.5	374.5
Lower	821	8.9	829.9

Trap Efficiency and Annual P-Budget for the JRA

The estimated annual load at Galena from the upper James River Basin is 473 Mg/yr entering the JRA, with an annual yield of 185 kg/km^2/yr (Table 5.25). The lower James River Basin load is only 7 Mg/yr with a yield of 6 kg/km^2/yr. The load decreases with distance from Galena from 206 Mg/yr (upper) to 93 Mg/yr (middle) to 45 Mg/yr (lower). The reading at the lower section is actually the entire James River Basin load going to the White River. Loads from the lower basin are based on estimated inflow P concentration of only 16 ug/L and probably are low for watersheds such as Aunts Creek, which has the highest amount of urban area of any watershed in the lower basin. However, these loads would still be dwarfed by the high discharge and P concentrations entering the JRA at Galena.

Annual P storage in the upper section is 272.8 Mg, 113.5 Mg in the middle section, and 48.7 Mg in the lower section (Table 5.26). Based on these estimates, the trap efficiency of each section of the JRA is roughly 50% (52% - 57%) diminishing the load by half in each section. Total annual sediment-P mass storage decreased down arm from 271 Mg (upper), to 105 Mg (middle), to 40 Mg in the lower section. The sedimentation rates based on P storage in the upper section was 14.6 cm/yr, 1.4 cm/yr in the middle section, and 0.2 cm/yr in the lower section. This sedimentation rate does not take into account biological uptake. Even though the sedimentation rate may be overestimated in the upper section, coupled with the low loading time, this area receives high P load in a short amount of time. Totals for the entire JRA show a total annual P storage of 435 Mg for a trap efficiency of 91%. Total annual sediment P storage is 416 Mg with a P sedimentation rate of 1.6 cm/yr. Figure 5.31 is a summary of the annual JRA P budget.

Table 5.25. Annual P Load and Yield Estimates

Location	Ad km^2	mean Q cms	Avg P (mg/L)	Daily Load (Mg/d)	Annual Load (Mg/yr)	Annual Yield (kg/km2/yr)
Upper James River Basin	2,562	29.41	0.51	1.296	473	185
Lower James River Basin	1,205	13.83	0.016	0.019	7	6
Upper Coves	1,000	11.48	0.016	0.016	5.8	6
Upper JRA	3,562	40.9	0.16	0.565	206	58
Middle Coves	92	1.06	0.016	0.001	0.5	6
Middle JRA	3,654	41.95	0.07	0.254	93	25
Lower Coves	113	1.3	0.016	0.002	0.7	6
Lower JRA	3,767	43.25	0.033	0.123	45	12

Table 5.26. Annual P Budget, Trap Efficiency, and Accumulation

Location	Annual Load (Mg)	Annual Storage (Mg)	Trap Efficiency (%)	Water Column-P (Mg)	P Deposit-ion Rate (Mg/yr)	P in top 5 cm (Mg)	Sediment-ation Rate (cm/year)	Loading Time
James River	473							
Upper Coves	5.8							
Upper JRA	206	272.8	57	1.9	271	93	14.6	4.1 months
Middle Coves	0.5							
Middle JRA	93	113.5	55	8.5	105	366	1.4	3.5 years
Lower Coves	0.7							
Lower JRA	45	48.7	52	8.9	40	821	0.2	20.5 years
Totals (at White River)	45	435	91	19.3	416	1280	1.6	3.1 years

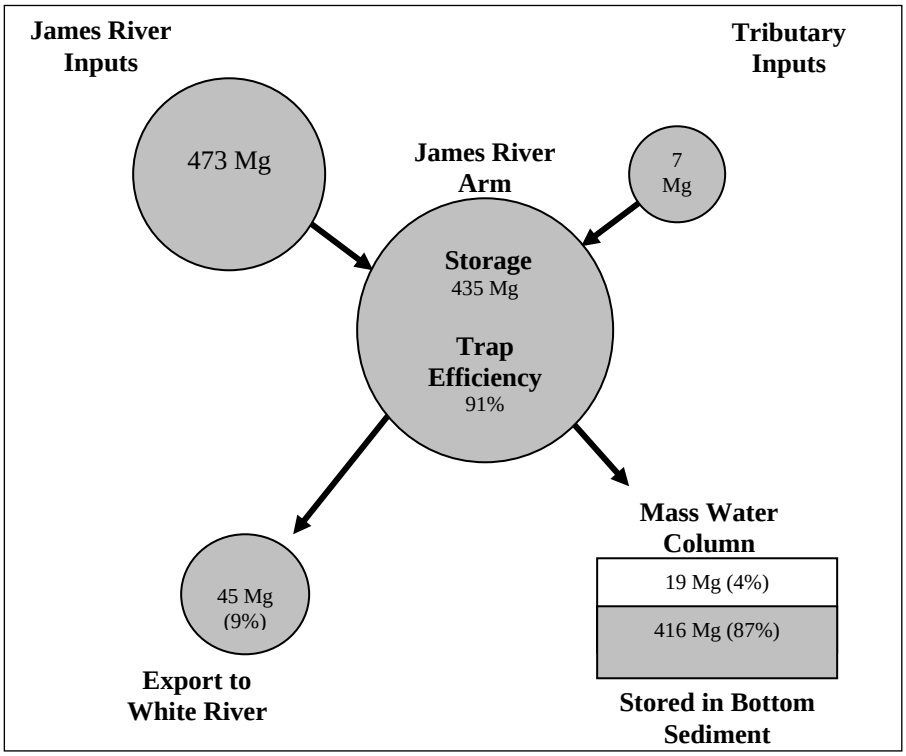

Figure 5.31. Annual P-Budget and Estimated Storage

SUMMARY

Spatial Patterns

In the main valley of the JRA, P concentrations increase down-arm from Galena in bottom sediments following the old channel. Concentrations of P also increase toward the deepest part of a transect across the main valley. However, variation in P concentrations is greatest in the shallower areas in the upper section of the main valley. Generally, P concentrations increase with depth along the main valley.

Cove sediments contain less P than the main valley of the JRA. Further investigation revealed the coves might actually dilute P concentrations in the main valley near confluences. This does not suggest the cove watershed areas are not polluting the lake, but P inputs at Galena are overwhelming the system and it would be more cost

effective to focus management efforts there. Regression modeling aimed at linking watershed characteristics, such as land use, to high P concentrations in cove sediments were unsubstantiated.

Sediment Geography, Composition, and Geochemistry

Statistical analyses show that Fe is highly correlated with P in bottom sediments of the main valley, while Fe and Ca are more P important in the coves. Iron, in aerobic or anaerobic conditions, is highly correlated with P within the entire JRA at all depths. In addition, sediment clay percentage and Fe concentration are also positively related. In the coves, Ca emerges as an important variable. It is unclear exactly how Ca is correlated with P, but previous studies suggest during low flow the majority of P entering the JRA is dissolved and the precipitation of $CaCO_3$ is the major source of P sedimentation at these flows (Knowlton and Jones, 1989).

Comparing shallow and deep areas of the main valley also helps to show differences in the P cycling process. In the shallow areas (< 12 m) of the main valley, Fe, distance, and silt % explain 88% of the variance of P in bottom sediments. Again, the actual geochemical role Fe has in P accumulation at these depths is unknown, only that there is a significant correlation. Distance actually has a negative correlation in the shallow sediments and could be misinterpreted as having higher P concentrations closer to Galena. This is not necessarily true because shallow samples from transect sites further down-arm have lower concentrations because sediment focusing transports fine-grain sediments and higher P concentrations near the channel at these locations, which are at depths >12 meters. Relatively high amounts of silt are present in these sediments,

so changes in silt % would tend to predict better than sand %, which is found at much lower amounts.

Approximately 81% of the variability of P in deep (>12 m) sediments of the main valley can be explained by the concentration of Fe in sediments. Again, the specific geochemical relationship between Fe and P was not measured and the possible relationships in sediments have been discussed previously. The delivery of both Fe and P is probably due to fine-grain particles settling at these depths, but the accumulation is likely due to redox changes at these depths.

More than any other single variable, lake depth is the best at predicting P concentrations in sediment of the JRA. This is due to the fact that studying the depth of sediment in a reservoir situation can give a 3-dimensional picture of P concentrations in sediment by describing the geography of the JRA and identifying two very influential processes that account for its accumulation. Spatially, the old channel is the deepest point at any cross-section of the JRA and gradually increases in depth down-arm. The first process is the variable of sediment composition or grain-size. Since fine-grain sediment can absorb more P than coarse sediments, the fining of sediment down-lake and sediment focusing move fine grain sediment into the deeper areas of the JRA. The second process the depth variable accounts for is aerobic conditions. Summer stratification of the JRA cause anaerobic conditions below the 12-15 meter mark where sediments are a sink for P and other important geochemical variables.

Anthropogenic Enrichment

The anthropogenic influences of P are described by two methods. The first is the often used P/Al ratio. This ratio takes out the influence of grain size and highlights

enrichment because Al is so closely related to clay particles with high absorptive surfaces and is stable under changing aerobic conditions. Comparing the P/Al ratio in the main valley with that in the coves shows an important point about cove size. Smaller coves and the main valley have the same ratio of P to Al suggesting a movement of sediments from the main valley into these small coves. On the other hand, the larger coves have a much lower P/Al ratio which may have sediment P concentrations closer to background. Looking down-arm, the P/Al ratio is fairly consistent from Galena to after Piney Creek cove where it is elevated to the confluence of the White River.

The amount of enrichment displayed in the main valley over that in the coves is shown in an enrichment ratio developed from regression modeling of sediment-P from the coves using main valley samples. The only variable in the model was depth and it was compared to the main valley depth model to achieve the ratio. Enrichment ranged from 1.15 (13 %) to 1.3 (24 %) times the cove background in main valley sediments. The lower ratio was found in the shallow areas and the higher ratio in the deep areas of the main valley of JRA. This shows that even a relatively small enrichment of P in sediments can result from a eutrophic condition in a reservoir setting.

Loading Balance and Annual P-Budget

Estimating the storage of P in the top 5 cm of sediments showed an increase down-arm from Galena. While previous studies show higher P concentrations in the upper sections of the main valley, total P in the water-column by volume increases down-arm. Nevertheless, by using an annual P-budget, it is estimated that the JRA traps approximately 91% of P coming in at Galena. The contributions of P from the coves are minimal, however, an estimated 45 Mg of P is delivered to the White River annually.

If conservative behavior between P concentration and sediment transport is assumed, the annual P-budget also shows that the upper section of the main valley receives sediment at a rate of 14.6 cm/yr. While much of that P is not stationary, this does show that this section can receive high amounts of P quickly. It is in this section where algal blooms have been noted. The shallow nature of this section already makes this area susceptible to eutrophic conditions because sunlight can penetrate to the bottom and is fed by how rapidly P can be delivered. The sedimentation rate decreases down-arm from 1.4 cm/yr in the middle section, to 0.2 cm/yr in the lower section. The total sedimentation rate for the JRA based on P storage is 1.6 cm/yr. Slight error in estimation of water-column total P can influence storage estimates due to relatively narrow lake and steeply decreasing total P concentration in the water-column.

Future Study

The overwhelming majority of P in the JRA is coming into the lake at Galena and that P has been linked to wastewater treatment facilities located in the upper James River Basin. The number one goal for management is without a doubt to reduce P coming from those facilities. Already, Springfield has reduced its P output by over 90% reducing P concentrations at Galena during baseflow from 510 ug/L to 108 ug/L (Pavlowsky, 2001). However, even after this reduction physical and chemical changes in the arm will take a long period of time due to the total amount of P stored in sediments that has the potential to be re-released when P loading is reduced. Fortunately, P can be trapped in sediments but only a detailed investigation using coring techniques and geochemical fractionation will be able to estimate the total mass P available to the water column. Furthermore, the amount of P being removed by biological uptake is unknown.

CHAPTER 6

CONCLUSIONS

The JRA of Table Rock Lake has suffered from higher than normal P contributions from the James River Basin. This influx of P has resulted in degraded water quality in the form of eutrophic conditions. Previous studies have shown that the upper JRA has some of the highest P concentrations of any reservoir in Missouri. Many of these studies tend to focus on dissolved-P in the water column and P absorbed to suspended sediments. These studies typically do not account for P stored in bottom sediment, which is important in P-cycling in aquatic environments. This study examines the spatial distribution of P in the top 5 cm of bottom sediment throughout the JRA to identify key variables for P accumulation in sediments, identify potential sources, estimate available P in storage, and develop an annual P-budget based on these findings. The major findings of this study are:

1. Phosphorus concentrations in the JRA increase with depth and distance from the mouth of the river at Galena for the main valley and at the stream mouth for coves.

These basic spatial patterns of P concentrations are actually a good explanation for the sedimentation and geochemical factors that cause P to be concentrated in some areas and not in others. The further the distance from the mouth of the stream entering the lake the more clay is found in the sample. Clay has a higher ability to absorb P than coarser sediments such as sand. First, fine grained sediments get focused in the deepest portion of the lake. This is true down-arm as the mean depth of the lake increases, but also along a particular transect across the lake due to wind and wave action. Second, depth is important for the presence or absence of oxygen. In aerobic conditions during

the fall, winter, and spring, P will be concentrated in sediments and Fe and Mn oxide coatings. In the shallow portions of the lake, <12 meters, late spring eutrophic conditions can deplete the dissolved oxygen in the water and P can hence be released to the water column. During summer stratification, an anaerobic layer below 12 meters in depth can cause P to chemically release from sediments. At this depth however, P is confined to the sediments due to limited upward mobility at the redox boundary and lack of current and wind action. Therefore, high P concentrations can be relatively immobile at these depths.

2. Phosphorus concentrations in the JRA are highly predictable using a combination of spatial, sediment composition, and geochemical variables.

Empirical multi-variat regression modeling was used to explain the spatial distribution of P in bottom sediments of the JRA. Variables used in this modeling included spatial, sediment composition, and geochemical data from bottom sediment sampling sites. An overall model was used and P concentrations had very good correlations with depth of the sample, Mn, and Ca accounting for 91% of the variability within an error of 15%. This suggests that a wide range of factors account for overall P storage in bottom sediments including grain size, aerobic conditions, and the various ways Ca can be associated with P. However, when modeling for specific areas within the JRA, more representative variables can be highlighted. These specific areas were the shallow sediments of the main valley (Fe, Distance, and Silt, R^2=0.88, SE=19%), the deep sediments of the main valley (Fe, R^2=0.81, SE=12%), and cove sediments (Fe and Ca, R^2=0.86, SE=16%). The cove model using the spatial variable depth was then used to estimate enrichment within the main valley.

3. Phosphorus concentrations in the main valley of the JRA are 13 - 24 % higher than in the coves.

Comparisons of bottom sediment samples at confluences of coves showed higher P concentrations in the main valley. This occurred even at similar depths suggesting coves have sediment-P concentrations closer to background levels. When adjusting for differences in grain size using the P:Al ratio, samples in the coves with small watersheds had similar concentrations to the main valley. This implies P could be entering these small coves from the main valley. This phenomena did not exist in the larger coves suggesting these coves may have the ability to flush out P from the main valley.

Using the cove model to conservatively estimate P enrichment, main valley concentrations are 1.15 (13 %) times higher in the shallow areas to 1.3 (24 %) times higher than in cove sediments. This does not imply the coves are not enriched in P, but that concentrations in coves are lower than in the main valley. The spatial distribution of P enrichment shows the highest area of enrichment occurs in the lower section of the main valley. This section of the main valley is the furthest from the source, at the greatest depth, and is the closest section to the main lake.

4. Annual P-budget shows 91% trap efficiency and a sedimentation rate of 1.6 cm/yr for the JRA.

While P loading decreases down-lake, storage increases with each section of the main valley reducing the load approximately in half. The JRA receives about 473 Mg/yr P at Galena from the upper basin and 7 Mg/yr P from the JRA coves and exports approximately 45 Mg of P per year for a trap efficiency of 91%. Estimated sediment accumulation rates decrease down-arm from 14.6 cm/yr in the upper section, to 1.4 cm/yr

in the middle section to 0.2 cm/yr in the lower section, averaging 1.6 cm/yr for the entire JRA.

5. Implications for lake and reservoir bottom sediment research

Bottom sediment studies in reservoirs rarely incorporate the spatial distribution of pollution storage when predicting temporal loading rates. Typically, researchers take a few cores and use a stratigraphic marker, such as Cs-137, to estimate loadings and storage. What this research seems to miss is accounting for differences in concentrations and sediment with distance from mouth, depth, and lateral position on the flooded reservoir floor. Depth is a very important factor in the spatial distribution of P for a couple of reasons. This high correlation between depth and P displays reservoir sedimentation and seasonal aerobic conditions are responsible for the presence of P in the sediments attached to clay particles, incorporated in the mineral matrix and organic matter, or by absorption by Fe and Mn coatings. A sampling scheme must incorporate channel and valley bottom sediments at several transect locations down-lake to account for the 3-dimensional variation in concentrations and mass storage within a river-lake transition system such as studied here in the James River Arm of Table Rock Lake.

LITERATURE CITED

Adamski, J.C., J.C. Petersen, D.A. Freiwald, and J.V. Davis, 1995. Environmental and Hydrologic Setting of the Ozark Plateaus Study Unit, Arkansas, Kansas, Missouri, and Oklahoma. U.S. Geological Survey Water-Resources Investigations Report 94-4022.

Aldrich, M.W., D. Meinert, 1994. Soil Survey of Barry County, Missouri. United States Department of Agriculture Soil Conservation Service.

Anderson, J.R., E. Hardy, J. Roach, and R. Witmar, 1976. A Land Use and Land Cover Classification System for Use with Remote Sensing Data. Washington DC. U.S. Geological Survey Professional Paper 964, 28 p.

Aslan, A. and W. J. Autin, 1998. Holocene Flood-plain Soil Formation in the Southern Lower Mississippi Valley: Implications for Interpreting Alluvial Paleosols. GSA Bulletin 110(4):433-449.

Baccini, P., 1985. Phosphate Interactions at the Sediment-Water Interface. Chemical Processes in Lakes. Edited by W. Stumm. New York: John Wiley and Sons, 189-205.

Beach, T., 1994. The Fate of Eroded Soil: Sediment Sinks and Sediment Budgets of Agrarian Landscapes in Southern Minnesota, 1851-1988. Annual of the Association of American Geographers, 84(1):5-28.

Berkas, W.R. 1989. Sedimentation of Lake Taneycomo, Missouri, 1913-1987. U.S. Geological Survey Water-Resources Investigations Report 89-4160.

Brenner, M., L.W. Keenan, S.J. Miller, and C.L. Schelske, 1999. Spatial and Temporal Patterns of Sediment and Nutrient Accumulation in Shallow Lakes of the Upper St. Johns River Basin, Florida. Wetlands Ecology and Management, 6:221-240.

Calcagno, T.H. and G.M. Ashley, 1984. Sedimentation Processes in an Impoundment, Union Lake, New Jersey. Environmental Geology Water Science, 6(4):237-246.

Carlson, J.L., 1999. Zinc Mining Contamination and Sedimentation Rates of Historical Overbank Deposits, Honey Creek Watershed, Southwest Missouri. Unpublished Masters Thesis. Springfield, Missouri: Southwest Missouri State University, Department of Geography, Geology, and Planning.

Chalmers, A.T., 1998. Distribution of Phosphorus in Bed Sediments of the Winoosk River Watershed, Vermont, 1997. U. S. Geological Survey Fact Sheet FS-108-98.

Clark, G.M., D.K. Mueller, and M.A. Mast, 2000. Nutrient Concentrations and Yields in Undeveloped Stream Basins of the United States. Journal of the American Water Resources Association, 36(4), 849-860.

Combest, K.B., 1991. Trace Metals in Sediments: Spatial Trends and Sorption Processes. Water Resources Bulletin, 27(1), 19-28.

Davison, W., 1985. Conceptual Models for Transport at a Redox Boundary. Chemical Processes in Lakes. Edited by W. Stumm. New York: John Wiley and Sons, 31-49.

Eadie, B. J., H. A. Vanderploeg, J. A. Robbins, and G. L. Bell, 1990. Significance of Sediment Resuspension and Particle Settling. In Large Lakes Ecological Structure and Function. Edited by Max M. Tilzer and Colette Serruya. Berlin: Springer-Verlag.

Elliot, W. J., and A. D. Ward, 1995. Soil Erosion and Control Practices. Environmental Hydrology. Edited by A.D. Ward and W.J. Elliot. Boca Raton: Lewis Publishers, 177-202.

Faulkner, D. and S. McIntyre, 1996. Persisting Sediment Yields and Sediment Delivery Changes. Water Resources Bulletin, 32(4):817-829.

Forstner, U., 1989. Contaminated Sediments. Lecture Notes in Earth Sciences. Edited by S. Bhattacharji, G.M. Friedman, H.J. Neugebauer and A. Seilacher. Berlin: Springer-Verlag, 31-55.

Fredrick, B. S. 2001. Spatial Distribution of Phosphorus in Fluvial Sediments from the James River, SW Missouri. Unpublished Masters Thesis. Springfield, Missouri: Southwest Missouri State University, Department of Geography, Geology, and Planning.

Graf, W. L. 1996. Transport and Deposition of Plutonium-Contaminated Sediments by Fluvial Process, Los Alamos Canyon, New Mexico. GSA Bulletin, 108(10):1342-1355.

Graneli, W., 1999. Internal Phosphorus Loading in Lake Ringsjon. Hydrobiologia, 404:19-26.

Greene County Missouri, 2003. Greene County Regulations and Standards for On-Site Wastewater Systems. Greene County Resource Management Department, October 2001.

Hakanson, L and M. Jansson, 1983. Principles of Lake Sedimentology. Berlin: Springer-

Verlag.

Hem, J.D. 1985. Study and Interpretation of the Chemical Characteristics of Natural Water (3rd Edition). U.S. Geological Survey Water-Supply Paper 2254.

Hilton, J., J. P. Lishman, and P. V. Allen, 1986. The Dominant Processes of Sediment Distribution and Focusing in a Small, Eutrophic, Monomictic Lake. Limnol. Oceanogr., 31(1): 125-133.

Horowitz, A. J., 1991. Sediment-Trace Element Chemistry (2nd Edition). Lewis Publishers: Chelsea, Michigan.

Hughes, H.E., 1982. Soil Survey of Greene and Lawrence Counties, Missouri. United States Department of Agriculture Soil Conservation Service.

Hyatt, J. A. and Gilbert, R., 2000. Lancastrian Sedimentary Record of Human-Induced Gully Erosion and Land-Use Change at Providence Canyon, Southwest Georgia, USA. Journal of Paleolimnology, 23: 421-438.

Jacobson, R.B. and A.T. Primm, 1997. Historical Land-Use Changes and Potential Effects on Stream Disturbance in the Ozark Plateaus, Missouri. United States Geological Survey Water-Supply Paper 2484, 85 pp.

Johnson, M.G. and K. H. Nicholls, 1989. Temporal and Spatial Variability in Sediment and Phosphorus Loads to Lake Simcoe, Ontario. J. Great Lakes Res. 15(2): 265-282.

Jones, J. R. and M. F. Knowlton, 1993. Limnology of Missouri Reservoirs: An Analysis of Regional Patterns. Lake and Reservoir Management, 8: 17-30.

Juracek, K. E. 1998. Analysis of Lake-Bottom Sediment to Estimate Historical Nonpoint-source Phosphorus Loads. Journal of the American Water Resources Association, 34(6):1449-1463.

Kiner, L. K. and C. Vitello, 1997. James River Basin Inventory and Management Plan. Missouri Department of Conservation.

Klump J. K., D. N. Edgington, P. E. Sager, and D. M. Robertson, 1997. Sedimentary Phosphorus Mass Balance for the Green Bay Ecosystem. Can. J. Fish. Aquat. Sci. 54:10-26.

Knowlton, M.F. and J.R. Jones, 1989. Summer Distribution of Nutrients,

Phytoplankton and Dissolved Oxygen in Relation to Hydrology in Table Rock Lake, a Large Midwestern Reservoir. Arch. Hydrobiol./Suppl. 83(2):197-225.

Knox, J. C., 1977. Human Impacts on Wisconsin Stream Channels. Annuals of the Association of American Geographers, 67(3):323-342.

Knox, J. C., 1987. Historical Valley Floor Sedimentation in the Upper Mississippi Valley. Annuals of the Association of American Geographers, 75:583-594.

Lakes of Missouri Volunteer Program, 1998. Table Rock Lake and Lake Taneycomo 1998 Data Report.

Leece, S. A. and R. T. Pavlowsky, 1997. Storage of Mine-Related Zinc in Floodplain Sediments, Blue River, Wisconsin. Physical Geography, 18:424-439.

Lewin, J., B. E. Davies, and P. J. Wolfenden, 1977. Interactions Between Channel Change and Historic Mining Sediments. River Channel Changes, Chichester: John Wiley, 353-367.

Logan, T.J., 1995. Water Quality. Environmental Hydrology. Edited by A.D. Ward and W.J. Elliot. Boca Raton: Lewis Publishers, 311-336.

Mantei, E. J. and E. J. Sappington, 1994. Heavy Metal Concentrations in Sediment of Streams affected by a Sanitary Landfill: A Comparison of Metal Enrichment in Two Size Sediment Fractions. Environmental Geology, 24: 287-292.

McCallister, D.L. and T.J. Logan, 1978. Phosphate Adsorption-Desorption Characteristics of Soils and Bottom Sediments in the Maumee River Basin of Ohio. Journal of Environmental Quality, 7(1):87-92.

Meals, D.W. and L.F. Budd, 1998. Lake Champlain Basin Nonpoint Source Phosphorus Assessment. Journal of the American Water Resources Association, 34(2):251-265.

Meade, R. H., 1982. Sources, Sinks, and Storage of River Sediment in the Atlantic Drainage of the United States. Journal of Geology, 90: 235-252.

Missouri Department of Natural Resources, 1999. Table Rock Lake Phosphorus Advisory Committee Report.

Missouri Department of Natural Resources, 2001[a]. What are TMDL's? Division of Environmental Quality Water Pollution Control Program Fact Sheet.

Missouri Department of Natural Resources, 2001[b]. Draft: Total Maximum Daily Load Analysis James River near Springfield in Webster, Greene, Christian and Stone

Counties, Missouri.

Morris, G. L. and J. Fan, 1998. Reservoir Sedimentation Handbook. McGraw-Hill: New York.

Novotny, V. and G. Chesters, 1989. Delivery of Sediment and Pollutants from Nonpoint Sources: A Water Quality Perspective. Journal of Soil and Water Conservation, November-December, 568-576.

Owen, M.R., 2000. Historical Mining Pollution and Overbank Sedimentation along the James River, SW Missouri. Illustrated Paper. The Association of American Geographers 96th Annual Meeting 4-8 April 2000, Pittsburgh Pennsylvania.

Pavlowsky, R. T., 1995. Spatial Variability of Mining-Related Zinc and Lead in Fluvial Sediments, Galena Watershed, Wisconsin-Illinois. Ph.D. Dissertation, Department of Geography, University of Wisconsin, Madison.

Pavlowsky, R. T., 2001. TMDL Report.

Pavlowsky, R.T., 2002. Personal Communication.

Petersen, J. C.; J. C. Adamski; R. W. Bell; J. V. Davis; S. R. Femmer; D. A. Freidwald; and R. L. Joseph, 1998. Water Quality in the Ozark Plateaus, Arkansas, Kansas, Missouri, and Oklahoma, 1992-1995. United States Geological Survey Circular 1158.

Petersen, M.S., 1986. River Engineering. Prentice-Hall: Englewood Cliffs, New Jersey.

Phillips, J.D., 1986. The Utility of the Sediment Budget Concept in Sediment Pollution Control. Professional Geographer, 38(3):246-252.

Pizzuto et al, 2000. Comparing Gravel-Bed Rivers in Paired Urban and Rural Catchments of Southeastern Pennsylvania. Geology, 28(1):79-82.

Pierzynski, G.M., J.T. Sims, and G.F. Vance, 1994. Soils and Environmental Quality. Lewis Publishers: Boca Raton

Rafferty, M.D., 1980. The Ozarks Land and Life. University of Oklahoma Press.

Reddy, K.R., G.A. O Connor, and P.M. Gale, 1998. Phosphorus Sorption Capacities of Wetland Soils and Stream Sediments Impacted by Dairy Effluent. Journal of Environmental Quality, 27:438-447.

Sanei, H., F. Goodarzi, L.R. Snowdon, L.D. Stasiuk, and E. Van Der Flier-Keller, 2000. Characterizing the Recent Sediments from Pigeon Lake, Alberta as Related to Anthropogenic and Natural Fluxes. Environmental Geosciences, 7(4):177-189.

Sauer, C.O., 1920. The Geography of the Ozark Highland of Missouri. Greenwood Press: New York.

Sharpley, A.N., T. Daniel, T. Sims, J. Lemunyon, R. Stevens, and R. Perry, 1999. Agricultural Phosphorus and Eutrophication. United States Department of Agriculture, Agriculture Research Service ARS-149.

Schumm S.A. and M.D. Harvey, 1982. Natural Erosion in the USA. Determinants of Soil Loss Tolerance. ASA special publication number 45. Published by the American Society of Agronomy and the Soil Science Society of America.

Spahr, N.E. and K.H. Wynn, 1997. Nitrogen and Phosphorus in Surface Waters of the Upper Colorado River Basin. Journal of the American Water Resources Association, 33(3):547-560.

Trimble, J. C., 2001. Spatial Patterns and Floodplain Contributions of Mining-Related Contaminants in Chat Creek Watershed, Southwest Missouri. Unpublished Masters Thesis. Springfield, Missouri: Southwest Missouri State University, Department of Geography, Geology, and Planning.

Trimble, S.W., 1977. The Fallacy of Stream Equilibrium in Contemporary Denudation Studies. American Journal of Science, 277:876-887.

Trimble, S. W., 1993. The distributed Sediment Budget Model and Watershed Management in the Paleozoic Plateau of the Upper Midwestern United States. Physical Geography, 14(3):285-303.

Uhlmann, D., M. Hupfer, and C. Appelt, 1997. Composition of Sediments in Drinking Water Reservoirs as a Basis for Assessment of Potential Changes in Water Quality. J Water SRT-Aqua, 46(2):84-94.

United States Army Corps of Engineers, 1985. Dissolved Oxygen Study Table Rock Dam and Lake White River, Missouri. Reconnaissance Report, Little Rock District.

Van Metre, P.C. and E. Callender, 1996. Identifying Water-Quality Trends in the Trintity River, Texas, USA, 1969-1992, using Sediment Cores from Lake Livingston. Environmental Geology 4:190-200.

Van Metre, P.C., E. Callender, and C.C. Fuller, 1997. Historical Trends in Organochlorine Compounds in River Basins Identified Using Sediment Cores from Reservoirs. Environmental Science and Technology, 31(8): 2339-2344.

Walling, D.E., T.A. Quine, and Q. He, 1992. Investigating Contemporary Rates of Floodplain Sedimentation. Lowland Floodplain Rivers: Geomorphological Perspectives. John Wiley & Sons Ltd.

Walling, D.E., 1999. Linking Land Use, Erosion and Sediment Yields in River Basins. Hydrobiologia, 410:223-240.

Watts, C.J., 2000. The Effect of Organic Matter on Sedimentary Phosphorus Release in an Australian Reservoir. Hydrobiologia, 431:13-25.

White, J.W., 2001. Spatial Assessment of Nonpoint Phosphorus Sources using Streambed Sediment Monitoring in the Kings River Basin, NW Arkansas. Unpublished Masters Thesis. Springfield, Missouri: Southwest Missouri State University, Department of Geography, Geology, and Planning.

Wilson, J.T. and P.C. Van Metre, 2000. Deposition and Chemistry of Bottom Sediments in Cochiti Lake, North-Central New Mexico. United States Geological Survey Water-Resources Investigations Report 99-4258.

APPENDIX A

Spatial Characteristics of Sample Locations

Site	Easting UTM NAD83 Zone 15n	Northing UTM NAD83 Zone 15n	Type	Location	Depth (m)	Distance (km)	Valley width (m)
1	454300	4070815	Channel	Main Valley	4.4	12.7	76
2	454219	4069591	Channel	Main Valley	8.0	14.0	46
3	455987	4069299	Channel	Main Valley	8.2	15.8	61
4	455653	4067555	Channel	Main Valley	8.8	17.9	168
5	454899	4066165	Channel	Main Valley	9.7	20.0	251
6	456191	4066311	Channel	Peach	4.3	0.6	3
7	453218	4068575	Channel	Flat	4.5	3.1	30
8	453602	4067507	Channel	Flat	5.4	4.9	175
9	454579	4067594	Channel	Flat	6.9	6.2	69
10	455285	4064917	Channel	Main Valley	11.2	22.2	305
11	455525	4063402	Channel	Main Valley	13.7	24.1	213
12	456654	4063392	Channel	Bear	6.3	0.7	84
13	454785	4061796	Channel	Main Valley	17.0	26.3	183
14	454012	4063338	Channel	Main Valley	17.6	28.4	206
15	452450	4063087	Channel	Main Valley	19.0	30.1	229
16	451490	4063822	Channel	Main Valley	20.4	32.0	267
17	452242	4062537	Channel	Main Valley	21.9	33.5	381
18	450396	4062598	Channel	Wooly	7.6	0.8	99
19	452109	4060620	Channel	Main Valley	23.7	35.4	290
20	453774	4059739	Channel	Main Valley	25.8	37.6	335
21	449165	4059526	Channel	Piney	5.6	1.0	30
22	449361	4059088	Channel	Piney	3.9	0.4	3
23	450255	4059835	Channel	Piney	12.3	2.2	114
24	451551	4059855	Channel	Piney	19.5	3.6	198
25	452532	4068158	Channel	Flat	1.2	0.5	3
26	452502	4069581	Channel	Flat	4.1	1.5	3
27	451465	4062432	Channel	Wooly	16.8	2.0	183
28	452619	4063968	Channel	Cape	8.3	0.4	84
29	454159	4071972	Channel	Main Valley	1.7	11.7	3
30	454100	4072594	Channel	Main Valley	3.8	11.1	3
31	454268	4073096	Channel	Swift	1.5	0.3	3
32	454538	4072898	Channel	Main Valley	4.5	10.4	49
33	454580	4072365	Channel	Main Valley	6.0	9.7	49
34	454663	4071666	Channel	Main Valley	2.6	9.0	49
36	454653	4071163	Channel	Main Valley	1.2	8.4	49
35	455126	4070773	Channel	Main Valley	-	7.8	49
37	455709	4071530	Channel	Main Valley	-	6.8	49
38	451858	4058950	Channel	Main Valley	27.3	39.9	442
39	450681	4057453	Channel	Main Valley	29.3	42.1	533
40	452414	4056135	Channel	Main Valley	31.2	44.1	762
41	454380	4055912	Channel	Main Valley	31.9	46.2	335
42	453490	4055119	Channel	Thompson	9.6	0.5	3
43	454105	4057091	Channel	Cedar	14.8	0.9	3

Site	Easting UTM NAD83 Zone 15n	Northing UTM NAD83 Zone 15n	Type	Location	Depth (m)	Distance (km)	Valley width (m)
44	455131	4057555	Channel	Main Valley	34.9	49.1	480
45	455334	4058402	Channel	Main Valley	36.4	51.4	869
46	455749	4059374	Channel	Main Valley	39.5	53.9	640
47	456481	4059967	Channel	Jackson	18.0	0.8	114
48	456813	4059440	Channel	Jackson	11.8	0.4	91
49	457443	4058198	Channel	Main Valley	41.3	56.1	457
50	456886	4055946	Channel	Main Valley	41.9	58.5	914
51	459327	4056172	Channel	Aunts	10.2	0.8	53
52	459148	4055913	Channel	Aunts	7.3	0.4	30
53	458457	4056063	Channel	Aunts	22.6	1.7	145
54	458172	4057204	Channel	Aunts	29.3	5.1	343
55	460684	4059973	Channel	Aunts	5.5	0.9	15
56	460222	4060104	Channel	Aunts	6.3	0.8	61
57	458928	4059146	Channel	Aunts	17.2	2.9	160
58	449883	4059679	Channel	Piney	9.7	1.7	191
59	450406	4060639	Channel	Piney	6.9	0.4	38
60	450935	4060243	Channel	Piney	16.9	3.0	183
61	463949	4082734	Stream	James	-	-	-
62	460477	4061328	Stream	Aunts	-	-	-
63	450031	4068206	Stream	Flat	-	-	-
64	445235	4061232	Stream	Piney	-	-	-
65	445438	4059943	Stream	Piney	-	-	-
66	460404	4076268	Stream	James	-	-	-
67	458728	4073760	Stream	James	-	-	-
68	458637	4072401	Stream	James	-	1.0	-
69	457712	4071774	Stream	James	-	2.7	-
70	457169	4070672	Stream	James	-	4.5	-
71	457222	4054959	Channel	Main Valley	45.1	60.9	686
72	458387	4053793	Channel	Main Valley	46.3	63.2	792
73	457707	4056575	Channel	Aunts	20.4	5.8	305
74	458784	4057615	Channel	Aunts	12.8	0.6	107
75	458395	4058284	Channel	Aunts	22.6	3.9	229
76	458694	4059674	Channel	Aunts	6.1	0.5	53
77	459865	4059461	Channel	Aunts	12.3	1.9	114
78	461307	4059922	Channel	Aunts	0.0	0.3	3
79	461509	4060023	Stream	Aunts	-	-	3
80	460913	4059628	Channel	Aunts	0.0	0.1	3
101	455622	4067941	Valley	Main Valley	1.7	17.7	91
102	455675	4067927	Valley	Main Valley	2.3	17.7	91
103	455718	4067894	Valley A	Main Valley	4.0	17.7	91
104	455718	4067894	Valley B	Main Valley	4.0	17.7	91
105	455718	4067894	Valley C	Main Valley	4.0	17.7	91
106	455772	4067876	Valley	Main Valley	5.8	17.7	91

Site	Easting UTM NAD83 Zone 15n	Northing UTM NAD83 Zone 15n	Type	Location	Depth (m)	Distance (km)	Valley width (m)
107	455791	4067843	Channel A	Main Valley	8.6	17.7	91
108	455791	4067843	Channel B	Main Valley	8.6	17.7	91
109	455791	4067843	Channel C	Main Valley	8.6	17.7	91
110	455268	4065076	Channel	Main Valley	11.3	22.2	305
111	455329	4065139	Valley	Main Valley	9.9	22.2	305
112	455446	4065158	Valley	Main Valley	7.9	22.2	305
113	455577	4065130	Valley	Main Valley	6.9	22.2	305
114	452327	4063864	Valley	Main Valley	1.7	30.7	221
115	452316	4063867	Valley	Main Valley	2.2	30.7	221
116	452256	4063821	Valley A	Main Valley	8.2	30.7	221
117	452256	4063821	Valley B	Main Valley	8.2	30.7	221
118	452256	4063821	Valley C	Main Valley	8.2	30.7	221
119	452189	4063790	Valley	Main Valley	17.8	30.7	221
120	452090	4063755	Channel A	Main Valley	19.1	30.7	221
121	452090	4063755	Channel B	Main Valley	19.1	30.7	221
122	452090	4063755	Channel C	Main Valley	19.1	30.7	221
123	451693	4058609	Valley	Main Valley	17.2	40.3	472
124	451757	4058592	Channel	Main Valley	27.6	40.3	472
125	451847	4058629	Valley	Main Valley	20.4	40.3	472
126	453751	4055915	Valley A	Main Valley	23.5	45.5	419
127	453751	4055915	Valley B	Main Valley	23.5	45.5	419
128	453751	4055915	Valley C	Main Valley	23.5	45.5	419
129	453710	4055991	Valley	Main Valley	23.5	45.5	419
130	453757	4056118	Channel A	Main Valley	31.5	45.5	419
131	453757	4056118	Channel B	Main Valley	31.5	45.5	419
132	453757	4056118	Channel C	Main Valley	31.5	45.5	419
133	453916	4056167	Valley	Main Valley	23.7	45.5	419
134	454000	4056232	Valley	Main Valley	22.9	45.5	419
135	456194	4058437	Valley	Main Valley	12.3	54.8	724
136	456219	4058592	Channel	Main Valley	38.2	54.8	724
137	456308	4058810	Valley	Main Valley	34.5	54.8	724
138	456389	4058976	Valley	Main Valley	22.3	54.8	724
139	457250	4054691	Valley	Main Valley	33.6	61.0	686
140	457262	4054797	Valley	Main Valley	34.2	61.0	686
141	457276	4054944	Channel A	Main Valley	44.9	61.0	686
142	457276	4054944	Channel B	Main Valley	44.9	61.0	686
143	457276	4054944	Channel C	Main Valley	44.9	61.0	686
144	457282	4055111	Valley A	Main Valley	35.4	61.0	686
145	457282	4055111	Valley B	Main Valley	35.4	61.0	686
146	457282	4055111	Valley C	Main Valley	35.4	61.0	686
147	457324	4056397	Valley	Aunts	38.5	6.3	488
148	457336	4056285	Valley	Aunts	33.3	6.3	488
149	457361	4056200	Valley	Aunts	23.1	6.3	488

Site	Easting UTM NAD83 Zone 15n	Northing UTM NAD83 Zone 15n	Type	Location	Depth (m)	Distance (km)	Valley width (m)
150	454690	4071823	Floodplain	Main Valley	1.4	-	-
151	454705	4071896	Stream	McCord	-	-	-
152	454620	4072102	Valley	Main Valley	1.4	9.4	49
153	454650	4072383	Valley	Main Valley	1.4	9.7	49
154	454812	4072650	Valley	Main Valley	6.6	10.0	49
155	454812	4072650	Channel	Main Valley	5.0	10.0	49
156	454812	4072650	Valley	Main Valley	5.7	10.0	49
157	454490	4072897	Valley	Main Valley	1.4	10.5	49
158	454151	4072165	Valley	Main Valley	0.5	11.6	84
159	454131	4072160	Valley	Main Valley	0.8	11.6	84
160	454111	4072163	Valley	Main Valley	1.4	11.6	84
161	454092	4072154	Valley	Main Valley	1.1	11.6	84
162	454083	4072147	Valley	Main Valley	1.4	11.6	84
163	454049	4072123	Channel	Main Valley	4.3	11.6	84
164	453953	4072133	Valley	Main Valley	1.9	11.6	84
165	454163	4071576	Valley	Main Valley	3.7	12.1	114
166	454163	4071576	Channel	Main Valley	3.6	12.1	114
167	454163	4071576	Valley	Main Valley	3.3	12.1	114
168	454002	4071506	Valley A	Main Valley	1.4	12.1	114
169	454002	4071506	Valley B	Main Valley	1.4	12.1	114
170	454002	4071506	Valley C	Main Valley	1.4	12.1	114
171	452943	4067822	Channel	Flat	3.4	4.2	38
172	454305	4068116	Channel	Flat	6.0	5.8	76
173	454214	4066676	Channel	Flat	8.7	7.5	183
174	455755	4066166	Channel	Main Valley	11.2	21.0	191
175	454716	4067378	Channel	Main Valley	9.3	19.0	107
201	458940	4049767	Channel	White R	50.3	69.0	732
202	457381	4050467	Channel	White R	48.1	67.2	800
203	457591	4051567	Channel	White R	49.3	65.8	777
204	457107	4052879	Channel	White R	49.3	63.9	869
205	455984	4052044	Channel	White R	47.2	61.9	572
206	454835	4051332	Channel	White R	46.9	60.0	701

APPENDIX B

Sediment Composition and Geochemistry

Site	% Sand	% Silt	% Clay	% Organic Matter	Al%	Ca%	Cu ppm	Fe%	Hg ppb	Mn ppm	P ppm	Pb ppm	Zn ppm
1	9.32	66.88	23.80	4.99	0.83	2.87	3	1.07	60	575	780	20	74
2	0.99	70.23	28.78	7.49	1.19	4.55	10	1.46	80	1135	1300	28	114
3	0.46	67.12	32.42	7.71	1.22	4.85	10	1.54	80	1105	1330	28	112
4	0.68	63.87	35.44	8.38	1.3	4.78	10	1.65	80	1365	1480	30	110
5	1.19	67.76	31.04	7.17	1.03	4.63	4	1.34	70	955	1110	22	88
6	8.92	68.14	22.94	12.27	0.64	5.97	0.5	0.94	50	440	710	12	30
7				7.40	1.04	3.71	0.5	1.31	50	1010	700	18	84
8	45.28	34.62	20.10	4.58	0.47	1.62	0.5	0.78	30	355	350	8	42
9	0.96	66.69	32.34	7.42	1.09	4.33	1	1.43	50	1025	800	20	90
10	0.63	71.94	27.44	7.48	1.15	4.46	5	1.45	70	1150	1180	24	88
11	0.76	57.83	41.40	9.09	1.3	5.32	6	1.74	60	1275	1410	26	92
12	1.39	76.70	21.91	7.22	0.84	9.08	0.5	1.02	50	405	870	16	34
13	0.49	61.02	38.49	7.93	1.33	5.71	5	1.74	70	1150	1580	26	88
14	0.66	62.25	37.08	8.21	1.26	5.61	4	1.59	60	950	1350	24	82
15	1.39	63.99	34.62	8.07	1.22	6.31	3	1.56	60	955	1470	22	80
16	0.63	57.59	41.78	8.54	1.35	6.03	3	1.64	60	910	1370	24	82
17	0.62	51.33	48.05	9.20	1.35	4.87	4	1.74	60	955	1620	28	86
18	2.79	74.84	22.36	8.61	0.65	5.96	0.5	0.85	50	275	650	12	26
19	0.56	48.03	51.41	10.05	1.49	5.4	8	1.87	60	950	1570	28	96
20	0.97	50.57	48.45	20.31	1.4	6.02	5	1.76	60	810	1570	24	80
21	4.01	68.75	27.24	10.54	0.85	3.08	1	1.09	50	345	560	14	34
22	19.39	49.68	30.93	20.15	0.81	2.77	3	1.26	60	350	560	18	30
23	10.46	53.80	35.74	10.15	1.03	5.86	3	1.4	60	450	1030	18	46
24	0.49	48.47	51.04	10.20	1.62	5.19	6	1.99	60	530	1270	26	80
25				-									
26				-									
27	0.69	48.87	50.43	9.84	1.34	5.8	2	1.67	60	655	1350	22	70
28	1.73	73.30	24.97	6.99	0.61	8.44	0.5	0.77	40	275	710	12	28
29	3.57	74.79	21.65	7.24	0.88	3.31	5	1.11	70	545	830	22	78
30	31.98	50.27	17.75	4.82	0.59	2.3	0.5	0.88	40	345	640	10	46
31	17.07	56.90	26.03	21.26	0.71	6.71	0.5	0.96	70	395	890	14	58
32	75.36	15.24	9.40	1.93	0.36	1.44	0.5	1.37	20	280	460	6	46
33	12.85	63.94	23.21	5.41	0.81	2.34	0.5	1.12	60	475	800	16	70
34	68.11	19.90	11.99	4.54	0.35	1.31	0.5	0.75	120	200	300	1	24
36	55.87	30.22	13.91	4.85	0.46	1.9	0.5	0.88	30	250	440	8	38
35				-									
37				-									
38	0.41	49.27	50.32	10.31	1.59	7.4	3	2.09	70	1090	1910	22	82
39	5.81	45.56	48.63	10.67	1.14	7.32	0.5	1.4	50	480	1080	14	52
40	0.95	46.60	52.46	10.50	1.43	6.11	0.5	1.78	60	845	1620	20	68
41	0.32	43.99	55.69	10.40	1.42	6.71	18	1.75	50	760	1390	24	86
42				-									
43				-									
44	2.45	41.52	56.04	10.76	1.32	6.23	16	1.86	50	1150	1930	22	84
45	0.23	45.31	54.46	11.26	1.34	6.72	18	1.77	50	800	1550	22	80
46	0.56	37.29	62.15	10.59	1.53	5.39	19	2	60	1035	1660	26	94
47	1.73	61.54	36.74	11.05	1.15	7.79	15	1.36	40	475	990	16	56
48				5.89	1.52	1.21	14	2.19	30	405	500	12	44

Site	% Sand	% Silt	% Clay	% Organic Matter	Al%	Ca%	Cu ppm	Fe%	Hg ppb	Mn ppm	P ppm	Pb ppm	Zn ppm
49	0.82	43.88	55.30	10.97	1.37	6.33	19	1.98	50	1090	2140	24	84
50	0.68	44.18	55.13	10.98	1.48	5.71	21	2.21	60	1400	2360	26	88
51	1.54	65.65	32.81	9.11	0.87	3.04	16	1.1	50	275	550	16	64
52	6.55	62.00	31.44	7.69	0.83	3.63	12	1.07	50	300	510	18	56
53	4.93	54.95	40.12	11.23	0.85	4.37	16	1.14	40	395	690	14	58
54	0.42	44.76	54.83	11.34	1.35	4.19	21	1.87	50	610	1040	24	72
55	3.26	66.51	30.23	8.40	0.78	2.5	11	1.22	60	545	420	14	46
56	4.95	65.24	29.81	7.73	0.72	2.69	12	1.07	60	300	400	14	54
57	0.93	51.02	48.05	10.23	1.32	3.57	18	1.75	60	400	800	18	72
58	12.92	44.69	42.39	9.31	0.84	4.54	13	1.25	30	355	640	14	38
59	27.18	40.93	31.89	9.10	0.61	3.88	12	1.01	40	385	490	12	40
60	23.98	26.96	49.07	7.69	1.14	2.94	14	1.62	30	410	630	14	48
61	82.02	4.50	13.48	2.10	0.27	1.19	5	1.06	30	275	290	18	38
62	80.01	6.49	13.50	2.78	0.32	1.65	4	1.4	10	635	220	10	30
63	54.36	24.33	21.31	4.75	0.47	2.4	6	1.21	20	505	440	10	54
64	47.72	22.53	29.75	6.08	0.83	1.9	11	1.83	40	1110	390	14	48
65	48.13	22.66	29.22	4.35	0.87	0.47	12	1.87	40	1285	340	14	50
66	90.80	0.79	8.41	1.17	0.22	0.21	3	1.82	10	385	310	10	62
67	81.93	6.54	11.53	1.44	0.31	1.38	3	1.01	5	250	210	6	34
68	38.58	35.36	26.06	10.03	0.59	3.29	12	1.79	40	765	850	16	92
69	87.71	0.81	11.48	1.64	0.24	0.59	6	2	5	485	380	12	64
70	42.26	33.08	24.66	3.46	0.69	0.47	8	1.35	40	930	310	24	62
71	0.44	44.47	55.09	12.27	1.45	5.75	22	2.06	60	1015	1850	26	84
72	1.33	39.50	59.17	10.73	1.66	3.52	22	2.38	70	1820	2520	28	92
73	2.63	50.82	46.55	11.67	1.26	5.47	21	1.69	50	780	1160	24	70
74	2.14	60.37	37.49	9.80	1.16	4.06	19	1.43	50	365	800	22	88
75	0.91	49.49	49.60	10.89	1.55	3.94	21	1.98	60	630	990	24	80
76	6.46	67.78	25.76	8.24	0.76	3.04	11	1.01	40	250	420	14	36
77	0.59	55.51	43.90	10.17	1.35	2.33	17	1.86	60	685	720	20	76
78	12.23	57.19	30.58	12.98	0.83	3.9	9	1.39	40	600	580	12	46
79	69.40	15.18	15.43	3.71	0.55	1.98	6	1.64	30	960	280	12	34
80	7.01	52.71	40.28	14.40	1.07	1.96	15	1.51	60	545	520	20	56
101	39.63	45.10	15.27	2.83	0.44	2.74	7	0.76		245	5	10	30
102	48.87	36.59	14.54	2.61	0.36	2.19	6	0.74	30	185	5	6	26
103	2.71	74.47	22.82	4.81	0.8	3.84	14	1.02		355	5	12	66
104	2.31	75.13	22.57	4.98	0.64	3.6	11	0.84	50	330	210	8	52
105	2.75	73.09	24.16	5.01	0.7	3.8	13	0.88	60	340	280	12	58
106	3.46	74.89	21.65	5.24	0.77	4.1	13	0.99	60	485	530	16	66
107	0.34	58.43	41.24	8.70	1.47	4.58	23	1.71	80	1225	1160	24	114
108	0.39	56.98	42.64	8.26	1.45	4.3	22	1.68	80	1200	1150	26	112
109	0.51	58.34	41.14	8.68	1.47	4.36	24	1.71	80	1235	1210	24	114
110	0.56	64.13	35.30	7.94	1.35	4.89	19	1.57	60	1085	1100	20	98
111	0.95	64.45	34.61	7.38	1.35	4.86	19	1.48	70	895	880	22	98
112	2.95	71.88	25.18	5.60	0.84	6.54	21	1.06	70	525	580	20	78
113	2.45	72.33	25.23	5.06	0.75	5.33	17	0.94	70	370	340	14	66
114	62.19	22.91	14.90	1.13	0.46	0.14	6	1.34	10	405	5	12	10
115	83.75	6.33	9.93	1.25	0.38	0.23	5	2.42	10	600	170	16	22
116	4.76	73.70	21.54	3.79	0.58	4.93	11	0.73	50	295	150	14	42
117	9.13	71.89	18.97	3.37	0.56	4.91	10	0.76	50	310	150	12	38

Site	% Sand	% Silt	% Clay	% Organic Matter	Al%	Ca%	Cu ppm	Fe%	Hg ppb	Mn ppm	P ppm	Pb ppm	Zn ppm
118	4.30	75.99	19.72	4.00	0.67	4.9	11	0.8	50	315	180	10	46
119	19.73	51.83	28.44	5.70	1.02	4.68	14	1.25	50	670	750	16	66
120	0.38	48.44	51.18	8.82	1.56	7.44	21	1.69	60	775	1080	20	90
121	0.43	47.51	52.06	9.08	1.34	6.84	19	1.78	60	885	1210	30	102
122	0.77	51.60	47.63	9.12	1.5	6.61	22	2.02	60	1070	1450	30	118
123	47.99	25.93	26.08	7.62	0.86	5.93	13	1.55	40	515	910	26	64
124	0.59	41.19	58.22	10.61	1.64	6.53	22	2.13	60	985	1660	28	104
125	49.38	27.81	22.81	4.18	0.72	1.64	9	1.17	50	395	600	20	70
126	0.23	47.72	52.06	9.39	1.55	8.76	21	1.9	50	670	1420	28	86
127	0.39	48.50	51.12	9.14	1.58	9.4	21	1.85	60	695	1440	28	86
128	0.43	49.06	50.51	9.35	1.52	8.91	21	1.87	60	695	1410	26	82
129	0.33	45.74	53.93	8.57	1.59	8.58	21	1.95	60	830	1540	28	90
130	0.18	40.54	59.28	9.94	1.59	7.02	23	2.09	50	975	1920	28	100
131	0.30	40.53	59.16	10.53	1.51	6.76	21	2	60	915	1710	28	94
132	0.51	50.64	48.84	10.88	1.53	7.08	22	2.02	50	915	1770	30	98
133	3.10	56.84	40.06	8.22	1.25	8.83	18	1.69	60	955	1660	30	86
134	0.59	48.98	50.43	10.43	1.43	9.44	20	1.77	50	610	1350	26	84
135	40.37	28.28	31.35	35.50	0.54	5.32	13	1.08	60	310	830	14	38
136	0.57	52.92	46.51	10.78	1.46	7.7	22	2.07	50	865	1910	24	86
137	0.59	53.94	45.47	10.57	1.43	8.13	21	2.03	50	960	1930	28	82
138	6.05	55.67	38.28	10.25	1.25	8.68	19	1.55	70	645	1080	26	80
139	0.77	62.83	36.41	12.24	1.37	7.65	23	1.87	50	860	1320	28	76
140	0.82	59.58	39.60	11.19	1.63	7.05	25	2.03	60	1175	1600	32	90
141	0.46	58.22	41.31	11.76	1.64	5.43	23	2.4	60	1280	2380	26	88
142	0.34	55.03	44.63	12.10	1.48	5.52	23	2.3	50	1145	2300	24	84
143	0.31	58.22	41.48	12.44	1.5	6.35	24	2.26	50	1175	2240	28	84
144	1.97	48.12	49.91	11.33	1.62	5.22	21	2.15	60	1040	1680	28	86
145	1.26	48.78	49.96	11.94	1.53	6.04	23	2.2	50	1150	1950	30	82
146	2.84	51.27	45.89	10.53	1.6	5.15	22	2.12	60	1080	1590	30	86
147	2.02	51.42	46.56	10.88	1.51	5.08	22	2.08	50	1060	1670	32	78
148	2.42	55.03	42.54	10.11	1.56	6.13	22	1.79	50	765	1290	28	76
149	4.10	56.86	39.04	8.95	1.37	4.81	19	1.53	60	520	900	28	74
150	58.04	21.79	20.17	2.31	0.88	0.41	8	1.68	10	380	350	20	48
151	37.65	43.38	18.97	12.34	0.61	0.42	9	1	30	125	460	18	46
152	56.59	28.22	15.19	4.52	0.54	1.16	7	1.09	20	235	400	14	48
153	49.24	31.17	19.59	2.42	0.66	0.94	5	1.02	10	495	260	12	36
154	9.37	67.21	23.42	6.54	0.78	3.14	15	1.02	50	500	790	24	86
155	37.09	43.23	19.68	5.50	0.62	2.7	11	1.01	40	400	660	14	70
156	52.17	30.83	17.00	4.21	0.54	2.32	9	0.99	30	340	560	18	64
157	26.06	49.56	24.38	2.07	0.9	0.19	7	1.45	10	500	270	14	34
158	25.13	59.99	14.88	2.36	0.69	0.38	7	0.96	20	435	300	14	36
159	12.64	72.39	14.96	3.50	0.55	2.24	8	0.78	30	245	360	12	48
160	3.93	73.90	22.17	5.71	0.82	3.19	14	1.02	50	345	520	22	76
161	26.80	52.57	20.63	13.85	0.69	3.23	15	1.05	60	420	640	22	84
162	38.01	45.02	16.97	7.23	0.66	2.93	12	0.99	50	330	490	18	74
163	11.19	62.81	26.00	5.83	0.87	3.34	15	1.25	60	815	910	22	96
164	33.40	50.84	15.75	4.90	0.48	2.06	8	0.79	50	240	410	16	50
165	59.88	25.06	15.05	3.20	0.41	2.11	6	1.15	30	340	490	14	58
166	26.23	55.55	18.22	5.73	0.51	3.31	10	0.85	40	370	540	14	64

Site	% Sand	% Silt	% Clay	% Organic Matter	Al%	Ca%	Cu ppm	Fe%	Hg ppb	Mn ppm	P ppm	Pb ppm	Zn ppm
167	22.71	57.21	20.08	5.47	0.62	3.15	12	0.94	50	400	580	22	72
168	8.92	72.86	18.22	4.86	0.65	3.01	12	0.89	50	250	420	18	68
169	8.27	74.03	17.70	4.88	0.59	2.87	11	0.81	50	230	400	18	62
170	7.19	73.84	18.98	5.11	0.62	2.93	11	0.84	50	240	410	16	64
171	15.81	65.90	18.28	4.97	0.59	1.9	7	0.84	30	310	300	14	62
172	2.50	69.43	28.07	7.18	0.94	3.45	12	1.21	40	625	550	20	94
173	0.97	65.36	33.67	7.41	1.18	4.51	15	1.58	50	960	810	24	112
174	0.59	66.33	33.09	8.49	1.08	4.19	19	1.52	70	1035	1130	28	108
175	0.41	64.75	34.85	7.62	1.07	4.56	21	1.53	70	1010	1100	32	116
201	1.54	46.55	51.91	11.77	1.48	1.8	23	2.36	60	2780	2210	28	78
202	1.10	45.64	53.26	11.54	1.6	2.24	24	2.57	60	3050	2460	32	86
203	0.98	46.72	52.30	12.69	1.58	2.89	25	2.41	60	2370	2460	24	84
204	1.27	45.21	53.52	12.19	1.52	1.62	21	2.53	60	3150	2090	28	74
205	1.47	45.50	53.03	12.20	1.42	1.14	21	2.51	50	3080	1860	26	66
206	0.56	53.35	46.08	11.66	1.27	0.85	20	2.49	60	3010	1720	30	60

APPENDIX C

Cove Spatial Characteristics

Site	Cove Name	Drainage Area (km^2)	# of Docks	Road Length (km)	Lake Surface Area (km^2)	% Urban	% Forest	% Agriculture
6	Peach	8.444	0	6	0.04	0.3	56.3	42.4
7	Flat	835.128	0	1109	0.26	1.3	41.3	56.7
8	Flat	836.573	0	1112	0.59	1.3	41.3	56.6
9	Flat	838.649	2	1121	0.90	1.3	41.4	56.5
12	Bear	13.806	0	13	0.07	1.8	72.4	24.7
18	Wooly	14.92	5	16	0.09	0.0	92.3	6.7
21	Piney	28.988	0	13	0.08	0.0	98.2	1.1
22	Piney	6.596	0	2	0.02	0.0	97.6	1.4
23	Piney	39.61	0	15	0.39	0.0	97.3	1.1
24	Piney	44.41	0	19	0.86	0.0	96.2	1.1
27	Wooly	17.285	8	22	0.42	0.0	90.0	7.0
28	Cape	3.444	0	7	0.07	0.7	64.4	31.1
31	Shift	2.249	0	3	0.02	0.4	78.9	20.0
47	Jackson	3.264	1	9	0.17	0.1	89.4	5.5
48	Jackson	0.585	0	1	0.03	0.0	97.7	0.0
51	Aunts	5.265	1	10	0.09	8.5	84.2	5.6
52	Aunts	2.464	0	7	0.03	6.5	84.2	5.2
53	Aunts	8.515	14	19	0.31	8.4	81.2	5.5
54	Aunts	52.975	78	63	1.63	2.0	81.4	13.2
55	Aunts	20.268	3	15	0.12	3.4	83.6	12.2
56	Aunts	20.932	0	18	0.06	0.4	81.3	17.8
57	Aunts	43.299	51	40	0.64	1.9	81.7	14.6
58	Piney	37.892	0	15	0.29	0.0	97.5	1.1
59	Piney	2.241	0	1	0.03	0.0	97.2	0.9
60	Piney	43.292	0	17	0.65	0.0	96.6	1.1
73	Aunts	54.339	87	69	2.11	2.5	80.4	13.0
74	Aunts	2.074	5	10	0.09	5.3	86.3	5.4
75	Aunts	49.418	56	50	1.07	1.9	81.8	13.9
76	Aunts	3.403	0	2	0.03	0.0	87.2	11.5
77	Aunts	42.103	27	37	0.39	1.9	82.0	14.9
78	Aunts	16.361	0	11	0.04	3.6	83.8	12.1
80	Aunts	3.624	0	4	0.01	2.6	83.5	13.6
147	Aunts	63.91	121	91	3.00	3.3	79.9	11.8
148	Aunts	63.91	121	91	3.00	3.3	79.9	11.8
149	Aunts	63.91	121	91	3.00	3.3	79.9	11.8
171	Flat	835.763	0	1110	0.45	1.3	41.3	56.7
172	Flat	838.406	2	1120	0.84	1.3	41.4	56.5
173	Flat	839.2	2	1121	1.15	1.3	41.4	56.5

APPENDIX D

Triplicate Analysis

Site	Sample	Al%	Ca%	Cu ppm	Fe%	Hg ppb	Mn ppm	P ppm	Pb ppm	Zn ppm
104	A	0.6	3.75	11	0.87	90	380	530	20	66
104	B	0.57	3.69	12	0.83	80	355	510	16	66
104	C	0.67	3.57	12	0.87	70	365	530	22	68
108	A	1.45	4.46	24	1.75	90	1300	1270	30	128
108	B	1.38	4.23	22	1.66	90	1230	1210	30	122
108	C	1.27	4.45	24	1.66	90	1270	1310	34	120
117	A	0.52	4.93	8	0.75	40	330	440	16	52
117	B	0.47	4.41	7	0.69	50	305	400	14	48
117	C	0.51	4.9	9	0.75	50	335	430	14	52
121	A	1.33	7.04	20	1.74	70	935	1250	28	106
121	B	1.24	6.64	19	1.63	70	875	1180	24	102
121	C	1.22	6.44	19	1.6	60	865	1190	24	100
127	A	1.36	8.74	20	1.58	70	615	1210	20	72
127	B	1.42	9.06	20	1.65	70	640	1310	22	76
127	C	1.35	8.96	21	1.61	80	630	1280	24	74
131	A	1.43	6.75	21	1.81	70	850	1560	24	80
131	B	1.42	6.71	21	1.83	70	860	1560	24	80
131	C	1.42	6.81	22	1.83	60	855	1630	24	82
142	A	1.42	5.64	25	2.19	70	1130	2190	24	74
142	B	1.37	5.55	25	2.16	70	1090	2100	24	76
142	C	1.36	5.19	23	2.05	70	1030	2050	22	72
145	A	1.52	5.61	23	1.95	70	1025	1590	24	72
145	B	1.44	5.41	22	1.87	70	995	1580	20	68
145	C	1.41	5.52	22	1.89	70	1000	1620	24	68
2	A	1.09	4.24	21	1.39	80	1075	1130	24	102
2	B	1.11	4.27	21	1.41	80	1085	1110	24	106
2	C	1.11	4.23	21	1.39	80	1065	1100	26	102
8	A	0.39	1.36	6	0.69	30	300	230	8	40
8	B	0.42	1.51	7	0.73	30	335	250	10	44
8	C	0.43	1.57	7	0.74	30	345	260	12	44
13	A	1.24	5.64	21	1.71	70	1135	1430	26	94
13	B	1.37	6.2	22	1.88	70	1245	1590	28	104
13	C	1.29	5.81	20	1.76	70	1170	1450	26	98
19	A	1.49	6.11	22	2.05	80	1060	1600	30	104
19	B	1.42	5.77	21	1.93	70	1000	1460	26	98
19	C	1.36	5.58	20	1.86	60	970	1460	24	94
23	A	1	6.44	19	1.52	60	510	1020	20	54
23	B	1	6.41	19	1.5	60	505	1000	20	54
23	C	0.94	5.96	18	1.43	60	475	960	18	50
34	A	0.32	1.28	6	0.77	30	195	330	10	32
34	B	0.35	1.33	7	0.8	40	215	360	12	36
34	C	0.34	1.35	6	0.82	50	210	350	10	34
41	A	1.42	8.02	22	1.89	80	845	1540	24	84
41	B	1.33	7.34	19	1.75	60	780	1440	22	78
41	C	1.36	7.76	20	1.83	60	825	1520	22	80

Site	Sample	Al%	Ca%	Cu ppm	Fe%	Hg ppb	Mn ppm	P ppm	Pb ppm	Zn ppm
54	A	1.39	4.55	23	1.94	60	640	1100	22	66
54	B	1.36	4.44	22	1.89	60	625	1060	22	64
54	C	1.32	4.43	21	1.87	50	620	1080	22	62

APPENDIX E

Water-Column Data

USGS 07052910 TABLE ROCK LAKE (JAMES R. ARM) AT CAPE FAIR, MO.		
Latitude 36°43'24",	**Source:** http://waterdata.usgs.gov/nwis/qwdata?	
Longitude 93°29'35"	Retrieved on 2003-05-22 21:27:04 EDT	
NAD27	Department of the Interior, U.S. Geological Survey	
Date and time	**Sampling depth, feet**	**Phosphorus, water, unfltrd mg/L**
7/6/1975 13:55	0	
7/6/1975 14:00	9	0.09
7/6/1975 14:30	36	0.15
10/21/1975 13:40	0	
10/21/1975 13:45	8	0.09
10/21/1975 13:50	33	0.21
2/25/1976 11:49	0	
2/25/1976 11:50	9	0.25
2/25/1976 12:30	36	0.24
7/13/1976 14:14	0	
7/13/1976 14:15	7	0.09
7/13/1976 14:30	28	0.12
10/13/1976 10:51	0	
10/13/1976 10:59	0	
10/13/1976 11:00	6	0.08
10/13/1976 11:01	6	
10/13/1976 11:15	24	0.1
10/13/1976 11:16	24	
4/11/1977 12:21	0	
4/11/1977 12:25	0	
4/11/1977 12:30	6	0.22
4/11/1977 12:31	6	
4/11/1977 12:40	24	0.22
4/11/1977 12:41	24	
9/25/1977 11:14	0	
9/25/1977 11:15	0	
9/25/1977 11:20	7	0.13
9/25/1977 11:21	7	
9/25/1977 11:55	26	0.22
9/25/1977 11:56	26	
3/21/1978 10:25	0	
3/21/1978 10:30	8	0.2

3/21/1978 10:45	32	0.2
6/21/1978 13:40	0	
6/21/1978 13:45	9	0.06
6/21/1978 13:50	37	0.09
10/4/1978 16:45	0	
10/4/1978 16:50	8	0.07
10/4/1978 16:55	32	0.11
3/14/1979 9:35	0	
3/14/1979 9:40	9	0.08
3/14/1979 9:45	36	0.08
6/13/1979 8:10	0	
6/13/1979 8:15	9	0.01
6/13/1979 8:20	36	0.09
8/23/1979 8:50	0	
8/23/1979 8:55	7	0.07
8/23/1979 9:00	28	0.1
12/6/1979 10:15	0	
12/6/1979 10:20	6	.120
12/6/1979 10:25	24	0.13
5/8/1980 17:30	0	
5/8/1980 17:35	9	0.1
5/8/1980 17:40	36	0.21
8/28/1980 8:45	0	
8/28/1980 8:50	7	0.08
8/28/1980 8:55	28	0.22
12/11/1980 9:15	0	
12/11/1980 9:20	5	0.46
12/11/1980 9:25	21	0.47
5/14/1981 8:10	0	
5/14/1981 8:15	6	0.52
5/14/1981 8:20	24	0.49
8/13/1981 8:00	0	
8/13/1981 8:05	8	0.07
8/13/1981 8:10	32	0.12
12/10/1981 10:55	0	
12/10/1981 11:00	9	0.11
12/10/1981 11:05	35	0.17
5/20/1982 13:55	0	
5/20/1982 14:00	9	< .010
5/20/1982 14:05	37	0.15
8/19/1982 7:45	0	
8/19/1982 7:50	9	0.06
8/19/1982 7:55	36	0.19
12/9/1982 8:15	0	
12/9/1982 8:16	3	
12/9/1982 8:20	12	0.13
12/9/1982 8:25	48	0.15

5/19/1983 10:35	0	
5/19/1983 10:36	3	
5/19/1983 10:40	10	0.07
5/19/1983 10:45	40	0.1
8/17/1983 13:05	0	
8/17/1983 13:06	3	
8/17/1983 13:10	9	0.05
8/17/1983 13:15	36	0.23
12/7/1983 12:05	0	
12/7/1983 12:06	3	
12/7/1983 12:10	8	0.05
12/7/1983 12:15	34	0.04
5/22/1984 10:15	0	
5/22/1984 10:16	3	
5/22/1984 10:20	10	0.05
5/22/1984 10:25	40	0.08
8/14/1984 13:30	0	
8/14/1984 13:31	3	
8/14/1984 13:35	9	< .010
8/14/1984 13:40	35	0.28
12/12/1984 9:00	0	
12/12/1984 9:01	3	
12/12/1984 9:05	10	0.09
12/12/1984 9:10	40	0.12
5/9/1985 16:00	0	
5/9/1985 16:01	3	
5/9/1985 16:05	10	0.04
5/9/1985 16:10	40	0.05
8/8/1985 18:00	0	
8/8/1985 18:01	3	
8/8/1985 18:05	9	0.01
8/8/1985 18:10	35	0.14
12/11/1985 14:30	0	
12/11/1985 14:31	3	
12/11/1985 14:35	11	0.1
12/11/1985 14:40	43	0.1
5/8/1986 8:30	0	
5/8/1986 8:31	3	
5/8/1986 8:35	9	0.08
5/8/1986 8:40	35	0.1
8/7/1986 13:30	0	
8/7/1986 13:31	3	
8/7/1986 13:35	9	0.08
8/7/1986 13:40	33	0.29
1/14/1987 13:30	0	
1/14/1987 13:31	3	
1/14/1987 13:35	8	0.19

1/14/1987 13:40	32	0.26
5/12/1987 10:20	0	
5/12/1987 10:21	3	
5/12/1987 10:25	9	0.08
5/12/1987 10:30	36	0.09
8/18/1987 10:00	0	
8/18/1987 10:01	3	
8/18/1987 10:05	8	0.07
8/18/1987 10:10	32	0.16
12/2/1987 13:40	0	
12/2/1987 13:41	3	
12/2/1987 13:45	8	0.15
12/2/1987 13:50	30	0.17
5/11/1988 12:00	0	
5/11/1988 12:01	3	
5/11/1988 12:05	8	0.08
5/11/1988 12:10	32	0.11
8/9/1988 7:30	0	
8/9/1988 7:31	3	
8/9/1988 7:35	8	0.08
8/9/1988 7:40	32	0.67
1/5/1989 11:30	0	
1/5/1989 11:31	3	
1/5/1989 11:35	8	.120
1/5/1989 11:40	32	0.14
5/3/1989 8:20	0	
5/3/1989 8:21	3	
5/3/1989 8:25	10	0.1
5/3/1989 8:30	39	0.13
8/9/1989 9:25	0	
8/9/1989 9:26	3	
8/9/1989 9:30	9	0.09
8/9/1989 9:35	36	0.6
1/9/1990 11:50	0	
1/9/1990 11:51	3	
1/9/1990 11:55	7	0.05
1/9/1990 12:00	28	0.42
5/15/1990 9:00	0	
5/15/1990 9:01	3	
5/15/1990 9:05	10	0.08
5/15/1990 9:10	40	0.12
8/1/1990 14:25	0	
8/1/1990 14:26	3	
8/1/1990 14:30	10	0.06
8/1/1990 14:35	40	0.2
5/30/1991 14:30	0	
5/30/1991 14:31	3	

5/30/1991 14:32	6	
5/30/1991 14:33	7	
5/30/1991 14:35	9	
5/30/1991 14:36	10	0.1
5/30/1991 14:37	13	
5/30/1991 14:38	18	
5/30/1991 14:40	20	
5/30/1991 14:41	30	
5/30/1991 14:42	35	
5/30/1991 14:43	36	
5/30/1991 14:44	37	
5/30/1991 14:45	39	
5/30/1991 14:46	40	0.11
5/30/1991 14:47	50	
5/30/1991 14:48	51	
8/14/1991 8:35	0	
8/14/1991 8:36	3	
8/14/1991 8:37	9	0.1
8/14/1991 8:39	10	
8/14/1991 8:40	20	
8/14/1991 8:41	28	
8/14/1991 8:42	30	
8/14/1991 8:43	31	
8/14/1991 8:44	32	
8/14/1991 8:45	33	
8/14/1991 8:46	35	
8/14/1991 8:47	36	.340
8/14/1991 8:48	37	
8/14/1991 8:49	40	
8/14/1991 8:50	41	
8/14/1991 8:51	46	
1/8/1992 8:30	0	
1/8/1992 8:31	3	
1/8/1992 8:35	23	0.14
5/7/1992 7:25	0	
5/7/1992 7:26	3	
5/7/1992 7:30	22	0.14
8/13/1992 7:40	0	
8/13/1992 7:41	3	
8/13/1992 7:45	10	0.09
8/13/1992 7:50	39	0.26
1/27/1993 8:05	0	
1/27/1993 8:06	3	
1/27/1993 8:10	24	0.07
5/6/1993 7:29	0	
5/6/1993 7:30	3	
5/6/1993 7:31	25.1	0.06

8/25/1993 8:28	0	
8/25/1993 8:29	3	
8/25/1993 8:30	9	0.07
8/25/1993 8:31	36.1	0.38
1/11/1994 11:07	0	
1/11/1994 11:08	3	
1/11/1994 11:09	23.9	0.08
5/4/1994 8:30	0	
5/4/1994 8:31	3	
5/5/1994 8:35	24.1	0.08
8/11/1994 12:50	0	
8/11/1994 12:53	3	
8/11/1994 12:54	7.1	0.04
8/11/1994 12:55	28	0.15
1/12/1995 8:52	0	
1/12/1995 8:53	3	
1/12/1995 8:55	21	0.16
5/24/1995 10:51	0	
5/24/1995 10:52	3	
5/24/1995 10:53	17	0.02
8/23/1995 9:47	0	
8/23/1995 9:48	3	0.05
8/23/1995 9:49	12	0.06

USGS 07052920 TABLE ROCK LAKE (JAMES R) NR KIMBERLING CITY, MO		
Latitude 36°38'23"	**Source:** http://waterdata.usgs.gov/nwis/qwdata?	
Longitude 93°29'27"	Retrieved on 2003-05-21 21:23:51 EDT	
NAD27	Department of the Interior, U.S. Geological Survey	
Date and time	**Sampling depth, feet**	**Phosphorus, water, unfltrd mg/L**
7/6/1975 16:00	10	
7/6/1975 16:15	50	
10/21/1975 15:10	0	
2/25/1976 14:30	0	
7/16/1976 16:30	0	

10/13/1976 12:53	0	
10/13/1976 13:00	0	
10/13/1976 13:05	12	
10/13/1976 13:10	48	
4/12/1977 15:16	0	
4/12/1977 15:20	0	
4/12/1977 15:25	15	
4/12/1977 15:30	60	
9/25/1977 14:22	0	
9/25/1977 14:25	0	
9/25/1977 14:30	25	
9/25/1977 14:35	102	
3/21/1978 11:55	0	
3/21/1978 12:00	19	
3/21/1978 12:15	76	
6/21/1978 12:30	0	
6/21/1978 12:35	30	
6/21/1978 12:40	120	
10/4/1978 15:45	0	
10/4/1978 15:50	28	
10/4/1978 15:55	112	
3/14/1979 15:10	0	
3/14/1979 15:15	28	
3/14/1979 15:20	112	
6/13/1979 11:00	0	
6/13/1979 11:05	29	
6/13/1979 11:10	116	
8/23/1979 13:50	0	
8/23/1979 13:55	28	
8/23/1979 14:00	112	
12/6/1979 15:45	0	
12/6/1979 15:50	27	
12/6/1979 15:55	108	
5/8/1980 14:00	0	
5/8/1980 14:05	20	
5/8/1980 14:10	80	
8/28/1980 12:35	0	
8/28/1980 12:40	24	
8/28/1980 12:45	96	
12/11/1980 13:20	0	
12/11/1980 13:25	25	
12/11/1980 13:30	100	
5/14/1981 11:45	0	
5/14/1981 11:50	26	
5/14/1981 11:55	104	
8/13/1981 11:45	0	
8/13/1981 11:50	28	

8/13/1981 11:55	112	
12/10/1981 9:35	0	
12/10/1981 9:40	29	
12/10/1981 9:45	116	
5/20/1982 11:25	0	
5/20/1982 11:30	29	
5/20/1982 11:35	116	
8/19/1982 9:35	0	
8/19/1982 9:40	30	
8/19/1982 9:45	120	
12/9/1982 9:50	0	
12/9/1982 9:51	3	
12/9/1982 9:55	32	
12/9/1982 10:00	128	
5/19/1983 11:30	0	
5/19/1983 11:31	3	
5/19/1983 11:35	29	
5/19/1983 11:40	116	
8/17/1983 14:15	0	
8/17/1983 14:16	3	
8/17/1983 14:20	28	
8/17/1983 14:25	112	
12/7/1983 12:45	0	
12/7/1983 12:46	3	
12/7/1983 12:50	28	
12/7/1983 12:55	112	
5/22/1984 11:15	0	
5/22/1984 11:16	3	
5/22/1984 11:20	30	< .010
5/22/1984 11:25	109	0.05
8/14/1984 14:45	0	
8/14/1984 14:46	3	
8/14/1984 14:50	29	< .010
8/14/1984 14:55	116	0.03
12/11/1984 15:00	0	
12/11/1984 15:01	3	
12/11/1984 15:05	30	< .010
12/11/1984 15:10	120	< .010
5/9/1985 14:30	0	
5/9/1985 14:31	3	
5/9/1985 14:35	32	< .010
5/9/1985 14:40	128	0.05
8/8/1985 16:30	0	
8/8/1985 16:31	3	
8/8/1985 16:35	29	< .010
8/8/1985 16:40	116	0.08
12/17/1985 10:30	0	

12/17/1985 10:31	3	
12/17/1985 10:35	32	0.03
12/17/1985 10:40	128	0.07
5/8/1986 10:30	0	
5/8/1986 10:31	3	
5/8/1986 10:35	30	0.02
5/8/1986 10:40	120	0.05
8/7/1986 12:20	0	
8/7/1986 12:21	3	
8/7/1986 12:25	28	0.01
8/7/1986 12:30	112	0.09
1/14/1987 12:00	0	
1/14/1987 12:01	3	
1/14/1987 12:05	28	0.02
1/14/1987 12:10	112	0.02
5/12/1987 11:45	0	
5/12/1987 11:46	3	
5/12/1987 11:50	29	0.02
5/12/1987 11:55	116	0.03
8/18/1987 11:00	0	
8/18/1987 11:01	3	
8/18/1987 11:05	28	0.01
8/18/1987 11:10	112	0.08
12/3/1987 10:00	0	
12/3/1987 10:01	3	
12/3/1987 10:05	27	0.03
12/3/1987 10:10	108	0.07
5/11/1988 10:30	0	
5/11/1988 10:31	3	
5/11/1988 10:35	30	0.06
5/11/1988 10:40	120	0.08
8/9/1988 9:00	0	
8/9/1988 9:01	3	
8/9/1988 9:05	28	0.03
8/9/1988 9:10	112	0.08
1/5/1989 10:25	0	
1/5/1989 10:26	3	
1/5/1989 10:30	28	0.02
1/5/1989 10:35	112	0.05
5/3/1989 10:30	0	
5/3/1989 10:31	3	
5/3/1989 10:35	30	0.03
5/3/1989 10:40	120	0.09
8/9/1989 16:01	3	
8/9/1989 16:05	29	< .020
8/9/1989 16:10	116	0.08
1/9/1990 12:45	0	

1/9/1990 12:46	3	
1/9/1990 12:50	28	< .020
1/9/1990 12:55	112	0.02
5/15/1990 10:10	0	
5/15/1990 10:11	3	
5/15/1990 10:15	32	0.02
5/15/1990 10:20	128	0.06
8/1/1990 13:00	0	
8/1/1990 13:01	3	
8/1/1990 13:05	30	0.03
8/1/1990 13:10	120	0.08
5/30/1991 12:15	0	
5/30/1991 12:16	3	
5/30/1991 12:17	10	
5/30/1991 12:18	11	
5/30/1991 12:19	15	
5/30/1991 12:20	17	
5/30/1991 12:21	18	
5/30/1991 12:22	20	
5/30/1991 12:23	22	
5/30/1991 12:24	24	
5/30/1991 12:25	26	
5/30/1991 12:26	28	< .010
5/30/1991 12:27	30	
5/30/1991 12:28	34	
5/30/1991 12:29	37	
5/30/1991 12:30	40	
5/30/1991 12:31	45	
5/30/1991 12:32	50	
5/30/1991 12:33	60	
5/30/1991 12:34	70	
5/30/1991 12:35	80	
5/30/1991 12:36	90	
5/30/1991 12:37	100	
5/30/1991 12:38	114	0.03
5/30/1991 12:39	120	
5/30/1991 12:40	130	
5/30/1991 12:41	140	
5/30/1991 12:42	143	
8/14/1991 10:10	0	
8/14/1991 10:11	3	
8/14/1991 10:12	10	
8/14/1991 10:13	20	
8/14/1991 10:14	26	
8/14/1991 10:15	27	
8/14/1991 10:16	28	
8/14/1991 10:17	29	0.03

8/14/1991 10:18	30	
8/14/1991 10:19	31	
8/14/1991 10:20	32	
8/14/1991 10:21	33	
8/14/1991 10:22	35	
8/14/1991 10:23	37	
8/14/1991 10:24	40	
8/14/1991 10:25	43	
8/14/1991 10:26	48	
8/14/1991 10:27	50	
8/14/1991 10:28	55	
8/14/1991 10:29	60	
8/14/1991 10:30	70	
8/14/1991 10:31	80	
8/14/1991 10:32	90	
8/14/1991 10:33	100	
8/14/1991 10:34	110	
8/14/1991 10:35	116	0.09
8/14/1991 10:36	120	
8/14/1991 10:37	130	
8/14/1991 10:38	139	
1/8/1992 9:30	0	
1/8/1992 9:36	3	
1/8/1992 9:40	75	0.05
5/7/1992 8:45	0	
5/7/1992 8:46	3	
5/7/1992 8:50	70	0.01
8/13/1992 13:55	0	
8/13/1992 13:56	3	
8/13/1992 14:00	30	< .020
8/13/1992 14:05	120	0.04
1/27/1993 14:05	0	
1/27/1993 14:06	3	
1/27/1993 14:10	75	0.05
5/6/1993 13:15	0	
5/6/1993 13:16	3	
5/6/1993 13:17	75	0.02
8/24/1993 17:09	0	
8/24/1993 17:10	3	
8/24/1993 17:11	30.2	0.02
8/24/1993 17:12	120	0.16
1/11/1994 8:28	0	
1/11/1994 8:29	3	
1/11/1994 8:30	70	0.02
5/5/1994 9:30	0	
5/5/1994 9:31	3	
5/5/1994 9:34	75	0.06

8/11/1994 11:50	0	
8/11/1994 11:51	3	
8/11/1994 11:52	29	0.02
8/11/1994 11:54	116	0.12
1/12/1995 11:27	0	
1/12/1995 11:28	3	
1/12/1995 11:30	69.8	0.06
5/24/1995 12:25	0	
5/24/1995 12:26	3	
5/24/1995 12:28	80	.060
8/23/1995 8:32	0	
8/23/1995 8:33	3	
8/23/1995 8:34	10	0.02
8/23/1995 8:35	40	0.02

APPENDIX F

Phosphorus Fractionation Data

Table of Site and Sediment Characteristics for Geochemical Fractionation Samples*							
Sample	**Location**	**Distance**	**Depth**	**OM**	**Sand**	**Silt**	**Clay**
ID		**(km)**	**(m)**	**(%)**	**(%)**	**(%)**	**(%)**
JRA 58	Piney Ck	1.69	9.7	9.31	12.92	48.30	42.39
JRA 60	Piney Ck	2.98	16.9	7.69	23.98	43.25	49.07
JRA 75	Aunts Ck	3.94	22.6	10.89	0.91	39.52	49.60
JRA 160	JR-below McCord Bend	11.55	1.4	5.71	3.93	72.12	22.17
JRA 163	JR-below McCord Bend	11.55	4.3	5.83	11.19	68.17	26.00
JRA 110	JR-below Flat	22.22	11.3	7.94	0.56	56.76	35.30
JRA 112	JR-below Flat	22.22	7.9	5.60	2.95	69.23	25.18
JRA 117	JR-Cape Fair	30.68	8.2	3.37	9.13	77.65	18.97
JRA 121	JR-Cape Fair	30.68	19.1	9.08	0.43	38.86	52.06
JRA 124	JR-below Piney	40.28	27.6	10.61	0.59	31.16	58.22
JRA 125	JR-below Piney	40.28	20.4	4.18	49.38	73.01	22.81
JRA 136	JR-Jackson Hollow	54.77	38.2	10.78	0.57	42.71	46.51
JRA 143	JR-Jackson Hollow	54.77	22.3	10.25	6.05	51.46	38.28
JRA 139	JR-below Aunts	61.01	33.6	12.24	0.77	51.35	36.41
JRA 138	JR-below Aunts	61.01	44.9	12.44	0.31	46.08	41.48

Table of Site and Sediment Characteristics for Geochemical Fractionation Samples*							
Sample	**Location**	**Distance**	**Depth**	**Al (aq)**	**Ca (aq)**	**S (aq)**	**Hg (aq)**
ID		**(km)**	**(m)**	**(%)**	**(%)**	**(%)**	**(ug/kg)**
JRA 58	Piney Ck	1.69	9.7	0.84	4.54	0.09	30
JRA 60	Piney Ck	2.98	16.9	1.14	2.94	0.07	30
JRA 75	Aunts Ck	3.94	22.6	1.55	3.94	0.15	60
JRA 160	JR-below McCord Bend	11.55	1.4	0.82	3.19	0.06	50
JRA 163	JR-below McCord Bend	11.55	4.3	0.87	3.34	0.07	60
JRA 110	JR-below Flat	22.22	11.3	1.35	4.89	0.08	60
JRA 112	JR-below Flat	22.22	7.9	0.84	6.54	0.07	70
JRA 117	JR-Cape Fair	30.68	8.2	0.56	4.91	0.06	50
JRA 121	JR-Cape Fair	30.68	19.1	1.34	6.84	0.12	60
JRA 124	JR-below Piney	40.28	27.6	1.64	6.53	0.18	60
JRA 125	JR-below Piney	40.28	20.4	0.72	1.64	0.07	50
JRA 136	JR-Jackson Hollow	54.77	38.2	1.46	7.7	0.24	50
JRA 143	JR-Jackson Hollow	54.77	22.3	1.25	8.68	0.15	70
JRA 139	JR-below Aunts	61.01	33.6	1.37	7.65	0.26	50
JRA 138	JR-below Aunts	61.01	44.9	1.5	6.35	0.22	50

Table of Results for Phosphorus, Iron, and Manganese Fractionation Experiments*							
Sample ID	**Location**	**Distance (km)**	**Depth (m)**	**P (total) mg/kg**	**P (avail) mg/kg**	**Fe (aq) %**	**Fe (CD) %**
JRA 58	Piney Ck	1.69	9.7	706	73	1.25	1.08
JRA 60	Piney Ck	2.98	16.9	705	73	1.62	1.36
JRA 75	Aunts Ck	3.94	22.6	995	62	1.98	1.35
JRA 160	JR-below McCord Bend	11.55	1.4	540	71	1.02	0.59
JRA 163	JR-below McCord Bend	11.55	4.3	936	125	1.25	0.83
JRA 110	JR-below Flat	22.22	11.3	1196	153	1.57	1.07
JRA 112	JR-below Flat	22.22	7.9	840	93	1.06	0.71
JRA 117	JR-Cape Fair	30.68	8.2	438	40	0.76	0.48
JRA 121	JR-Cape Fair	30.68	19.1	1300	121	1.78	1.20
JRA 124	JR-below Piney	40.28	27.6	1686	131	2.13	1.41
JRA 125	JR-below Piney	40.28	20.4	567	28	1.17	0.73
JRA 136	JR-Jackson Hollow	54.77	38.2	1397	141	2.07	1.48
JRA 143	JR-Jackson Hollow	54.77	22.3	2088	171	1.55	1.53
JRA 139	JR-below Aunts	61.01	33.6	1272	111	1.87	1.27
JRA 138	JR-below Aunts	61.01	44.9	995	91	2.26	0.89

Table of Results for Phosphorus, Iron, and Manganese Fractionation Experiments*							
Sample ID	**Location**	**Distance (km)**	**Depth (m)**	**Fe (oxalate) %**	**Mn (aq) mg/kg**	**Mn (CD) mg/kg**	**Mn (oxalate) mg/kg**
JRA 58	Piney Ck	1.69	9.7	0.46	355	369	238
JRA 60	Piney Ck	2.98	16.9	0.47	410	378	273
JRA 75	Aunts Ck	3.94	22.6	0.50	630	533	371
JRA 160	JR-below McCord Bend	11.55	1.4	0.21	345	274	223
JRA 163	JR-below McCord Bend	11.55	4.3	0.26	815	649	488
JRA 110	JR-below Flat	22.22	11.3	0.41	1085	923	811
JRA 112	JR-below Flat	22.22	7.9	0.31	525	461	373
JRA 117	JR-Cape Fair	30.68	8.2	0.21	310	230	205
JRA 121	JR-Cape Fair	30.68	19.1	0.48	885	736	565
JRA 124	JR-below Piney	40.28	27.6	0.73	985	822	550
JRA 125	JR-below Piney	40.28	20.4	0.26	395	289	240
JRA 136	JR-Jackson Hollow	54.77	38.2	0.90	865	763	517
JRA 143	JR-Jackson Hollow	54.77	22.3	0.83	645	999	608
JRA 139	JR-below Aunts	61.01	33.6	0.66	860	679	433
JRA 138	JR-below Aunts	61.01	44.9	0.29	1175	437	262

*METHODS

aq - (aqua regia digestion using hot 3:1 HCl:HNO3 at ALS Chemex Labs, Sparks Nevada)
total- (hot H2SO4 and HNO3 digestion)
avail- (NaHCO3 extraction using the Olsen method)
CD- (dithionite-citrate method)
Oxalate- (acid ammonium oxalate method)

Geochemical Fractionation of Phosphorus in James River Arm Sediments
(analyses by the University of Wisconsin-Milwaukee Soils Laboratory)*

Sample #	Location	Total P	Organic/residual	Apatite	Al/Fe Oxides	Carbonate	Exchangeable
	(distance/depth)	(mg/kg)	(%)	(%)	(%)	(%)	(%)
163	McCord (12km/4m)	936	29	12	19	35	5
110	Flat (22km/11m)	1196	4	7	31	40	18
121	Cape Fair (31km/19m)	1300	31	6	16	34	13
124	Piney (40km/28m)	1686	22	8	17	41	12
136	Jack Hol (55km/38m)	1397	27	11	19	30	13
143	Aunts (61km/45m)	2088	29	6	18	36	11
75	Aunts Ck (23m)	995	25	8	20	34	14
60	Piney Ck (17m)	705	37	9	17	30	8
58	Piney Ck (10m)	706	20	11	29	34	6

*METHODS

Fraction 1a (NaOH/NaCl extraction) measures nonoccluded Al and Fe bound P.

Fraction 1b (NaCl and Na citrate-Na bicarbonate (CB)) measures P sorbed by carbonates during the 1a extraction.

Fraction 2 (Na citrate-Na dithionite-Na bicarbonate (CDB)) measures P occluded within Al and Fe oxides and hydrous oxides.

Fraction 3 (HCl extraction) measures Ca-bound P.

Fraction 4 (calculated as difference between "total" P and "extractable" P using steps 1a through 3).

Fraction 5 (H2SO4 and HNO3 digestion) measures the total P in the sediment.

Table of Sed-P Fractionation Results for JR-Arm